UNIVERSITY OF OKLAHOMA
GRADUATE COLLEGE

RESERVOIR CHARACTERIZATION AND MODELING OF THE DESMOINESIAN SERIES GRANITE WASH, BUFFALO WALLOW FIELD, ANADARKO BASIN, TEXAS

A THESIS
SUBMITTED TO THE GRADUATE FACULTY
in partial fulfillment of the requirements for the
Degree of
MASTER OF SCIENCE

By

DOĞA ECEM ŞENOĞLU
Norman, Oklahoma
2017

RESERVOIR CHARACTERIZATION AND MODELING OF THE DESMOINESIAN SERIES GRANITE WASH, BUFFALO WALLOW FIELD, ANADARKO BASIN, TEXAS

A THESIS APPROVED FOR THE
CONOCOPHILLIPS SCHOOL OF GEOLOGY AND GEOPHYSICS

BY

_____
Dr. Matthew Pranter, Chair

_____
Dr. Roger Slatt

_____
Dr. Kurt Marfurt

Dedicated to my parents, my little sister and Uğur. Thank you for being the most wonderful family, making me feel like the luckiest girl in the whole world, giving me all the opportunities that I have, supporting and encouraging me no matter what and reminding me who I am and what I am capable of. Your existence is a blessing for me.

And a note to myself;

Stay gold.

Acknowledgment

This research was funded through the sponsors of the Reservoir Characterization and Modeling Laboratory and the Granite Wash Consortium: Chesapeake Energy, Devon Energy, QEP Resources, and SM Energy. I thank Devon Energy for providing the data for this study. I would also like to thank CGG and Schlumberger for their donation of Petrel and Hampson Russell software to the University of Oklahoma. I would like to acknowledge my advisor, Dr. Matthew Pranter, for his extensive guidance, constant support, time, advice, and direction throughout this project. I would also like to thank my committee members Dr. Kurt Marfurt and Dr. Roger Slatt for the advice and guidance. I would also like to thank John Mitchell for his help and input to this study. I would also like to thank my fellow graduate students: Burak Salantur, Gabriel Machado, Javier Tellez, Suriamin, Andreina Liborius, Niles Wethington, Yagmur Sumer, Oluwatobi Olorunsola and Richard Brito. I would also like to thank Juan Valdez and Yellowtail for keeping me awake and calm. Last but not least, I would like to thank my parents, for their unconditional love and endless support, to my little sister, just because her presence means world to me, to Uğur, for proving me once again there is no distance great enough that his love and support cannot travel, and to Ecenur, for always being there to encourage and comfort me.

Table of Contents

List of Tables

List of Figures

Abstract

The Desmoinesian Series Granite Wash at Buffalo Wallow Field represents deepwater deposits including slumps, channels, and submarine fan lobes that consist of six major lithofacies as mudstone, interbedded mudstone and sandstone, dark gray muddy sandstone, sandstone with mudstone clasts, fining upward sandstone, and laminated sandstone with mudstone. A combined artificial neural network and well-log cutoff approaches was followed to estimate lithology logs for non-cored wells with 84% accuracy. There are 10 stratigraphic intervals that, from top to bottom, include Marmaton, Caldwell, Cherokee, and Granite Wash A through G. These intervals are bounded by flooding surfaces which are capped by laterally extensive and distinctive mudstone layers. Furthermore, using well logs, a vertical proportion curve, and seismic data a sequence-stratigraphic framework was constructed and system tracts were interpreted that consist of five third-order regressive-transgressive cycles. Detailed 3-D lithological and effective porosity models that were constrained to cores, estimated lithology logs, porosity logs, spatial statistics from variography, and 3-D seismic data illustrate the stratigraphic variability in reservoir characteristics. Sandstone proportion within the study area decreases basinward from southwest to northeast. Moreover, while the sandstone proportion decreases stratigraphically upward, the muddy sandstone increases. In terms of sequence stratigraphy, lowstand and transgressive system tract deposits were combined and they contain a greater amount of sandstone and connectivity when compared to highstand deposits. Highstand deposit thickness increases vertically as well as the muddy sandstone occurrence, which represent more proximal deposits, thus suggesting that there is an overall progradation within the study area.

INTRODUCTION

The Desmoinesian Granite Wash deposits of the Buffalo Wallow Field area, in Wheeler and Hemphill counties, Texas (Figure 1, Appendix A) represent alluvial fans, fan deltas, proximal turbidites, and debris flows deposited during the formation of the Amarillo-Wichita uplift (Figure 2) (Dutton, 1985; Mitchell, 2011; Duggins, 2013, Holmes, 2015; Salantur, 2016). The deposits occur as several thousand feet of conglomerates, sandstones, and mudstones which form complex, low-permeability and generally low-porosity reservoirs. More basinward sandstones and mudstones were interpreted to have been deposited as medial- to distal turbidite and debris flows. Moreover, variation in the mineralogy, grain size, and sorting of these reservoirs causes significant challenges in subsurface interpretation and reservoir development (Sahl, 1970; Dutton, 1985; Dutton and Land, 1985; Mitchell, 2011; Gilman, 2012).

Dutton (1985) studied the Granite Wash of the Texas Panhandle, especially the Mobeetie Field in Wheeler County. Dutton (1985) used 37 wells with logs and a core to describe the mineralogy, lithology, depositional environment, and reservoir properties of the study area and stated that it is part of a fan-delta system and it is formed by terrigenous clastics that are interbedded with limestones, which both form the reservoirs. Duggins (2013), studied the Desmoinesian Granite Wash of the Texas Panhandle and western Oklahoma within Roger Mills, Custer, Washita, and Beckham counties in Oklahoma, and Wheeler, Hemphill, and Roberts counties in Texas. Using core, magnetic susceptibility, and spectral gamma-ray data Duggins (2013) interpreted the lithologies, lithofacies, sequence stratigraphy, and reservoir quality. Results showed

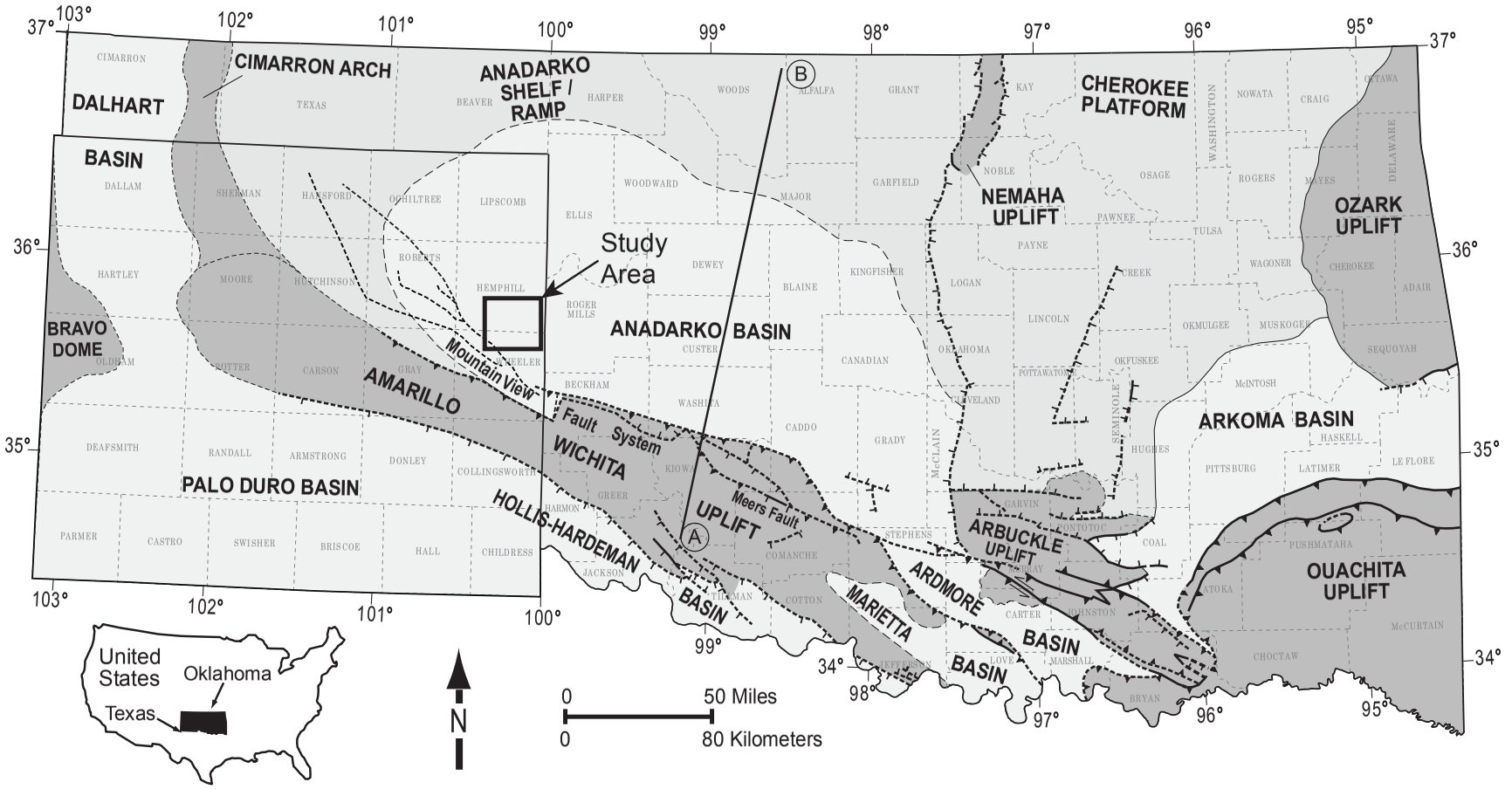

Figure 1. Regional basemap showing the geological provinces of Oklahoma and Texas. The study area resides in the deep Anadarko Basin just north of the Amarillo-Wichita Uplift Mountain View Fault System (modified from Johnson and Luza, 2008; Northcutt and Campbell, 1995; Campbell, et al., 1988; Dutton, 1984; McConnell, 1989; LoCriccho, 2012).

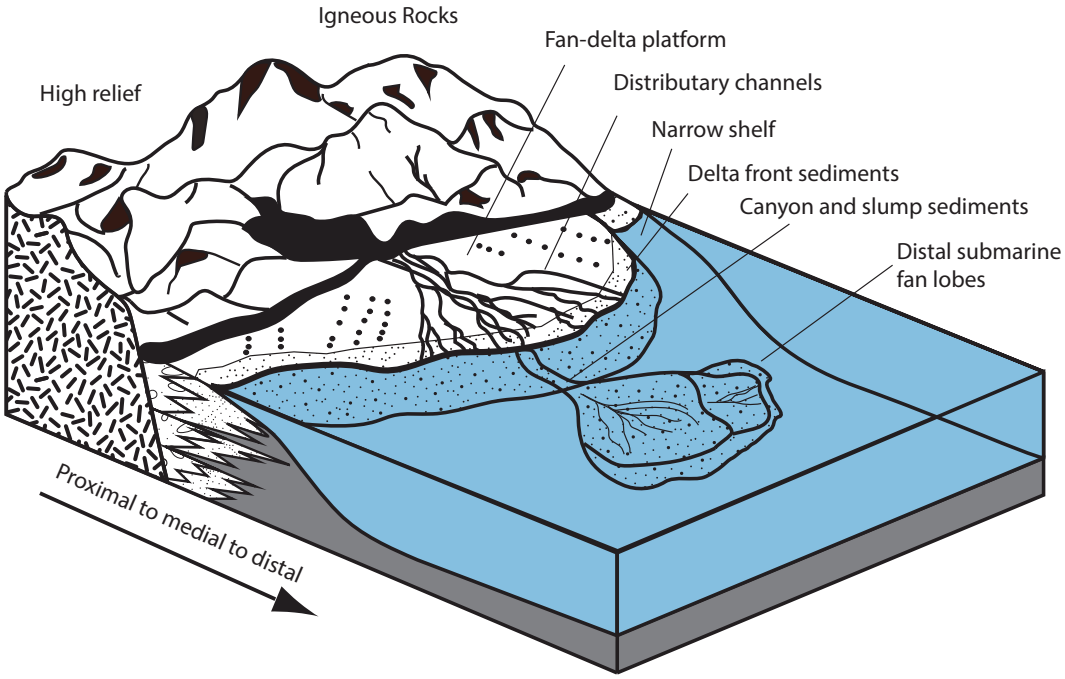

Figure 2. Schematic illustration of environments of deposition of the Granite Wash in deep Anadarko Basin. Sediments eroded from Amarillo-Wichita Mountains are deposited to the mountain front, mainly by fan-deltas. Fine - to coarse-grained submarine deposits transported by sediment gravity flows and slumps can be found in more distal areas. Coarse proximal deposits belong to alluvial fan and fan delta systems. Distal submarine fan lobes contain finer grains. (adapted from Bouma, 2000; Bruner and Smosna, 2000; from Salantur, 2016).

that the major depositional environment of the study area is fan-delta setting which mainly consists of fluvial, slump, debris flow, and deep-marine deposits. Holmes (2015) studied the stratigraphic architecture, facies characteristics, and distribution of deep-water deposits at Colony Granite Wash Field, Anadarko Basin, Oklahoma. Well-log, cores with porosity, permeability, density, and X-ray diffraction measurements, and four depth-converted interpreted seismic horizons were used. This study uses an artificial neural network approach for lithology and lithofacies and a combination of geostatistical methods including multiple-point statistics and sequential-indicator simulation to create 3-D models of the architectural elements. The depositional environment of the study area is marine that consist of conglomerates, sandstones and mudstones deposited as channels, levee, and overbank deposits, and upward-fining sandstone turbidite lobes. Salantur (2016) studied the lithology, stratigraphy, and reservoir characteristics of Marmaton Group Elk City Field in eastern Beckham and western Washita counties, Anadarko Basin, Oklahoma. Salantur (2016) also used the artificial neural network approach for lithology estimation and sequential-indicator simulation in order to map the spatial distribution and analyze static reservoir connectivity. Based on well-log and core data, the depositional environment is interpreted to be fan-delta that consists of conglomerates and sandstones. Moreover, Karis (2015), studied the Marmaton Group, located in Beckham County, Oklahoma and Wheeler County, Texas in terms of lithology, stratigraphy and reservoir characteristics. In this study, wire-line logs and three cored wells were used to explore key lithologies and combination of principal component analysis combined and cluster analysis used for estimating lithologies in the non-cored wells. In order to model the spatial

distribution of lithologies, sequential-indicator simulation was used whereas for petrophysical properties, which were calculated by well-logs, sequential-gaussian simulation was used. Karis (2015), interpreted this area as terrestrial to shallow marine that includes conglomerates, sandstones, and shales as major lithologies. Mitchell (2011) described a core from southeast Wheeler County as sheet sandstones deposited as proximal to distal turbidite lobes. Mitchell (2011) found these deposits to thin to the northeast and grade into siltstone and shale in Hemphill and Roger Mills Counties.

Granite Wash deposits consist of granite-, quartz-, and feldspar-rich deposits that derived from pre-Pennsylvanian sedimentary rocks and Cambrian igneous rocks and these are generally referred to as arkosic sandstone and conglomerate (Sahl, 1970; Dutton, 1985; Dutton and Land, 1985; Mitchell, 2011). The potassium feldspar content in the rock matrix results in high gamma-ray values in Granite Wash deposits sourced by granitic terranes while gabbroic sourced regions have higher iron and magnesium content which causes low resistivity values (Mitchell, 2011; Gilman, 2012).

In order to define stratigraphy of Granite Wash laterally continuous shale breaks which represent regional flooding surfaces were used (Mitchell, 2011; LoCricchio, 2012; Holmes, 2015; Karis, 2015; Salantur, 2016). LoCricchio (2014) studied the Desmoinesian Granite Wash deposits across the Anadarko Basin. Using approximately 30,000 wells, LoCricchio (2012) defined 11 zones separated by regionally correlative flooding surfaces and mapped them throughout the study area. Mitchell (2011) used regionally correlative flooding surfaces for the stratigraphic intervals of Granite Wash and divided Marmaton Group into 7 zones and divided Cherokee group into 5 zones as

Upper Skinner Shale, Upper Skinner Wash, Lower Skinner Shale, Lower Skinner Wash and Redfork. Moreover, Mitchell (2015) constructed a translation chart for Texas to Oklahoma nomenclature for Granite Wash in order to resolve inadequate correlation and confusion between two states. Gavidia (2012) studied Granite Wash at Wheeler and Hemphill counties in terms of seismic geomorphology and reservoir characteristics using the 3-D seismic attributes and poststack seismic inversion. Using a 3-D seismic survey and 53 wells, he defined 9 sesimic horizons of Desmoinesian Granite Wash as Caldwell, Cherokee, and Granite Wash A through G.

Porosity and permeability values vary considerably throughout the area. Duggins (2013) conducted tests of porosity and permeability and the best quality reservoir rock ranged from 11-29% for porosity and 0.1-0.8 md for permeability. Dutton (1985) stated that the porosity of the Granite Wash based on thin-section porosity in the sandstones varies from 0-14% and porosity from core plugs up to 21%. Horizontal permeability ranges from less than 0.1 mD to 1,450 mD. Also average porosity is calculated to be approximately 6% and permeability is generally below 0.1 mD (Mitchell, 2011).

Three-dimensional seismic attributes of the Pennsylvanian Granite Wash were also studied by Batista (2010) and Gavidia (2012). Batista (2010) used coherent energy, most positive and most negative curvature, and Sobel filter similarity to delineate Granite Wash deposits using a 3-D seismic survey and 18 wells from Pennsylvanian Granite Wash of the Dalhart Basin, Texas and an acoustic impedance volume to evaluate reservoir heterogeneity. Gavidia (2012) used seismic similarity and energy-weighted coherent- amplitude gradient to delineate the geomorphology of the Buffalo Wallow

Granite Wash reservoirs. Gavidia (2012) used an acoustic impedance (AI) volume to map the reservoir heterogeneity and it is found that the sandstones with relative high impedance are typical of reservoirs in the study area.

Although there are numerous studies related to the lithologies, depositional processes and petrophysical properties of the Desmoinesian Series Granite Wash deposits for different regions across the Anadarko Basin, the complexity of the Granite Wash deposits is still not fully understood. In order to further expand on the complexity and heterogeneities of this play, this study focuses on the Desmoinesian Series of the Granite Wash in the Wheeler and Hemphill counties, Texas (Figure 3). In this study, the key lithologies and lithofacies of the Desmoinesian Series and their corresponding well-log responses were evaluated and the depositional processes were interpreted with 2 cores and log data from 68 wells. A stratigraphic framework was established based on regional flooding surfaces from well logs and 3-D seismic data, total and effective porosities were calculated using well logs in order to evaluate the spatial distribution of the porosity. An acoustic impedance constrained 3-D lithology model was constructed utilizing artificial neural network (ANN) based lithology logs. The spatial distribution and connectivity of the lithologies were mapped and their relation to the stratigraphic framework was established.

The study area (Figure 3) covers 78 mi^2 (202 km^2). Three-dimensional seismic data cover 28 mi^2 (72 km^2) of the study area. An acoustic impedance volume, previously calculated for the 3-D seismic survey by Gavidia (2012), is also utilized. Sixty-eight wells with digital wireline logs and two wells with conventional core were also included in the data set. The logs were sorted by quality and data coverage and

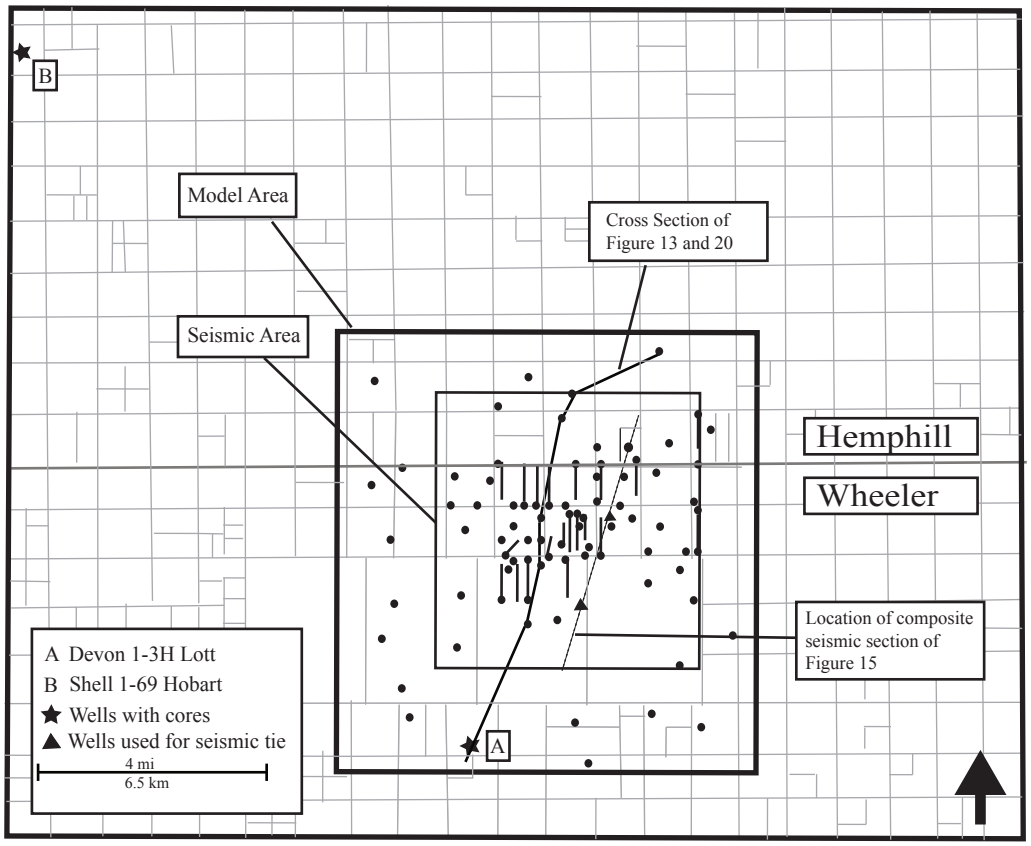

Figure 3. Detailed basemap of study area. There are 68 wells with wire-line logs. See Figure 1 for the location of the study area.

aliased by type for gamma ray (GR), neutron porosity (NPHI), density porosity (DPHI), deep resistivity (Res), sonic and spontaneous potential. Cored wells of the study area are Devon 1-3H Lott and Shell 1-69 Hobart. The Devon 1-3H Lott core is 345 ft (105 m) and corresponds to Caldwell, Cherokee, and Granite Wash A intervals and the Shell 1-69 Hobart well is 113 ft (34 m) and corresponds to Granite Wash B interval.

GEOLOGICAL SETTING

The Anadarko Basin of the southern Mid-continent is the deepest Phanerozoic sedimentary basin within the North American craton and is also one of the most productive basins in terms of hydrocarbons in the continental United States (Perry, 1989; Ball et al., 1991) (Figures 1 and 4). Locally it contains more than 40,000 ft (12,000 m) of Cambrian though Permian sediments (Ham and Wilson, 1967) that mostly were deposited in shallow-water environments. The Anadarko Basin is bounded on the east by the Nemaha ridge, on the north and west by shelf areas, and on the south by the Amarillo-Wichita uplift (Evans, 1987). The Anadarko Basin has a complex structural history that can be divided into four periods according to Perry (1989): (1) Precambrian crustal consolidation, (2) Late Precambrian to Middle Cambrian aulacogen development, (3) Cambrian through Early Mississippian development of the southern Oklahoma trough, and (4) Late Paleozoic tectonism associated with development of the Anadarko Basin on the northwestern flank of the trough. These events indicate that there is a trend of crustal weakness at an orientation of 60° NW that affects the entire subsequent tectonic history of the area (Perry, 1989; Gilbert, 1992).

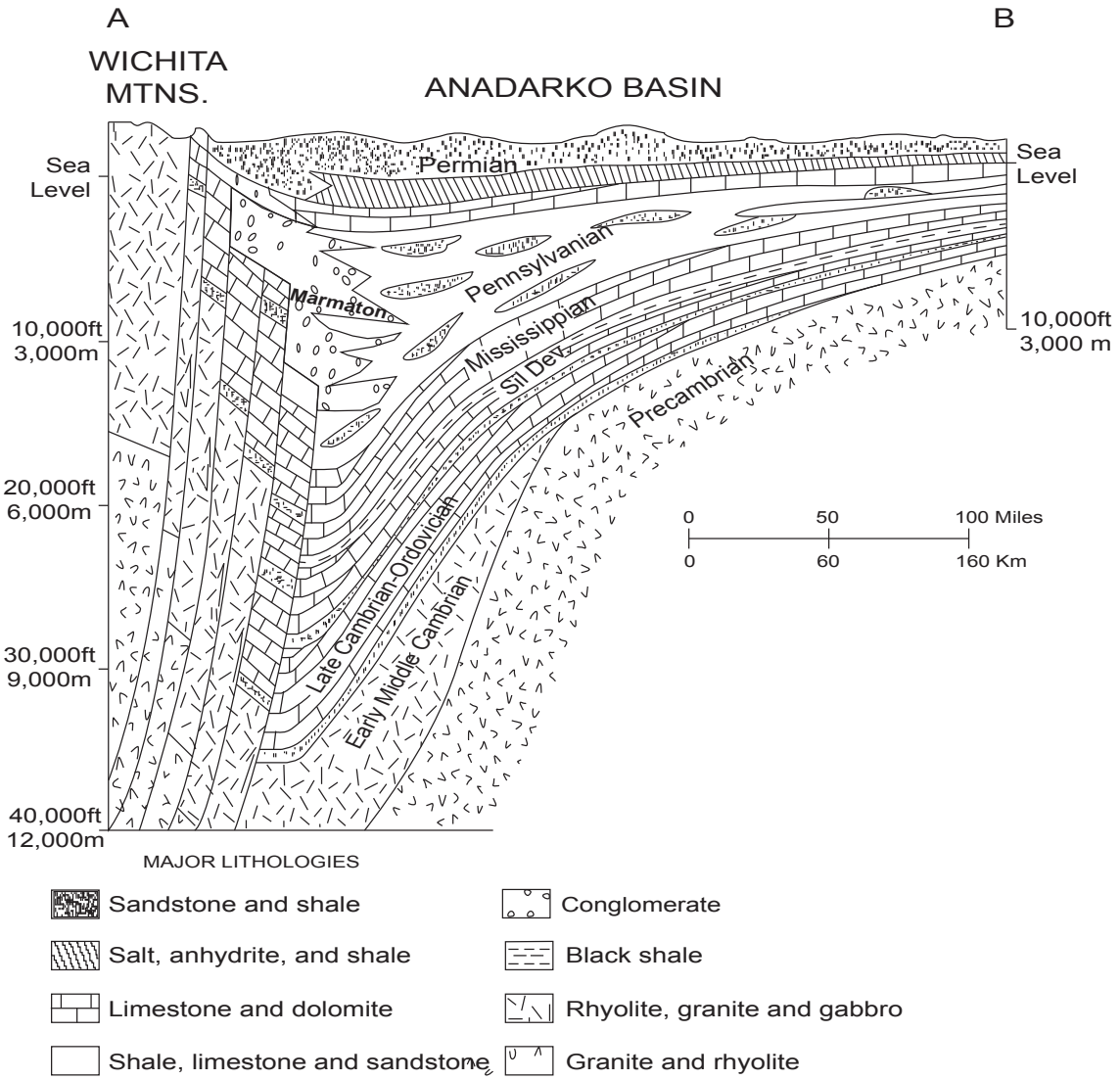

Figure 4. SW to NE structural cross section of the Anadarko Basin. With the change in the stress regime in Early Pennsylvanian, the materials of the Amarillo - Wichita uplift started to erode and were deposited in the basin overlying the igneous rocks and carbonates. Granite Wash deposits pinch out towards north and they are transitional with the sediments that are sourced from the north (modified from unpublished H.G. Davis; K.S. Johnson, 1989). See Figure 1 for the location of the cross section.

The Amarillo-Wichita uplift was the main source area for the Granite Wash (Dutton, 1985). And these deposits consist of conglomerates, sandstones, and mudstones derived from the adjacent Amarillo-Wichita uplift. Granite Wash sediments are thought to have been deposited as alluvial fans, fan deltas, proximal turbidites, and debris flows. The lithologic components of the Anadarko Basin Granite Wash commonly include granite, rhyolite, gabbro, dolomite, limestone, and chert. These were derived from bedrock source areas that included pre-Pennsylvanian sedimentary rocks as well as Cambrian igneous rocks (Dutton, 1985; Mitchell, 2011). Subsidence in the southern Anadarko Basin apparently occurred at a rate comparable to sedimentation, thus allowing thick accumulations of shallow-marine and non-marine sediment to develop adjacent to the Amarillo-Wichita uplift. The greatest volume of Granite Wash was deposited during the Desmoinesian, which is evidence for the timing of the major movement of the Wichita-Amarillo uplift which occurred during this time (Dutton, 1984).

The Pennsylvanian Granite Wash is divided into five series (Figure 5): Morrowan, Atokan, Desmoinesian, Missourian, and Virgilian. The Morrowan Series is represented by an initial flood of sediments shed northward off of the Amarillo-Wichita uplift into the Anadarko Basin as the uplift initiated during that time and Mississippian cherty carbonates were brought to the surface (Mitchell, 2011). The Morrowan Series is a predominantly clastic, prolific hydrocarbon-producing unit in the Lower Pennsylvanian. The sediments of the Morrowan interval are dominantly shales with discontinuous sandstones and limestones (Al-Shaieb et al., 1994). During Atokan time, uplifting was still occurring and the Atokan Series is represented by a thick wedge of clastic sediments: arkosic sandstone and conglomerates adjacent to the uplift that thin to

SYSTEM	SERIES	GROUP	UNIT	A	B
PENNSYLVANIAN	VIRGILIAN	Shawnee/Cisco	Shawnee Wash Heebner Sh		
		Douglas/Cisco	Haskell Sh Tonkawa Ss		
	MISSOURIAN	Lansing/Hoxbar	Cottage Grove Wash		
		Kansas City/Hoxbar	Hoxbar Wash/Shale Hogshooter Wash Checkerboard Wash Cleveland Wash		
	DESMOINESIAN	Marmaton (Glover/Big Lime/ Oswego)	Marmaton Wash Caldwell Cherokee GWA GWB GWC	Marmaton Wash Marmaton A Marmaton B Marmaton C Marmaton D Marmaton E Marmaton F	Marmaton Wash Britt GWB GWC GWD GWE GWF
		Cherokee (Skinner/Pink Lime/ Red Fork)	GWD GWE GWF GWG	Upper Skinner Wash Lower Skinner Wash	GWG GWH GWI GWJ
	ATOKAN	Atoka	Atoka Wash 13 Finger Ls		
	MORROWAN	Morrow	Upper Morrow Lower Morrow		

Figure 5. Stratigraphic nomenclature for the Granite Wash for the Eastern Texas Panhandle Anadarko Basin. As Desmoinesian Granite Wash has different nomenclature in different states and petroleum companies, the guide A (modified from Mitchell, 2011) and B (modified from LoCricchio, 2012) can be used to correlate between Texas and Oklahoma Granite Wash intervals.

the northeast. The Desmoinesian Series contain interbedded arkosic sandstones and conglomerates that thin into shales in the northeastern direction. It is subdivided into the Cherokee Group and is overlain by the Marmaton Group (Al-Shaieb et al., 1994, Mitchell, 2011). During the Late Pennsylvanian, the Ouachita Mountains and the Wichita-Amarillo uplift were a major sediment source for the Missourian-Virgilian sediments. Extensive clastic sediments were deposited during early Missourian time. During periods of low clastic influx, carbonates were deposited in the shelf areas. Deposition of carbonate units within the thicker intervals of clastic sediments was characteristic of these sequences (Al-Shaieb et al., 1994).

The main focus of this study is the Desmoinesian Series of Wheeler and Hemphill counties, Texas and uses a modification of the stratigraphic terminology for the eastern Texas Panhandle portion of the Anadarko Basin as presented by Mitchell (2011) (Figure 5). This region was filled with proximal to distal submarine fans that consists of mudstones and sandstones that are mainly arkosic in composition due to the presence of intrusive rocks caused by the uplift. These intervals were punctuated by distinctive radioactive mudstones in the region (Mitchell, 2011). Using these mudstones, Mitchell defined nine zones of Desmoinesian Granite Wash in Oklahoma and Texas, for Marmaton Group: Marmaton Wash, Marmaton A through F, and for the Cherokee Group: Upper Skinner Wash and Lower Skinner Wash. While LoCricchio (2012) interpreted 11 zones within the same age interval as Top Marmaton Wash, Britt, and GWB through GWJ. Their correspondence to each other and to the stratigraphic zonation used in this study is shown in Figure 5. Within the scope of this study, ten intervals were defined using laterally extensive and correlative mudstones as,

Marmaton, Caldwell, Cherokee, Granite Wash A (GWA), Granite Wash B (GWB), Granite Wash C (GWC), Granite Wash D (GWD), Granite Wash E (GWE), Granite Wash F (GWF), and Granite Wash G (GWG) (Figures 6 and 7).

METHODS

Lithologies and Lithofacies

Desmoinesian Series lithologies and lithofacies were examined and interpreted based on detailed core descriptions of two cores from the Shell 1-69 Hobart and Devon 1-3H Lott wells (see Figure 3 for locations). Descriptions include lithology, color, grain size, reaction to HCL, sorting, rounding, sedimentary structures, and additional remarks (Appendix B). Both cored intervals are almost completely continuous. The Shell 1-69 Hobart core is 113 ft (34 m) thick (Figure 6) and corresponds to Granite Wash B interval. The Devon 1-3H Lott core is 345 ft (105 m) thick (Figure 7) and corresponds to Caldwell, Cherokee, and Granite Wash A intervals.

Lithology Estimation

There are multiple methods for electrofacies estimation of lithology including K-means, artificial neural network (ANN) analysis, and well-log cutoffs. In this study, the well-log cutoff and ANN methods were used. The well-log cutoff method assigns lithologies for intervals of specific log values as determined from core lithologies and comparison with distinct well-log responses. For example, a specific gamma-ray value may be used to separate sandstones from mudstones as greater values indicate mudstones and smaller values indicate sandstones. An ANN is a more complex

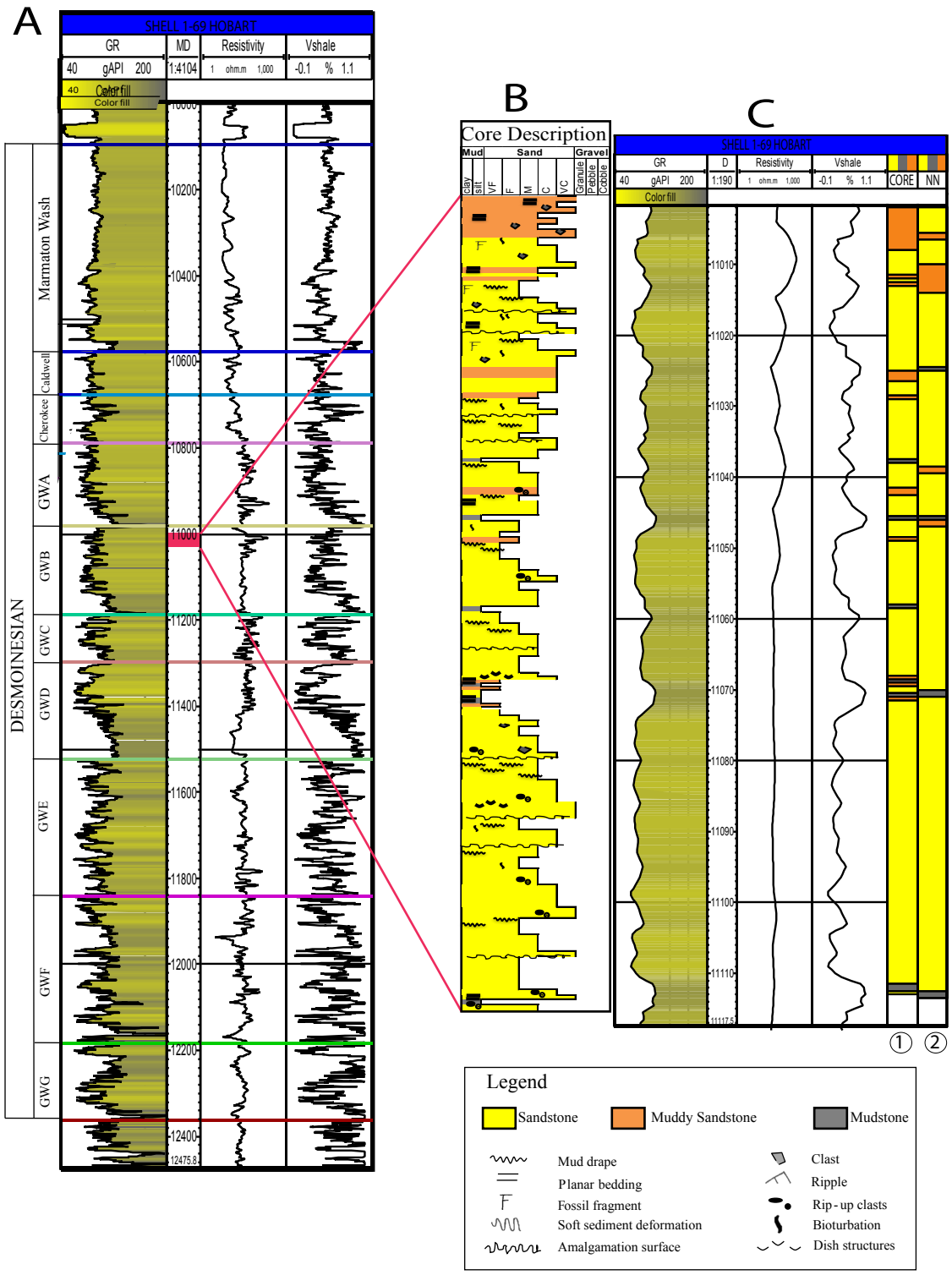
A
SHELL 1-69 HOBART
GR
MD
Resistivity
Vshale
40 gAPI 200
1:4104
1 ohm.m 1,000
-0.1 % 1.1
Color fill
DESMOINESIAN
Marmaton Wash
Caldwell
Cherokee
GWA
GWB
GWC
GWD
GWE
GWF
GWG
10200
10400
10600
10800
11000
11200
11400
11600
11800
12000
12200
12400
12475.8
B
Core Description
Mud
Sand
Gravel
clay
silt
VF
F
M
C
VC
Granule
Pebble
Cobble
C
SHELL 1-69 HOBART
GR
D
Resistivity
Vshale
40 gAPI 200
1:190
1 ohm.m 1,000
-0.1 % 1.1
CORE
NN
Color fill
11010
11020
11030
11040
11050
11060
11070
11080
11090
11100
11110
11117.5
1
2
Legend
Sandstone
Muddy Sandstone
Mudstone
Mud drape
Planar bedding
Fossil fragment
Soft sediment deformation
Amalgamation surface
Clast
Ripple
Rip-up clasts
Bioturbation
Dish structures

Figure 6. A) Gamma-ray (GR), resistivity and Vshale well-log responses for the cored well Shell 1-69 Hobart. Nine zones are separated by flooding surfaces. Red bar indicates the cored interval. B) Schematic core description from well Shell 1-69 Hobart C) Gamma-ray (GR), Resistivity and Vshale well-log responses for the cored interval. Sandstones have higher resistivity values relative to other lithologies. Mudstones have higher GR and Vshale values whereas sandstones have lower values. Mudstones have moderate GR and Vshale values. 1) Lithologies observed in the core. 2) Estimated lithology log by combining Artificial Neural Network (ANN) analysis and gamma-ray cut-off values.

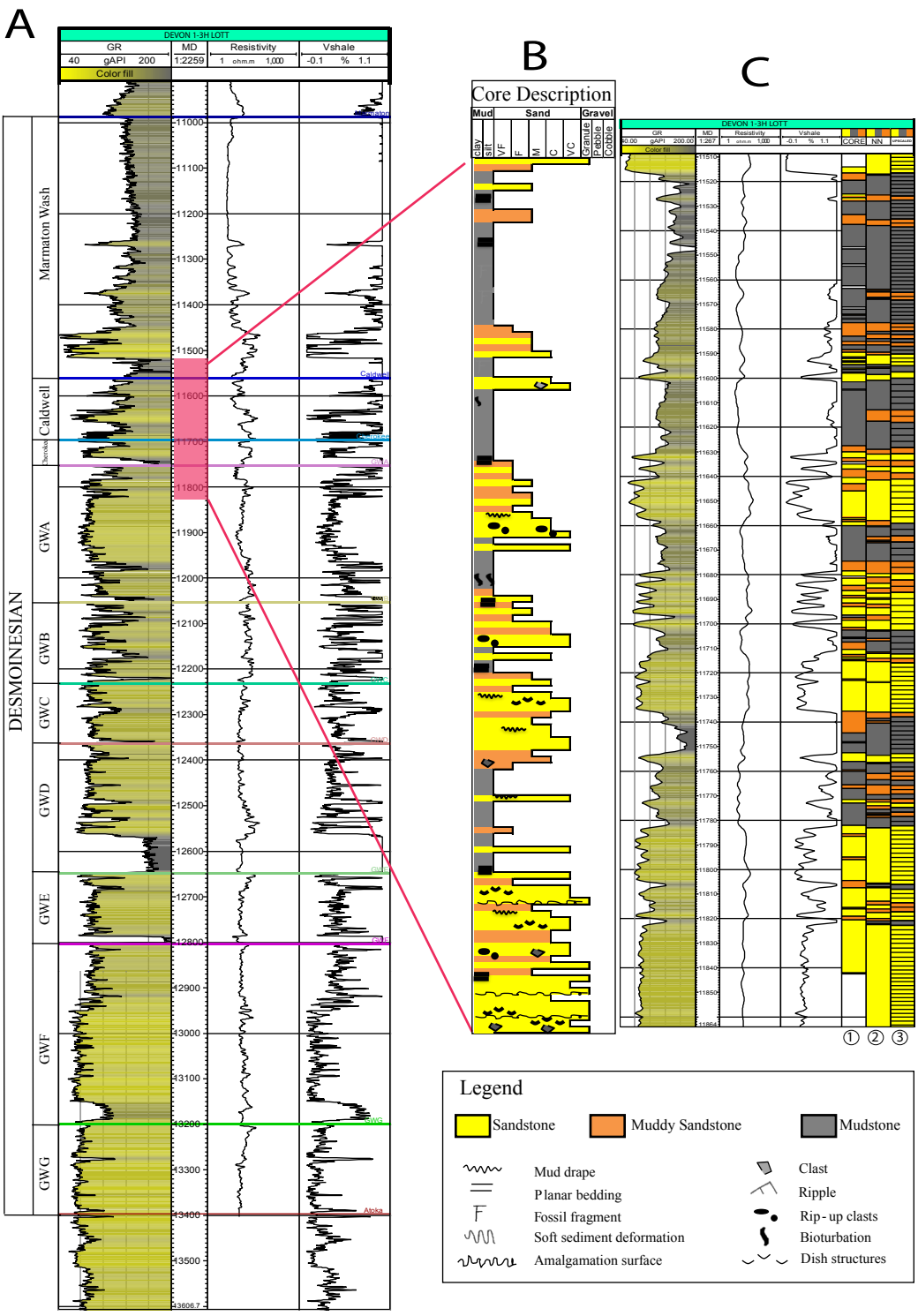
A
B
C
DEVON 1-3H LOTT
GR
MD
Resistivity
Vshale
Color fill
Core Description
Mud
Sand
Gravel
Clay
Silt
VF
F
M
C
VC
Granule
Pebble
Cobble
CORE
NN
DESMOINESIAN
Marmaton Wash
Caldwell
GWA
GWB
GWC
GWD
GWE
GWF
GWG
Atoka
Legend
Sandstone
Muddy Sandstone
Mudstone
Mud drape
Planar bedding
Fossil fragment
Soft sediment deformation
Amalgamation surface
Clast
Ripple
Rip-up clasts
Bioturbation
Dish structures

Figure 7. Type log for the Granite Wash Buffalo Wallow Field. A) Gamma-ray (GR), resistivity and Vshale well log responses for the cored well Devon 1-3H Lott. Red bar indicates the cored interval. B) Schematic core description from well C) Gamma-ray (GR), Resistivity and Vshale well logs for the cored interval. Sandstones have higher resistivity values relative to other lithologies. Mudstones have higher GR and Vshale values whereas sandstones have lower values. Mudstones have moderate GR and Vshale values. 1) Lithologies observed in the core. 2) Estimated lithology log by combining Artificial Neural Network (ANN) analysis, and gamma-ray cutoff. 3) Upscaled lithology logs used to constrain 3-D lithology model. Measured depth (MD) is in ft.

approach as it is able to integrate and recombine multiple types of inputs (Brouwer et al., 2011). The ANN system is a computational method which is inspired by the brain and its ability to learn by example and recognize patterns (Iloghalu and Azikiwe, 2003; Kumar and Kishore, 2006; Anggraini and Puspa, 2008; Brouwer et al., 2011). There are two types of neural networks, unsupervised and supervised. The unsupervised network does not use any constraints of interpreted data and only performs classification based on given input responses. In contrast, a supervised network uses interpreted data to recognize the patterns. This approach can also be utilized in geology for geological interpretation of lithologies, lithofacies, or architectural elements by using well-logs, core data or seismic attributes as inputs (Brouwer et al. 2011). The ANN is a multilayer system, including an input layer, output layer, and hidden layer(s). Each of these layers contains a number of nodes and these nodes are connected to the previous layer by simple weighted links. Each node multiplies its specific input value by the corresponding weight and then sums all the weighted inputs (Kumar and Kishore, 2006). The sum of the weighted inputs are then used to compute the output. The network then processes and compares the calculated output against the target output. Random weight connections are used at the beginning, and then the network adjusts these iteratively to attain the target output and minimize the errors (Anggraini and Puspa, 2008).

For this study, different sets of well logs were evaluated for the supervised ANN approach. These include the gamma-ray, resistivity, and Vshale. The Vshale log is calculated using gamma-ray method:

$$V_{shale} = (GR_{log} - GR_{sand}) / (GR_{shale} - GR_{sand}).$$

With supervised neural network analysis, the desired portion of the well-log responses were trained with the corresponding lithologies that were obtained from cores so that the network learns the relation between the selected well-log signatures and the corresponding lithology. The remaining core and well-log data were used in testing the result of the neural network. After obtaining the neural-network result for the cored well, the algorithm was tested by a confusion matrix to measure the overall accuracy. Construction of the confusion matrix is based on the number of correctly predicted cells that are divided by the total number of cells. In order to measure the accuracy of an individual lithology prediction, a confusion matrix was used in which the number of correctly predicted cells of a particular lithology was divided by the total number of actual samples that exist for that lithology. Use of this confusion matrix is commonly applied when there is a special emphasis on the accuracy of individual class predictions (Janssen and van der Wel, 1994; Foody, 2002, Allen, 2013). After yielding the desired accuracies for each lithology, the algorithm was applied to all of the non-cored wells that includes the set of gamma-ray, resistivity, and Vshale logs. In order to refine and constrain the neural network results, an additional gamma-ray cutoff was found to be necessary. Thus, a gamma-ray value was decided by comparing the well-log signatures and core lithologies. This cut-off value was applied to the wells for better classification between the lithologies.

Depositional Environment and Stratigraphy

In order to interpret the depositional environment of the Desmoinesian Series Granite Wash deposits, cores and well logs were used. Detailed core descriptions and lithology and sedimentary structure information gathered from the cores defining grain-size changes, sorting, rounding, bioturbation styles, and fossils, and their vertical relation to each other were evaluated and the depositional environment was interpreted. Furthermore, well-log signatures of the lithologies were evaluated in terms of their character, shape and correlation throughout the study area in order to interpret the depositional environment of the study area.

In order to interpret the stratigraphy of the Desmoinesian Series Granite Wash, cores, the ANN-derived lithology log, vertical proportion curve, well logs, and a time-migrated seismic survey were used. Well logs from 68 wells with the following logs: gamma ray, resistivity, density porosity, neutron porosity, sonic, spontaneous potential and ANN-derived lithology logs were used to establish cross sections for stratigraphic correlation (locations shown in Figure 3). Wells with sonic logs (N=2, locations shown in Figure 3) were tied to the migrated seismic volume using Hampson and Russell software (Appendix C). The seismic reflectors that correspond to the Desmoinesian Group intervals were interpreted, which are Marmaton, Oswego, GWA, GWE and GWG. Due to limited seismic resolution Caldwell, Cherokee, GWB, GWC, GWD, GWF and Atoka zones were solely interpreted from well data.

Using the formation tops of the Desmoineasian Granite Wash interpreted in the wells and horizons interpreted on the seismic, an average velocity model was generated.

The average velocity is based on the thicknesses from well logs and seismic data. The velocity model was used to depth convert the seismic horizons. As the model area is larger than the seismic area, in order to obtain surfaces for the whole model area, formation top data that were picked on the wells and the depth-converted seismic surfaces were combined for each zone. In order to do this, seismic surfaces were converted to points and appended with related formation top data points from wells. Using all data points for each zone a new surface was created for the whole model area per zone. While doing this, when seismic data is present both seismic and well data were honored, and when absent only well data were used. Thus, surfaces for each zone honor well and seismic data where available.

Also, surfaces for the formation tops that lack seismic horizons were developed by creating a surface that is conformable to the upper and lower seismic surfaces while still honoring the formation top data (from wells) of that interval. In this manner, the new surface honors both seismic and well data.

The depth surfaces for the Desmoinesian Series Granite Wash intervals were used as inputs to develop a 3-D model grid. The lithology logs were upscaled in a way that the lithology that exists in higher proportion within each cell was assigned as the upscaled cell lithology. The upscaled lithology logs were used to generate a vertical proportion curve in order to define the trends of lithologies associated with each zone. A vertical proportion curve is a vertical, 1-D trend (values between 0 and 1.0) that represents the variability in the percentage of lithology stratigraphically or by model

layer based on the upscaled lithology logs. The vertical proportion curve and well logs were used to interpret the sequence stratigraphy.

The ideal depositional package for one depositional sequence consists of lowstand, transgressive, and highstand systems tracts, formed in response to relative sea-level changes. Most deepwater sediments were deposited as the lowstand systems tract, although they can develop in other systems tracts depending on tectonism and sediment supply (Weimer and Slatt, 2007). There are two important surfaces in deepwater systems which are the maximum flooding surfaces and sequence boundaries. Maximum flooding surfaces (mfs) represent the greatest transgression of shallow-marine facies after relative rise in the sea level while sequence boundaries are significant erosional unconformities or their correlative conformities (Ross and Ross, 1988; Haq and Schutter, 2008). Another important surface for sequence stratigraphy is the transgressive surface (TS) which marks when the accommodation space is greater than the rate of sediment supply. The TS forms the base of the retrogradational parasequence stacking patterns of the transgressive systems tract but it might not extend into deepwater settings (Vail and Wornart, 1991). Moreover, during the transgressive and highstand systems tracts reduced sediment input causes little deposition in the deep basin causing the TST to be represented by a thin mudstone layer and the HST to be represented either by a thin mudstone layer as well or a thin package of progradational deposits (Vail and Wornart, 1991, Weimer and Slatt, 2006). From the vertical proportion curve and well logs, lithology proportions and their vertical arrangements were evaluated. Moreover distinctive mudstone layers that are capping flooding surfaces were interpreted on the vertical proportion curve as well as system tracts.

Spatial Distribution of Lithology and Porosity

In order to evaluate the spatial distribution of lithology, a 3-D lithology model of Desmoinesian Series Granite Wash deposits was generated for the study area. The model was constrained to the upscaled ANN-derived lithology logs, the histogram of lithology percentages, sandstone probability maps for each zone calculated from the acoustic impedance (AI) volume, vertical and horizontal variogram ranges and azimuths (by zone), the vertical lithology proportion curves for each zone, and seismic data. To map lithology, sequential-indicator simulation (SIS) was used. SIS is a cell-based (variogram-based) stochastic method that is commonly used for modeling facies or other rock types (Pyrcz and Deutsch, 2014). SIS divides geology into a series of cells. By visiting each cell sequentially, SIS assigns geologic and petrophysical properties to cells using geostatistics. Then, by using known data and trends, SIS predicts the geological properties where data are absent based mathematical and spatial relationships between data points.

For sandstone probability map generation, an acoustic impedance volume calculated by Gavidia (2012) was used. The relation between sandstone lithology and acoustic impedance values was confirmed on a cross plot of neutron-porosity versus AI and it was determined that higher acoustic impedance values are associated with sandstone lithology (Figure 8). Average AI maps were generated for each zone, and depending on the correlation between AI and sandstone occurrence, two AI cut-off values for each zone were determined from the cross plot of porosity vs AI where greater cut-off values were assigned to a sandstone probability of 1 and smaller cut-off

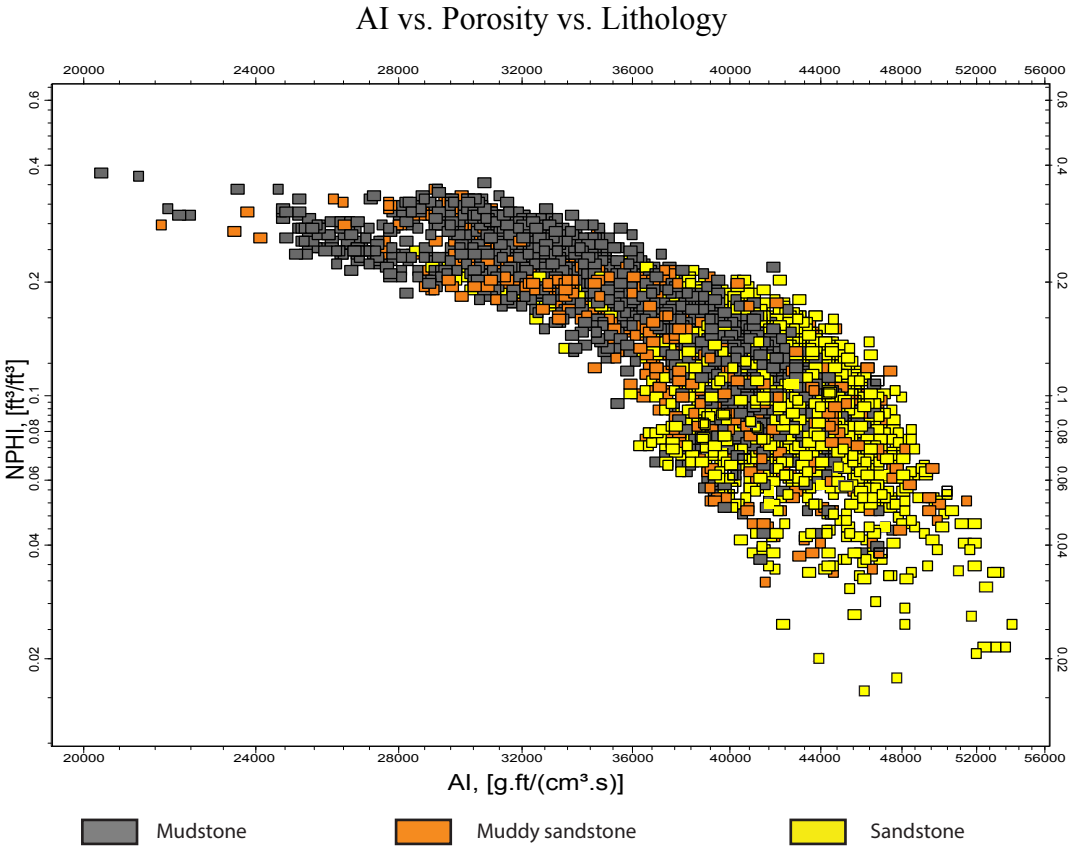

Figure 8. Crossplot of acoustic impedance versus porosity (as calculated from the logs) and color coded by lithology showing the relatively high impedance values are associated with sandstone. Because AI increases with depth, an average AI attribute map is generated for each zone and different cutoff values were determined to create sandstone probability maps.

values were assigned to a sandstone probability of 0. These cut-off values were then applied to the AI maps to generate the probability maps for each zone (Appendix D). As the model area is larger than the seismic volume, sandstone percentages of the wells that exist between the seismic and model area boundaries were used to complete the sandstone probability maps of each zone.

Variogram maps (polar plots) and vertical and horizontal variograms were calculated by zone and for each lithology, and they were used to determine the azimuth values for the directions of major continuity and the major and minor ranges of the lithologies (Appendix E). For sandstone lithology, as it is in correlation with AI, variogram maps were obtained from average AI maps of each zone in order to determine the azimuth values. For other lithologies, variogram maps were obtained from the lithology log.

To map effective porosity, sequential-gaussian simulation (SGS) was performed. In order to calculate the effective porosity, a total porosity (Φ_t) log was calculated using neutron porosity (NPHI) and density porosity (DPHI) logs in the following equation:

$$\Phi_t = \sqrt{(NPHI^2 + DPHI^2)}$$

Using total porosity and previously calculated Vshale logs the effective porosity (Φ_e) log was calculated for each well using equation below:

$$\Phi_e = \Phi_t - (Vshale * \Phi_{sh})$$

Calculated effective porosity logs were upscaled using the arithmetic average method in which the average of the values corresponding to each cell was assigned as the upscaled effective porosity. Vertical and horizontal ranges were estimated using vertical and horizontal variograms for effective porosity (Appendix F). The 3-D lithology model is the major constraint to map effective porosity which also honors the upscaled effective porosity logs and the variograms parameters.

Static connectivity analysis was performed using the 3-D lithology model and was calculated by dividing the connected volume of the desired lithology to wells by the bulk volume of the same lithology. This calculation gives the static connectivity of the target lithologies as a percentage. All of the wells within the model area were used for assessing connectivity. Also, porosity was used as a filter for the purpose of refining the connected volume of lithologies with porosity greater than 10%. Using porosity as a filter enabled evaluating and visualizing connected volumes of target reservoir lithologies with the desired porosity percentage. Furthermore, comparing lithologies for each zone in terms of connectivity and porosity provided better understanding of the relationship between reservoir characteristics and the sequence stratigraphic framework.

RESULTS

Lithologies and Lithofacies

Lithologies and lithofacies of Desmoinesian Series Granite Wash deposits were interpreted through core descriptions that include lithology, color, grain size, sorting, rounding, sedimentary structures, and additional remarks. Based on detailed core

descriptions, 3 lithologies were recognized; sandstone, muddy sandstone, and mudstone, which are divided into 6 lithofacies: 1) mudstone, 2) interbedded mudstone and sandstone, 3) dark gray muddy sandstone, 4) sandstone with mudstone clasts, 5) fining upward sandstone, and 6) laminated sandstone with mudstone (Figure 9 and Table 1).

Mudstone

Definition

Mudstone lithofacies consists of well-sorted mud, clay, and minor amounts of silt that are very dark gray to black in color. This lithofacies can be structureless or locally laminated and fissile. Bivalve, foraminifera, and ammonite fossil fragments are present locally. Few pyritizied fossils are present as well as pyrite minerals and nodules. Also, this lithofacies can react with HCL suggesting carbonate content. Bioturbation is not observed.

Interpretation

Mudstone lithofacies was interpreted to be deposited from the suspended material during very low energy conditions where the sediment influx is low. Lack of bioturbation and presence of pyrite indicates deep marine conditions.

Interbedded sandstone and mudstone

Definition

Interbedded sandstone and mudstone lithofacies feature alternating thin laminations of mudstone, muddy sandstone, and sandstone which are generally medium-grained and gray in color. This lithofacies features common convolute bedding and slumping. Mud and calcite clasts are embedded within the interbedded section. Some fossil fragments

are present within the mudstone layers. This lithofacies also includes mudstone clasts and occasional bioturbation.

Interpretation

This lithofacies was interpreted to be deposited in fluctuating energy conditions due to the change in the grain size. Moreover, convolute beddings were interpreted to be soft-sediment deformation caused by gravity flow and sudden deposition and mudstone clasts were decided to be rip-up clasts that were ripped up by a subsequent turbidity current which both require higher energy conditions and indicate a deep-marine setting.

Dark gray muddy sandstone

Definition

This lithofacies consists of poorly sorted medium- to coarse-grained sandstones which are dark gray in color. Convolute bedding is common, with occasional fossils. Pyrite is also present but rare. It typically alternates with thin mudstone layers or mudstone drapes which are generally wavy or convoluted. Local white to grey, sub-angular to sub-rounded, granule-to-pebble-sized clasts are present. Few bioturbation is observed.

Interpretation

Dark gray muddy sandstone lithofacies was interpreted to be deposited on or closer to the slope as debris flow deposits. Transportation mechanism is slumping which causes convoluted beds and soft-sediment deformations. Moreover, size and rounding of the clasts and frequency of soft-sediment deformation suggests high energy conditions and rapid deposition.

Sandstone with mudstone clasts

Definition

This lithofacies does not show any bedding and its grain size ranges from medium to very coarse sandstone. It is greenish-gray in color and moderately- to well-sorted. It does not show any vertical grading. Occasional bioturbation, mudstone clasts are present. Generally overlies a mudstone interval with a sharp contact.

Interpretation

Sandstone with mudstone clasts facies was interpreted to be deposited during high energy conditions by turbidity currents due to presence of very large clasts and abundance of rip-up mudstone clasts. Also absence of primary structures and grading suggests rapid deposition.

Fining-upward sandstone

Definition

Fining-upward sandstone lithofacies consists of fining upward light gray colored conglomerate- to coarse-grained sandstone that transitions into fine- to very fine-grained sandstone. Parallel laminations are common in the upper, fine-grained beds. Lower coarser parts are characterized with scoured bases, flame structures, and sub-angular mud clasts. Dish structures are also present occasionally. This lithofacies locally contains few bioturbation and mudstone clasts are also present. Amalgamation surfaces are also present.

Interpretation

This lithofacies was interpreted to be deposited by turbidity currents during waning flow as suggested by graded bedding. Lower parts are characterized by coarser grains as

higher energy is able to carry coarser grains and rip-up mudstone clasts. Abundance of dish structures are also indicative of deep-marine environment. Upper parts are characterized by finer grains which are deposited during lower energy conditions and show lamination.

Laminated sandstone with mudstone

Definition

Laminated sandstone with mudstone lithofacies consists of thin mudstone laminations or mudstone drapes in alteration with fine- to very fine-grained sandstone. Shale laminations and mudstone drapes are generally parallel to ripple cross bedded or locally convoluted. Flame structures are common.

Interpretation

This lithofacies always occurs on top of an upward-fining sandstone lithofacies with a smooth transitional base suggesting deposition during same flow but in a lower energy condition as it is only able to carry mud and fine- to very fine-grained sandstones. Presence of soft-sediment deformation like flame structures are also indicative of deep-marine condition which occurs due to water loss through more permeable layers and induce compaction of underlying deposits.

Lithology Estimation

In order to better evaluate the variations of lithology and porosity of the Desmoinesian Series Granite Wash deposits, lithologies were estimated in the non-cored wells. In this study two different approaches and their combination were evaluated to

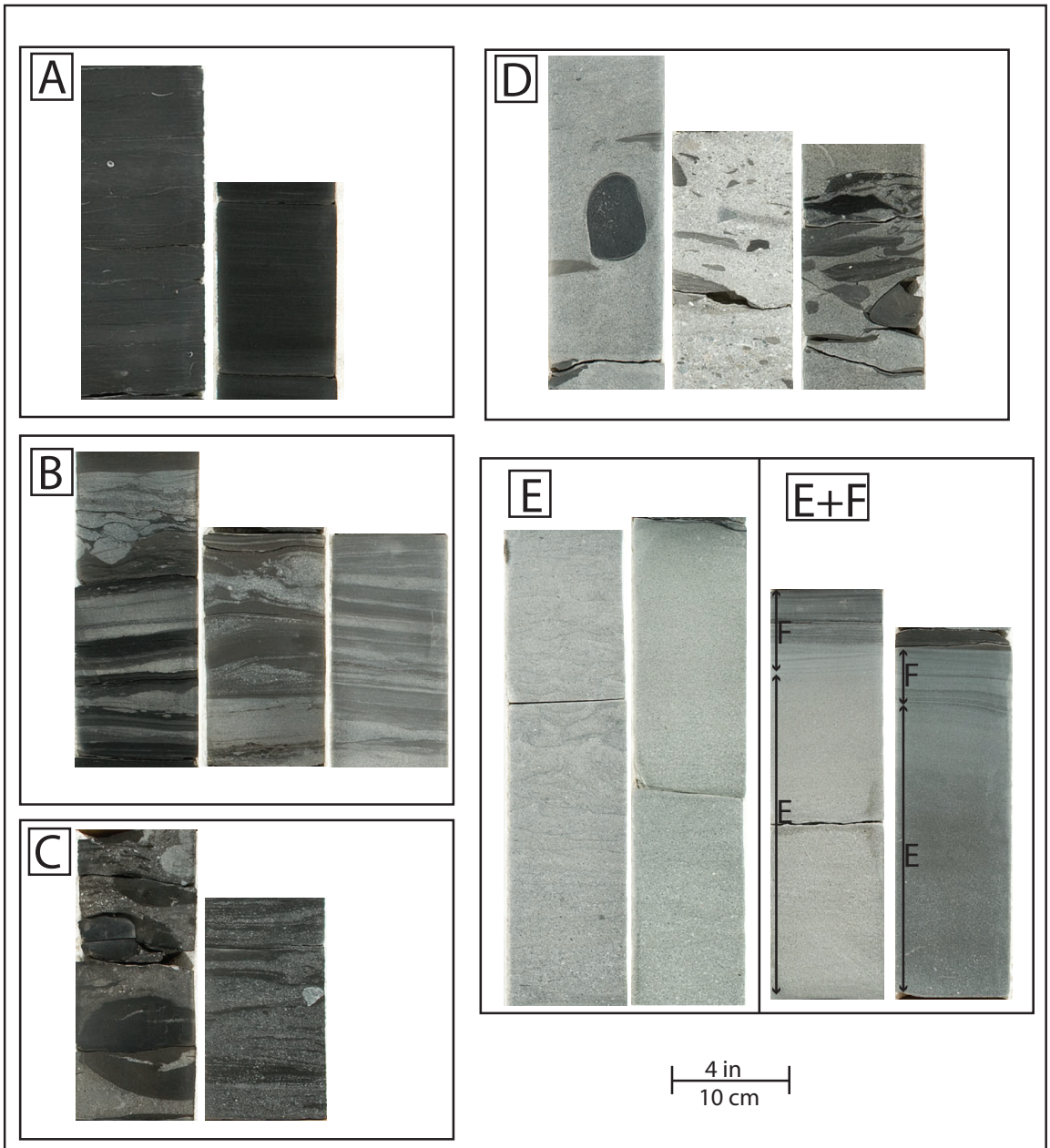

Figure 9. Representative images of the major Granite Wash lithofacies. A) Mudstone, measured depth (md) = 11537 ft, md = 11546 ft; B) Interbedded Mudstone / Sandstone, md = 11663 ft, md = 11666.2 ft, md = 11614.5 ft; C) Dark Gray Muddy Sandstone, md = 11625.5 ft, md = 11722 ft; D) Massive Sandstone, md = 11717.8 ft, md = 11676 ft, md = 11717.8 ft; E) Fining Upward Sandstone, md = 11784.5 ft, md = 11781.5 ft; F) Laminated Sandstone with Mudstone (overlying fining upward sandstones), md = 17777.5 ft, md = 11800.2 ft.

Table 1. Major Desmoinesian Series lithofacies with descriptions

	Lithofacies		Description	Depositional Processes
Mudstone	A	Mudstone	Very dark gray to black mudstone. Can be massive or laminated locally. Foraminifera and bivalve fossils. Pyrite mineralization and pyritized fossils locally. Calcitic at some parts.	Very low energy conditions; suspension sedimentation
Muddy Sandstone	B	Interbedded Mudstone / Sandstone	Alternating thin layers of mudstone, coarse- to fine-grained sandstone and muddy sandstone. Laminations are often convoluted. Abundant soft-sediment deformation and slumping with rip up clasts.	Turbidity currents; mudstones during low energy, sandstones during higher energy conditions
	C	Dark Gray Muddy Sandstone	Dark gray medium- to coarse-grained sandstone with occasional mud clasts distributed throughout. Local bioturbation.	Debris flow; slumping and soft-sediment deformation
Sandstone	D	Sandstone with mudstone clasts	Massive medium- to coarse-grained light gray sandstone with no change in grain size vertically. Local rip-up clasts. Occasional bioturbation.	High energy; rapid deposition
	E	Fining Upward Sandstone	Light gray sandstone that grades upward from conglomeratic sandstone to fine- to very fine- sandstone. Frequent parallel laminations at the top. Scoured at the bottom and flame structures. Dish structure is also present locally. Local bioturbation and mudstone clasts are also present.	Turbidity currents; waning flow. Grain size decreases vertically as energy decreases.
	F	Laminated Sandstone with Mudstone	Sandstone with mudstone laminations as mudstone drapes ranging from parallel to convoluted. Flame structures are common. Occurs at the top of a fining upward sandstone.	Turbidity currents; lower energy conditions

estimate lithologies in the non-cored wells. The best results were obtained by using a combination of Artificial Neural Network (ANN) and well-log cut-off approaches.

Well-log Cutoff Approach

One of the methods used for the lithology estimation is the cut-off method in order to obtain the lithologies for the Desmoinesian Series Granite Wash non-cored wells. Described lithologies from cored wells were used as a guide to obtain the cut-off values. By comparing core-derived lithology logs with gamma-ray logs, characteristics of sandstone, muddy sandstone, and mudstone lithologies were evaluated in terms of gamma-ray responses, and it was found out that sandstones have significantly lower GR values than mudstones as expected. Muddy sandstone lithologies showed slightly lower GR values than mudstones due to higher sandstone content when compared to mudstones. Two cutoff values were determined from the comparison of core and well-log responses; lithologies that have lower GR values than 100 API were assigned to be sandstone whereas higher GR values than 130 API were determined to be mudstone. The remaining part between 100-130 API was assigned as muddy sandstone lithology. The complex depositional patterns of the Granite Wash and co-occurrence of sandstone and mudstone together frequently prevented GR cut-off method to be accurate with an overall accuracy of 65% which is not adequate enough (Figure 10). It was found that the muddy sandstones were generally estimated to be mudstones causing an underestimation and lowering accuracy. In order to overcome this, an ANN was used.

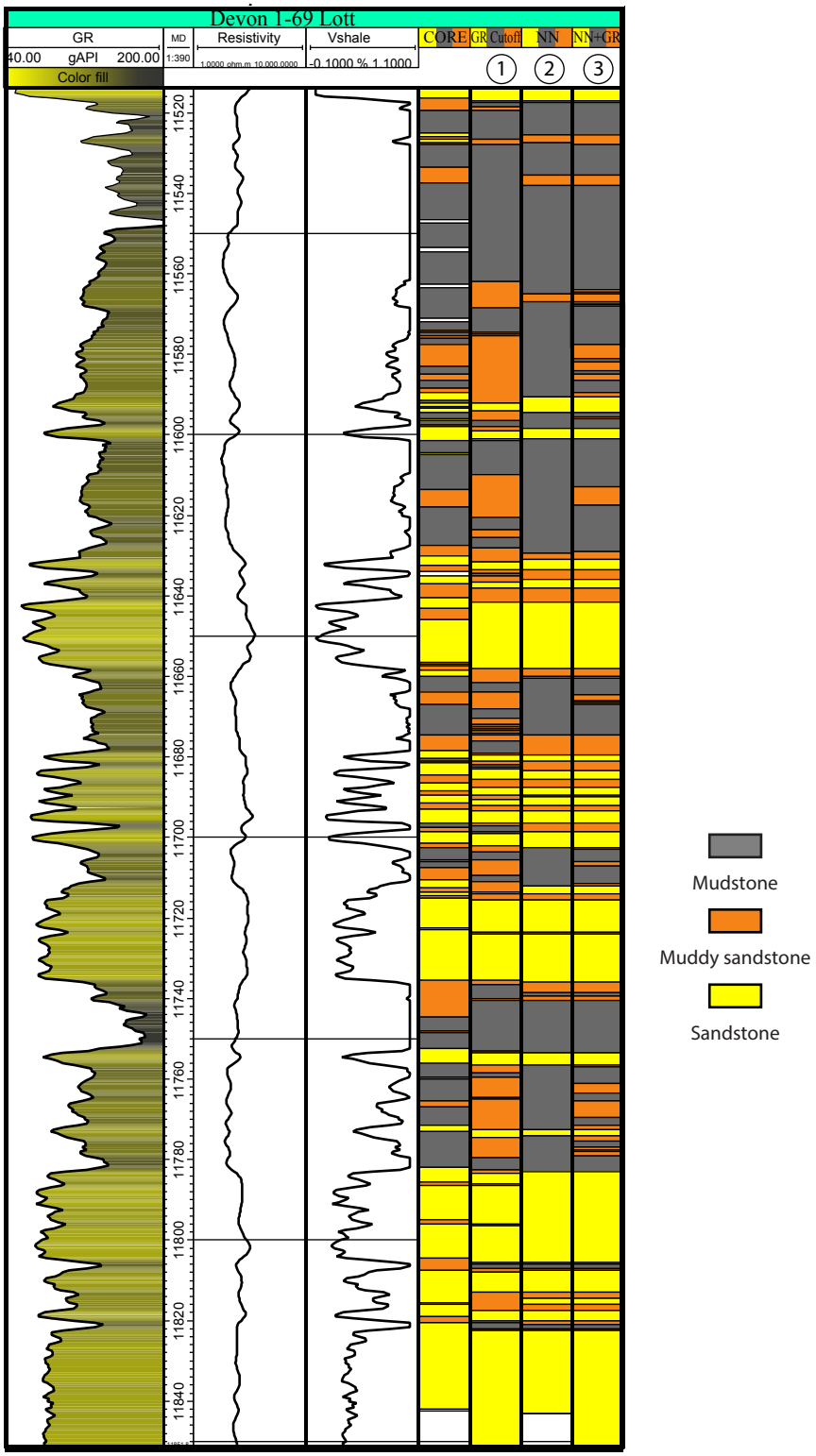

Figure 10: Well section of Devon 1-69 Lott showing gamma-ray, resistivity and Vshale logs together with the core lithology and resultant lithology logs 1) from gamma-ray cutoff method, 2) neural network method and 3) their combination. The accuracies of the methods are 0.65, 0.79, and 0.84, respectively. The best results are achieved by combining the neural network and cutoff approaches.

Artificial Neural Network Approach

With this approach, multiple well logs were taken into account in order to train the core-derived lithology log and use the same set of well logs to estimate lithology of non-cored wells. Several combinations of well-log sets were considered for this approach. Although SP and DT logs can be very helpful for lithology description, they were not present in most of the wells in the study area. Also, NPHI and DPHI logs could not be used due to their absence in the cored-wells. So, with the available logs, different combinations of gamma-ray, resistivity, and Vshale logs were evaluated (Figure 10). Evaluation of the available well-log combinations' ability to correctly predict the occurrences of the three lithologies achieved an overall accuracy of 78.8% when all three well logs were used together with the sandstone, muddy sandstone, and mudstone lithologies yielding the accuracies of 0.87, 0.31, and 0.93, respectively (Figure 11B). With the resultant confusion matrix, the overall accuracy was sufficient however, it was shown that the mudstone lithologies alone yielded a 0.31 accuracy was not sufficient (Figure 11B-C).

Refinement of Neural-Network Results by Well-log Cutoffs

With the purpose of refining the ANN-derived lithology log and differentiating muddy sandstone from shale lithologies better, a well-log cutoff was applied (Figure 10). This was necessary as the confusion matrix of the ANN results show that although the overall prediction and sandstone and mudstone lithology predictions were satisfactory, accurate prediction of the muddy sandstone lithology could not be achieved and it was frequently confused for the mudstone lithology. The GR cutoff value was

A

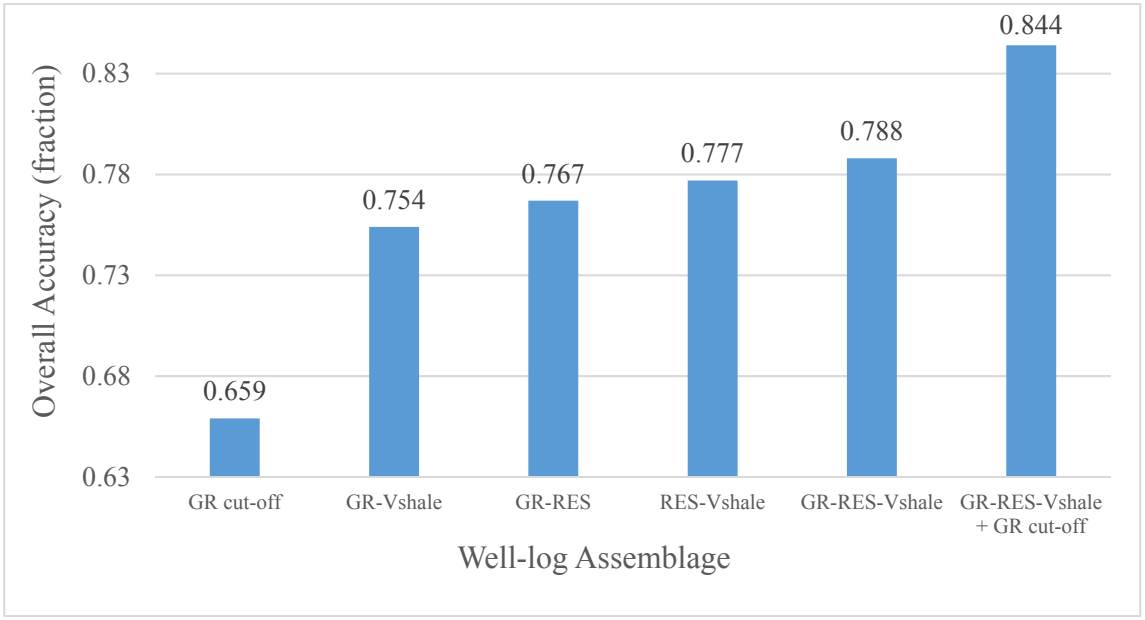

B

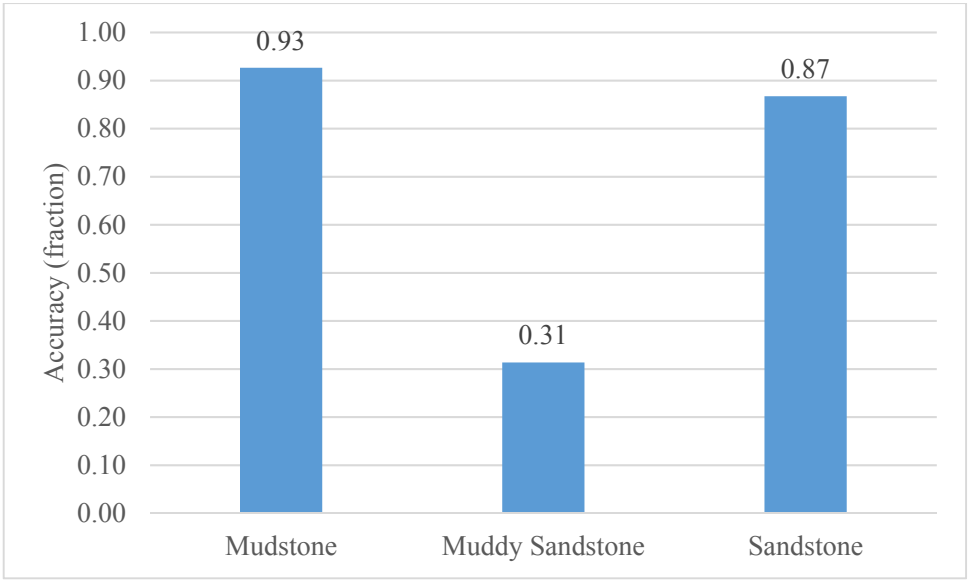

C

Actual Lithologies	Predicted Lithologies			Total
	Mudstone	Muddy Sandstone	Sandstone	
Mudstone	252	8	12	272
Muddy Sandstone	52	48	53	153
Sandstone	21	38	385	444

Figure 11. A) Histogram shows the overall accuracy of Artificial Neural Network results for estimating major lithologies within the cored interval for different combinations of well logs (GR: Gamma-ray; RES; and Vshale). Using three logs together resulted in the highest prediction accuracy which is 78.8%. B) Histogram shows the accuracy of the three estimated lithologies by the Artificial Neural Network using gamma-ray, Resistivity and Vshale logs. Accuracies were calculated by dividing the number of correctly estimated lithology by the total number of lithology in confusion matrix. C) Confusion matrix. Highlighted cells represent the number of correctly predicted lithologies in the cored intervals. All the other cells represent mis-predicted lithologies.

determined through evaluating and comparing the core-derived lithology log, ANN-derived lithology log, and the GR log. As the main confusion was between mudstone and muddy sandstone lithologies, a GR cutoff of 120 is applied to the lithology log which replaced mudstones having lower API values than 120 with muddy sandstones. With this refinement, the overall accuracy was increased to 84% thus satisfying confusion matrix results for each lithology (Figure 12).

Depositional Environment and Stratigraphy

The Desmoinesian Group Granite Wash was interpreted to be deposited within a proximal to distal deep-marine setting as suggested by the overall lack of bioturbation, abundance of dish structures, common fining-upward trend of the deposits, and the inferred fluxuating energy conditions from very high (rip-up clasts and graded beds) to very low (laminated mudstone). Desmoinesian Group Granite Wash deposits consists of slope-slump deposits, levee/overbank deposits, channel deposits, and submarine fan lobes. Dark gray muddy sandstone lithofacies was deposited as debris flow deposits and represents slope-slump deposits which are more proximal to the source. Levee/overbank deposits were represented by interbedded mudstone and sandstone lithofacies. Sandstone with mudstone clasts lithofacies was interpreted to be associated with submarine channel deposits. Submarine fan deposits include mudstone, laminated mudstone/sandstone, and fining upward sandstone facies which were interpreted to be the most distal deposits of all.

Desmoinesian Series Granite Wash consists of 10 stratigraphic intervals that are defined by distinctive laterally extensive mudstones. These mudstones were interpreted

A

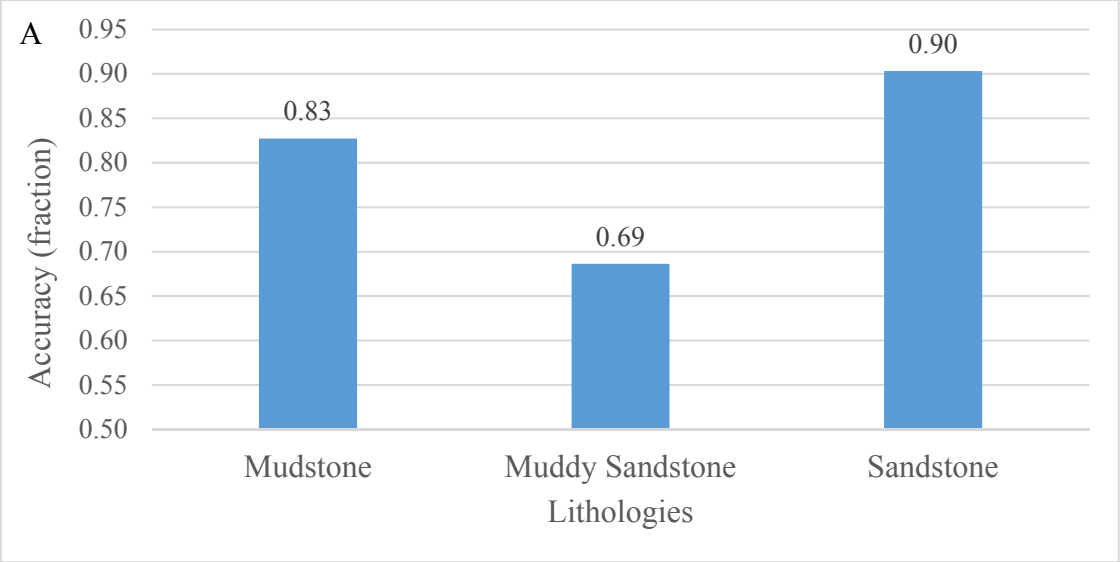

B

Actual Lithologies	Predicted Lithologies			Total
	Mudstone	Muddy Sandstone	Sandstone	
Shale	225	39	8	272
Muddy Sandstone	21	105	27	153
Sandstone	15	28	401	444

Figure 12. A) Histogram shows the accuracy of the three estimated lithologies by combining Artificial Neural Network and cutoff methods. Accuracies were calculated by dividing the number of correctly estimated lithology by the total number of lithology in confusion matrix. B) Confusion matrix. Highlighted cells represent the number of correctly predicted lithologies in the cored intervals. All the other cells represent mis-predicted lithologies.

to cap flooding surfaces based on the regional well-log correlations across the Anadarko Basin and into Kansas (Mitchell, 2011; LoCroccio, 2012; J. Mitchell, 2015, personal communication; Salantur, 2016). In this study, in order to define these 10 intervals, core, well logs, seismic data, and the vertical proportion curve were taken into account. A lithology log for 68 wells that was supervised by two core descriptions and estimated by ANN approach is utilized as well as gamma-ray and resistivity logs. The flooding surfaces that are defined by mudstones observed from the well logs and vertical proportion curve were picked on the wells at the highest gamma-ray and lowest resistivity responses and at the bases of the mudstones (Figures 13 and 14). On seismic data, five of the flooding surfaces were interpreted according to the corresponding formation top picks from wells and where there is negative amplitude contrast (Figure 15). Using these picks from seismic and wells 11 structure-contour maps were created that show the flooding surfaces and the top and base of the Desmoinesian Series. The top of the Desmoinesian Series is deepest to the south and is shallower towards the north in the study area (Figure 16A). Also, the isopach map of the Desmoinesian Series highlights the thickness distribution. The thickness is greatest to the southeast and thins to the northwest, parallel to the basin axis (Figure 16B). The thickest interval is the Marmaton Wash which has an average thickness of 800 ft (250 m) and the thinnest interval is the Caldwell interval with an average thickness of 100 ft (30 m).

In terms of sequence stratigraphy, the Desmoinesian Series Granite Wash was interpreted to consist of five third order cycles that are bounded by maximum flooding surfaces as defined by the vertical proportion curve and well logs (Figure 14). This cyclicity may be also due to eustatic sea-level changes, subsidence or uplift in the basin,

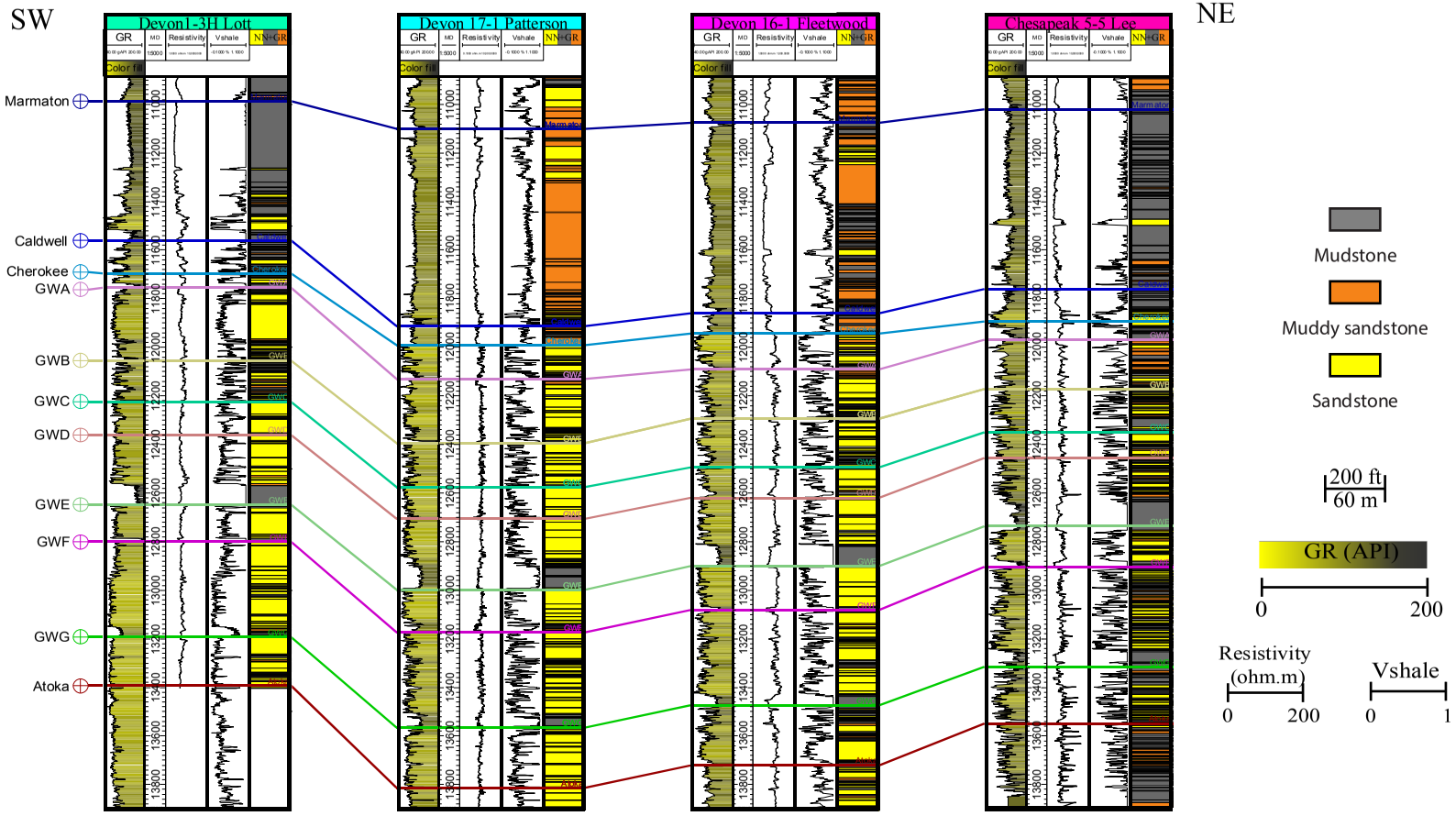

Figure 13: Structural cross section with estimated ANN-derived lithology log. Refer to figure 3 for the location of the cross section. Note that intervals with high gamma-ray values accompanied by low resistivity and high Vshale are classified as mudstones and flooding surfaces were picked at these locations.

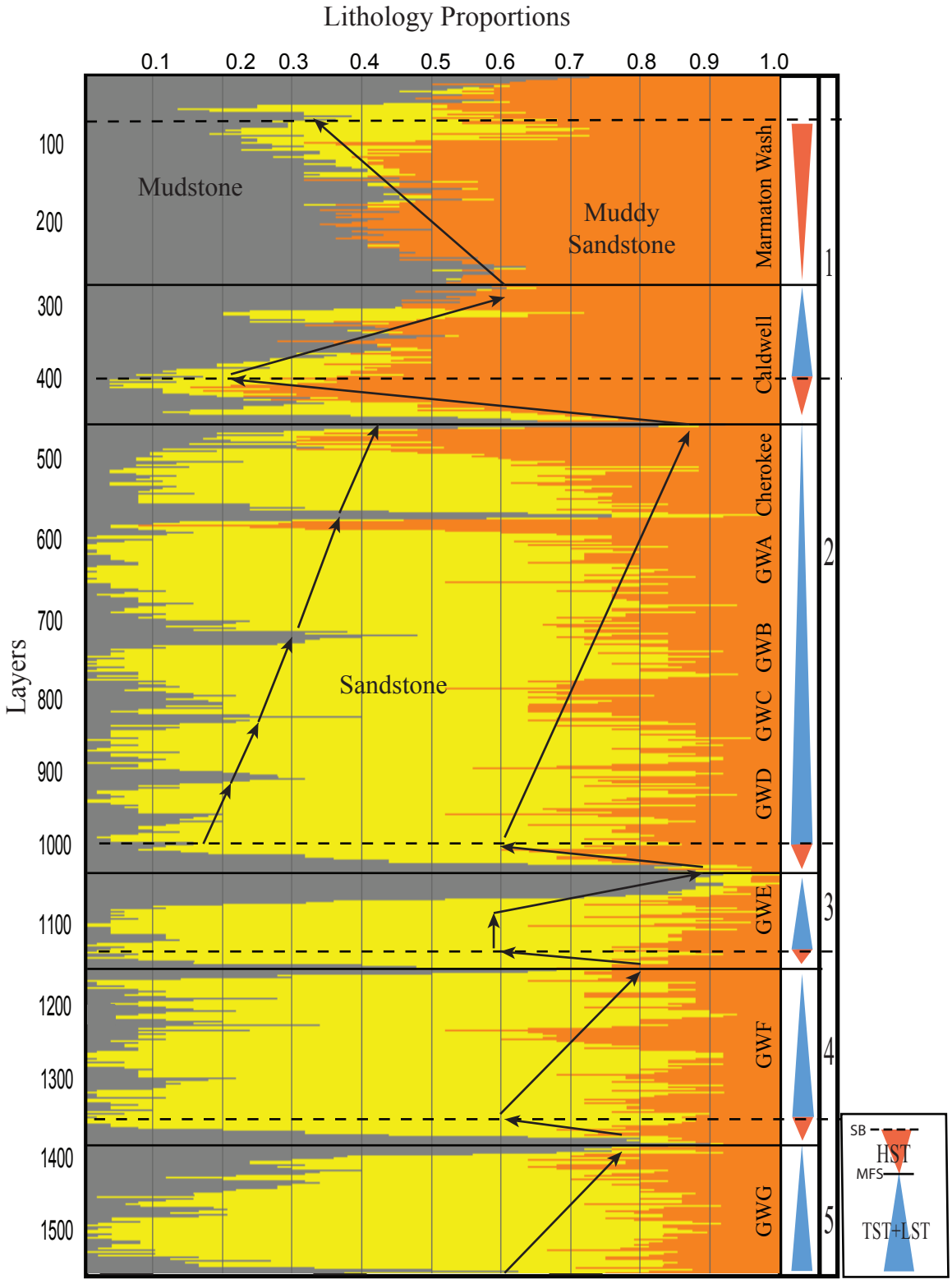
Lithology Proportions
0.1
0.2
0.3
0.4
0.5
0.6
0.7
0.8
0.9
1.0
Layers
100
200
300
400
500
600
700
800
900
1000
1100
1200
1300
1400
1500
Mudstone
Muddy Sandstone
Sandstone
Marmaton Wash
Caldwell
Cherokee
GWA
GWB
GWC
GWD
GWE
GWF
GWG
1
2
3
4
5
SB
HST
MFS
TST+LST

Figure 14. A) Lithology proportion curve showing the vertical proportion of three lithologies from the upscaled lithology logs. System tracts were interpreted from the vertical proportion curve and well-logs. The zones most likely represent 3rd-order regressive-transgressive cycles. MFS: Maximum flooding surface; SB: Sequence boundary; LST: Lowstand system tract; TST: Transgressive system tract; HST: Highstand system tract. Lowstand system tract (LST) and transgressive system tract (TST) were considered together as the transgressive surface does not extend to the sea-floor. In order to distinguish LST+TST deposits from highstand system tract (HST) deposits, maximum flooding surfaces (mfs) were used, which are defined by maximum mudstone proportion. They mark the turnaround point after which the regression starts, and coarsening upward deposits of HST start to develop. Sequence boundaries (SB) are defined by the highest proportion of sandstone deposition and change from coarsening upward to fining upward depositional trend. HST deposits are thin due to the distal location but with decreasing depth they become thicker and LST deposits become thinner due to change in depositional environment. For the 2nd sequence, higher order cycles are shown by smaller arrows.

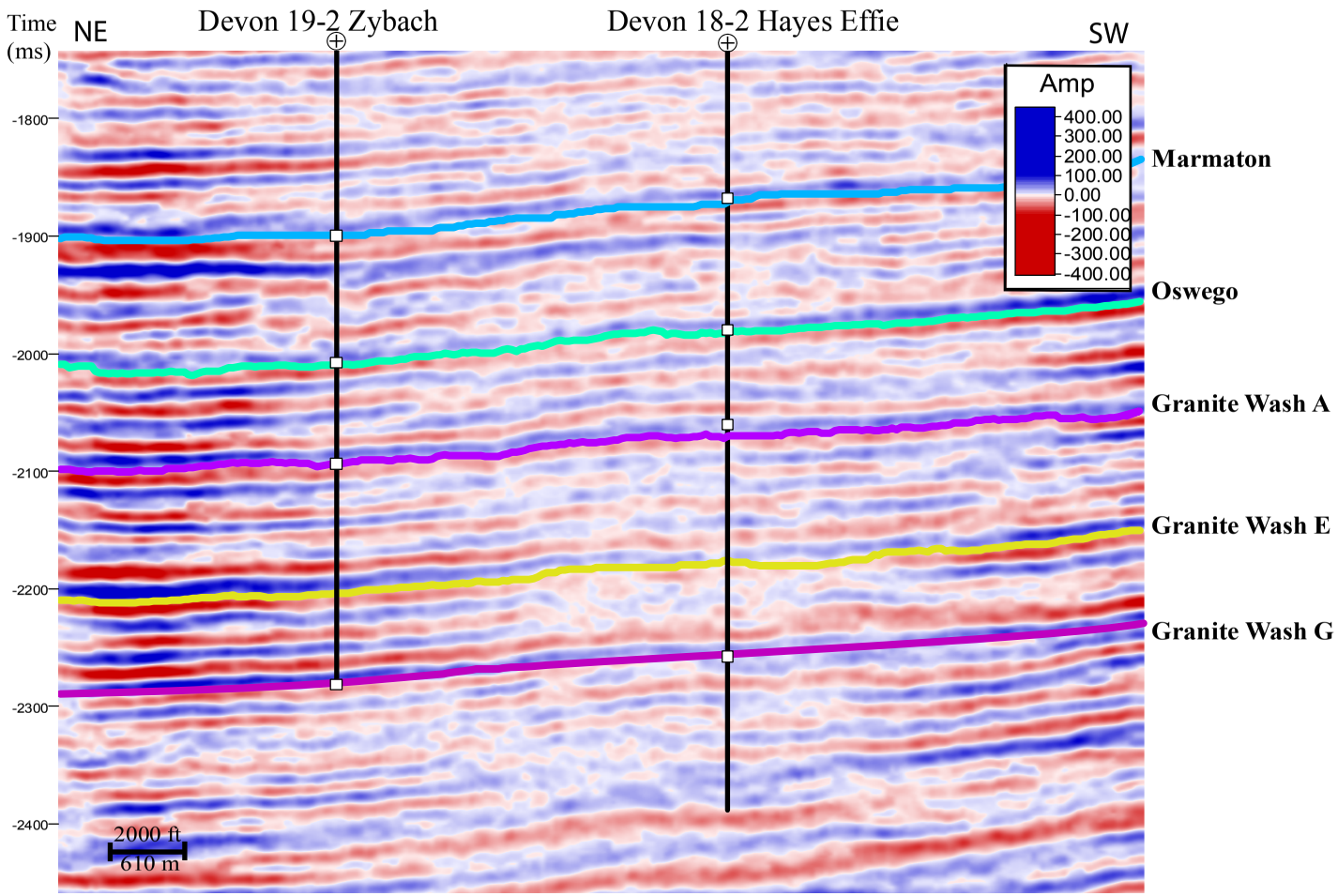

Figure 15. A composite section through seismic volume from northeast to southwest, between two wells that were used for the well-to-seismic tie using Hampson and Russell software. Footprint suppression was conducted and the data were subjected to structure-oriented filtering to remove noise. Five horizons that tie to the seismic include Marmaton, Oswego, Granite Wash A, Granite Wash E, and Granite Wash G.

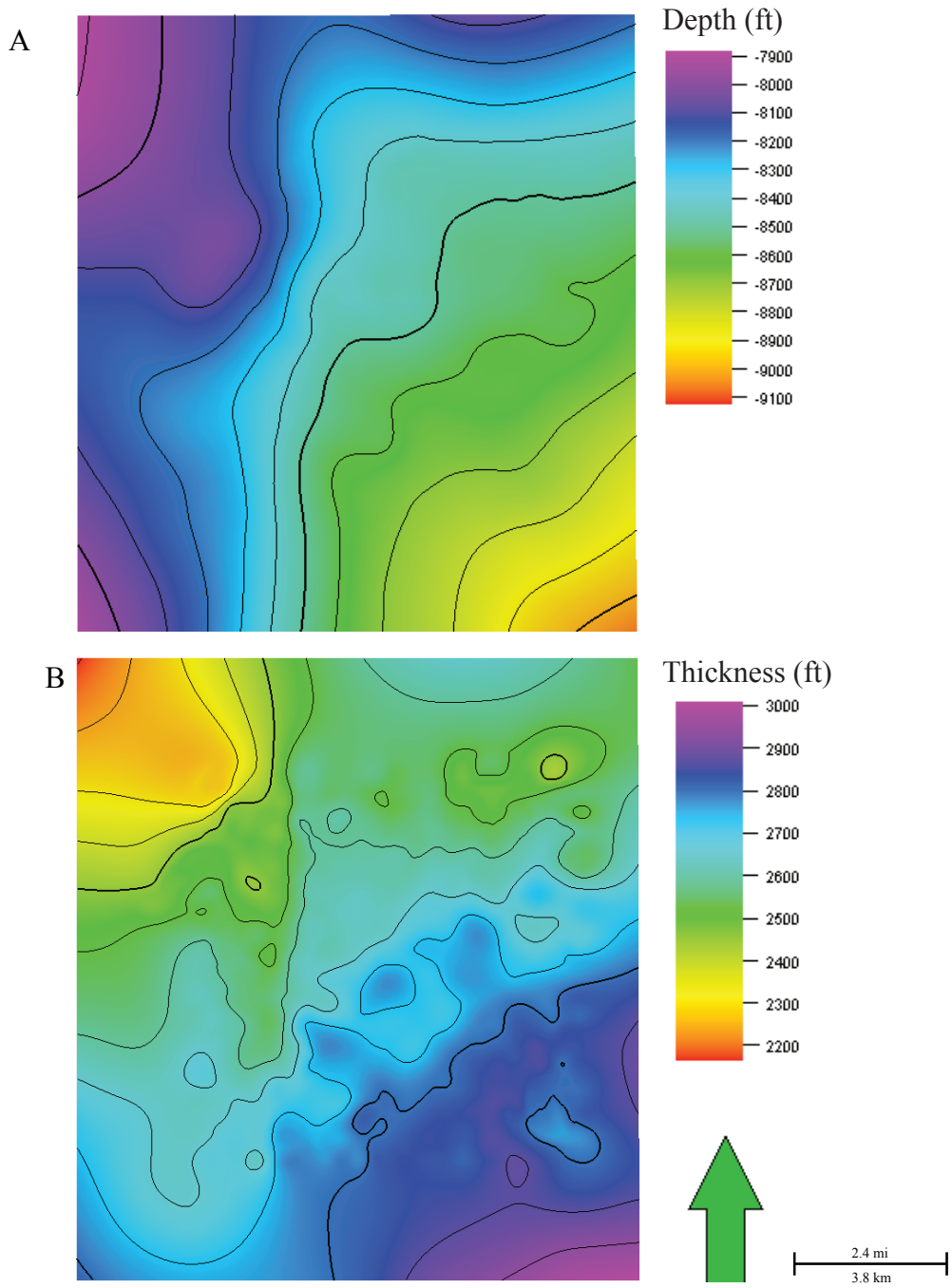

Figure 16. A) Structure-contour map of the top Desmoinesian Series Granite Wash. Map honors both seismic and well-log data and shows a trend of increasing structural elevation towards southeast. B) The isopach map for the Desmoinesian Series Granite Wash shows that thicker sediment accumulation occurs towards the southern boundary of the study area and thickness decreases towards northwest.

pulses of sediments or shifting of fan-delta lobes. On the vertical proportion curve, high proportion of mudstone corresponds to the correlated flooding surfaces on the well logs. Five of the flooding surfaces which corresponded to the highest occurrences of mudstones were interpreted to be related to the maximum flooding surfaces which correspond to the highest gamma ray values and high values of resistivity on the well logs. Sequence boundaries were interpreted where the proportion of sandstone is greatest and the mudstone proportion increases above it. The sequence boundaries were interpreted on the well logs at the bases of the blocky sandstones. The surface that defines the boundary between a lowstand system tract (LST) and transgressive system tract (TST) could not be identified. Due to this limitation, LST and TST deposits were evaluated together. In order to distinguish LST+TST deposits from highstand system tract (HST) deposits, maximum flooding surfaces were used, as they mark the turnaround point after which the regression starts, and progradational deposits start to develop.

The surfaces that honor both seismic and well data were used as inputs to develop a 3-D model grid stratigraphic framework. The model area is roughly square in shape and covers 78 mi^2 (202 km^2). The 3-D grid has 89 x 98 x 1525 cells (I x J x K) and 13,301,050 cells in total. Each cell is 500 x 500 ft (150 x 150 m) aerially and 4 ft (1.2 m) thick on average vertically with proportional layering (Figure 17). The lithology logs were upscaled to populate the grids cells in such a way that the lithology that exists in higher proportion within each cell was assigned as the upscaled cell (Figures 6, 7, and Appendix G).

On the vertical proportion curve, HST deposits are significantly thinner than the LST and TST deposits due to decreased sediment input in the deep-marine setting.

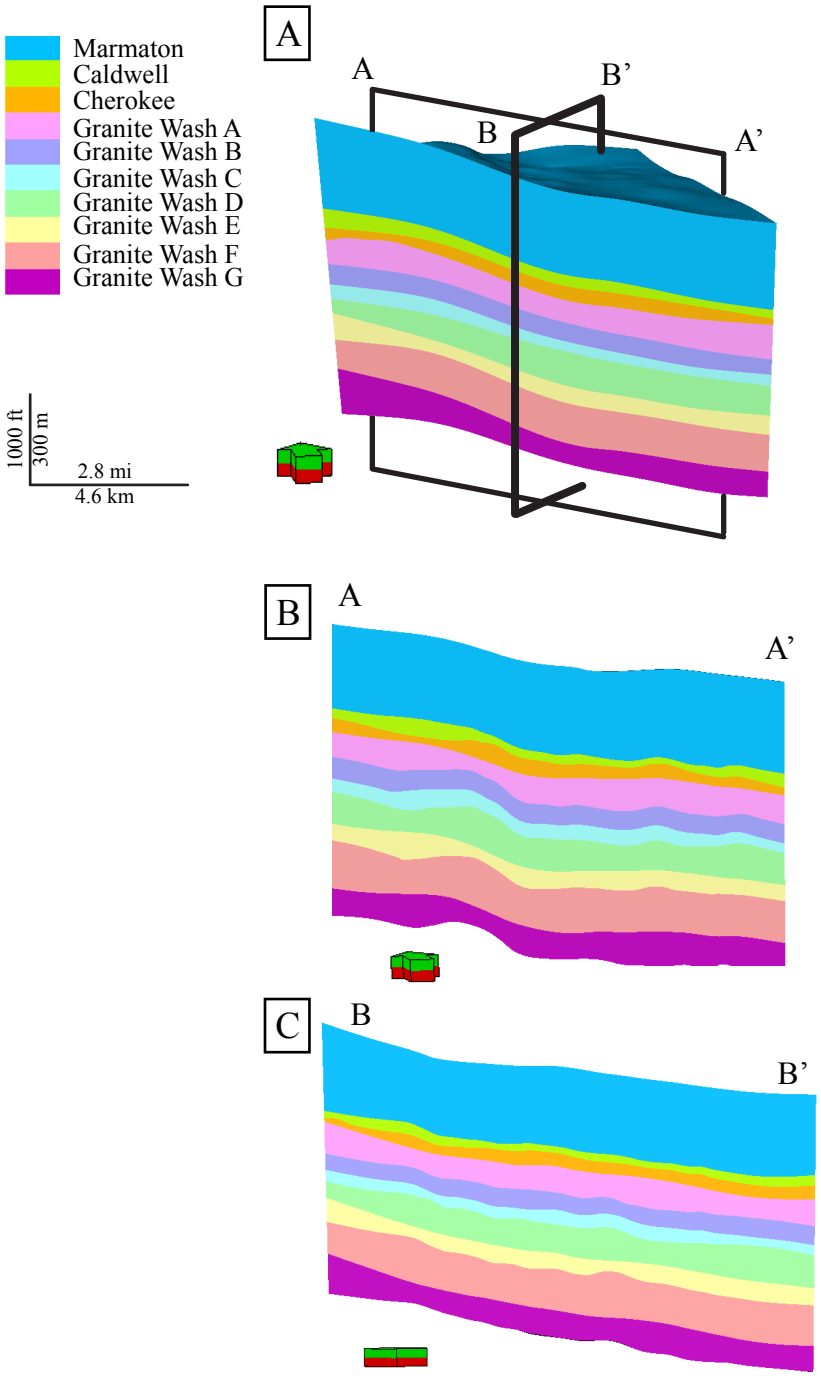

Figure 17. A) Stratigraphic and structural framework of the 3-D model (3-D grid) that illustrates nine stratigraphic intervals B) East-west oriented section and C) Longitudinal slice showing intervals across the study area. All figures are ten times vertically exaggerated.

But the thicknesses of the HST deposits increase stratigraphically upward, suggesting an increase in the sediment input by change of depocenter of the deposits or tectonism in the region. Moreover, muddy sandstone proportion increases stratigraphically upward indicating deposition of more proximal deposits, as muddy sandstones were interpreted to be deposited as slump and slope deposits. Overall, increase in the HST thickness and muddy sandstone proportion implies that this sequence is progradational (Figure 14). System tracts of Desmoinesian Granite Wash could not be identified on seismic due to the low resolution and quality of the data.

In terms of global sea-level cycles, the Desmoinesian Series corresponds to the upper Moscovian and lower Kasimovian stages of Pennsylvanian time which is between 306-312 mya on the international time scale (Ross and Ross; 1988, Haq and Schutter; 2008, Richards, 2013). This interval consists of 5 third order sea-level cycles that are approximately 1 million years each in duration in the global sea-level curve, which potentially corresponds to the 5 depositional cycles that were estimated on the vertical proportion curve and well logs (Appendix H).

Spatial Distribution of Lithologies and Porosity

Core descriptions, well logs, 3-D seismic data, and an acoustic impedance (AI) volume were used to construct 3-D lithology and porosity models. The resulting lithology model consists of 47% sandstone, 29% muddy sandstone, and 24% mudstone. From southwest to northeast, sandstone percentage decreases and mudstone percentage increases. Individual sandstone beds thin to the northeast which is basinward and coarser material is closer to the source near the southeast part of the study area and

grain size decreases towards the northeast. Stratigraphically, there is a significant increase in the proportion of muddy sandstone upward. As muddy sandstones were evaluated to be deposited more proximally, the increase in muddy sandstone occurrence suggests an overall progradation within the study area (Figure 18). LST+TST deposits have more sandstones than HST deposits, while HST deposits have more mudstones and muddy sandstones than LST+TST deposits. Also, HST deposits become thicker and muddy sandstone percent increases vertically within the HST deposits as well, which suggests that there is an overall progradation of the deposits within the study area (Figure 19).

The effective porosity model (Figure 20) illustrates the relationship between the sequence stratigraphy, lithologies and effective porosity. Average effective porosity maps for each lithology show the sandstone lithology has the highest average effective porosity, 8.5 %, while muddy sandstone lithology has a lower average effective porosity of 6.7 % which is most likely due to the increased content of mudstone. Also, the mudstone lithology has the lowest average effective porosity as expected which is only 3.3 % (Appendix I). Moreover, comparison of the sandstone percent map and average effective porosity map supports the idea of sandstone lithology having the highest porosity as higher percentage of sandstone corresponds to the areas of greater porosity (Figure 21). It can also be observed from the average porosity map for the entire study area, the highest porosity is aligned in the direction of southwest to northeast, which is also the direction of deposition. There is an observable decrease in effective porosity vertically which can be related to decreasing sandstone occurrence and change in depositional setting from distal to proximal as proximal deposits were evaluated to be

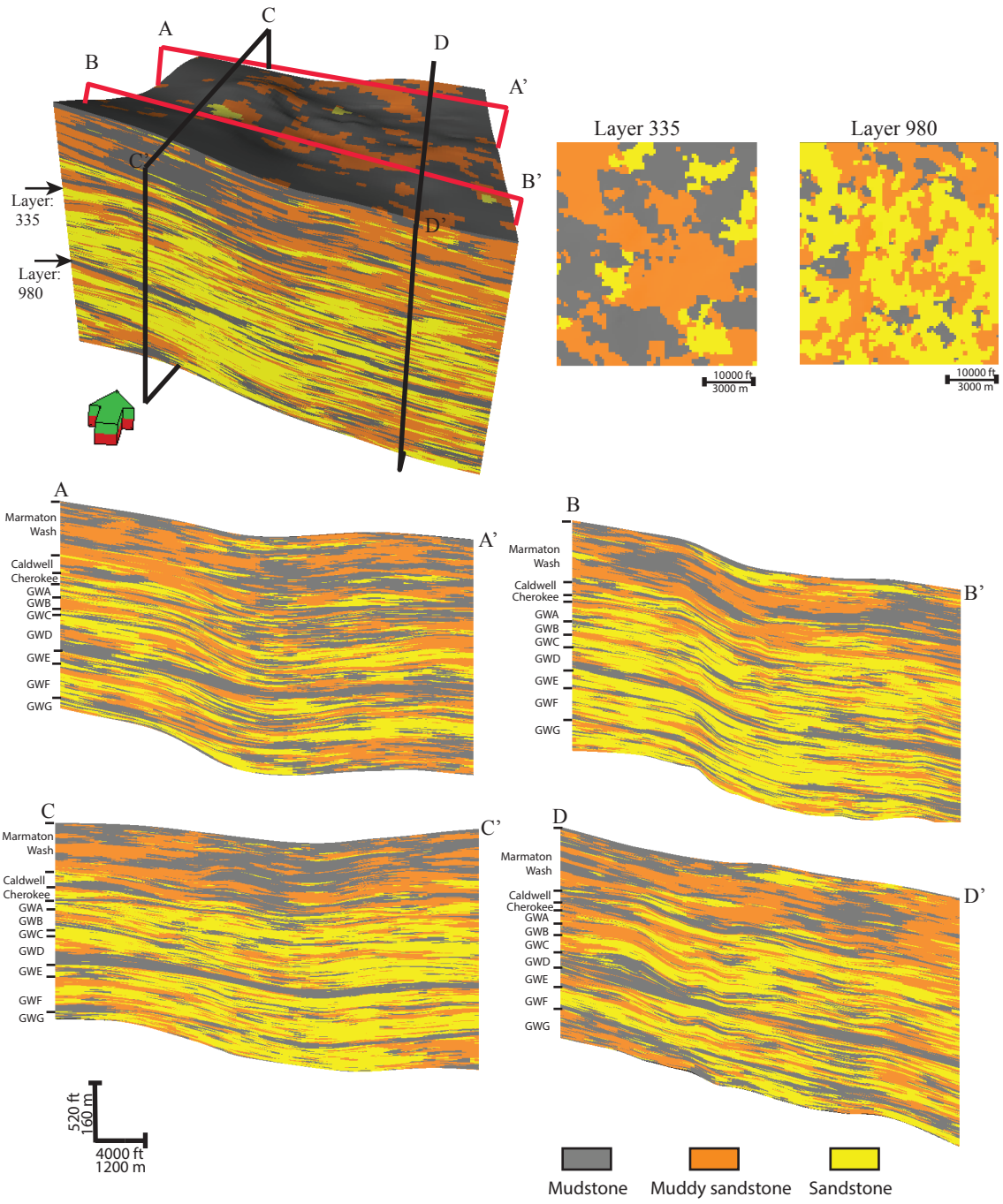

Figure 18. 3-D lithology model and its cross-sectional views. Note that mudstone content decreases with depth and sandstone proportion increases going from north to south whereas muddy sandstone proportion decreases. Also towards east side of the study area, amount of sandstone decreases and amount of mudstone increases. All views are 10x exaggerated.

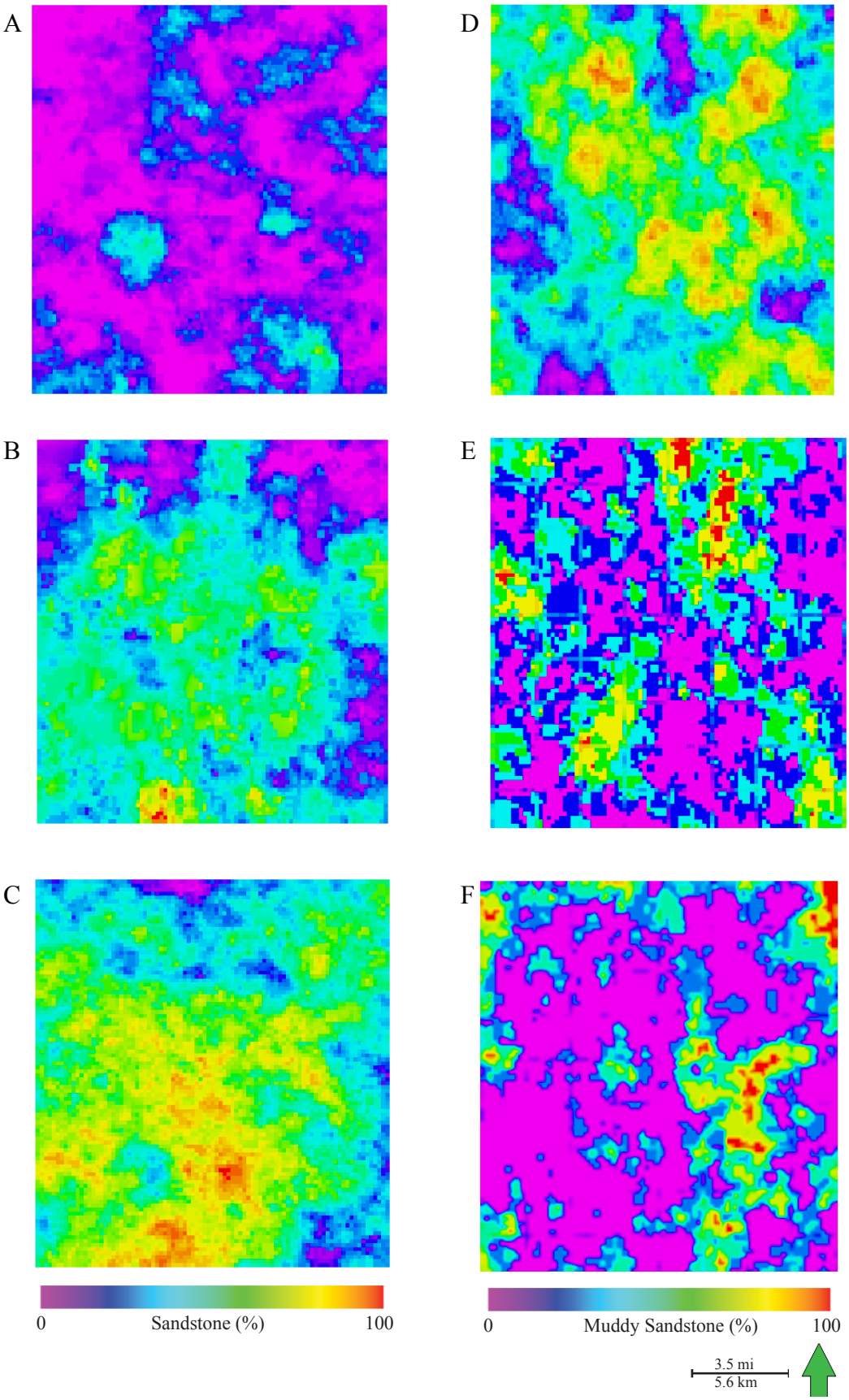
A
D
B
E
C
F
0
Sandstone (%)
100
0
Muddy Sandstone (%)
100
3.5 mi
5.6 km

Figure 19: Illustration of sandstone and muddy sandstone occurrences according to system tracts. A) Sandstone proportion map for LST+TST 1. B) Sandstone proportion map for LST+TST 3. C) Sandstone proportion map for LST+TST 4. D) Muddy sandstone proportion map for HST 1. E) Muddy sandstone proportion map for HST 3. F) Muddy sandstone proportion map for HST 4. Note that, while sandstone proportion decreases vertically for LST+TST deposits, muddy sandstone proportion increases for HST deposits.

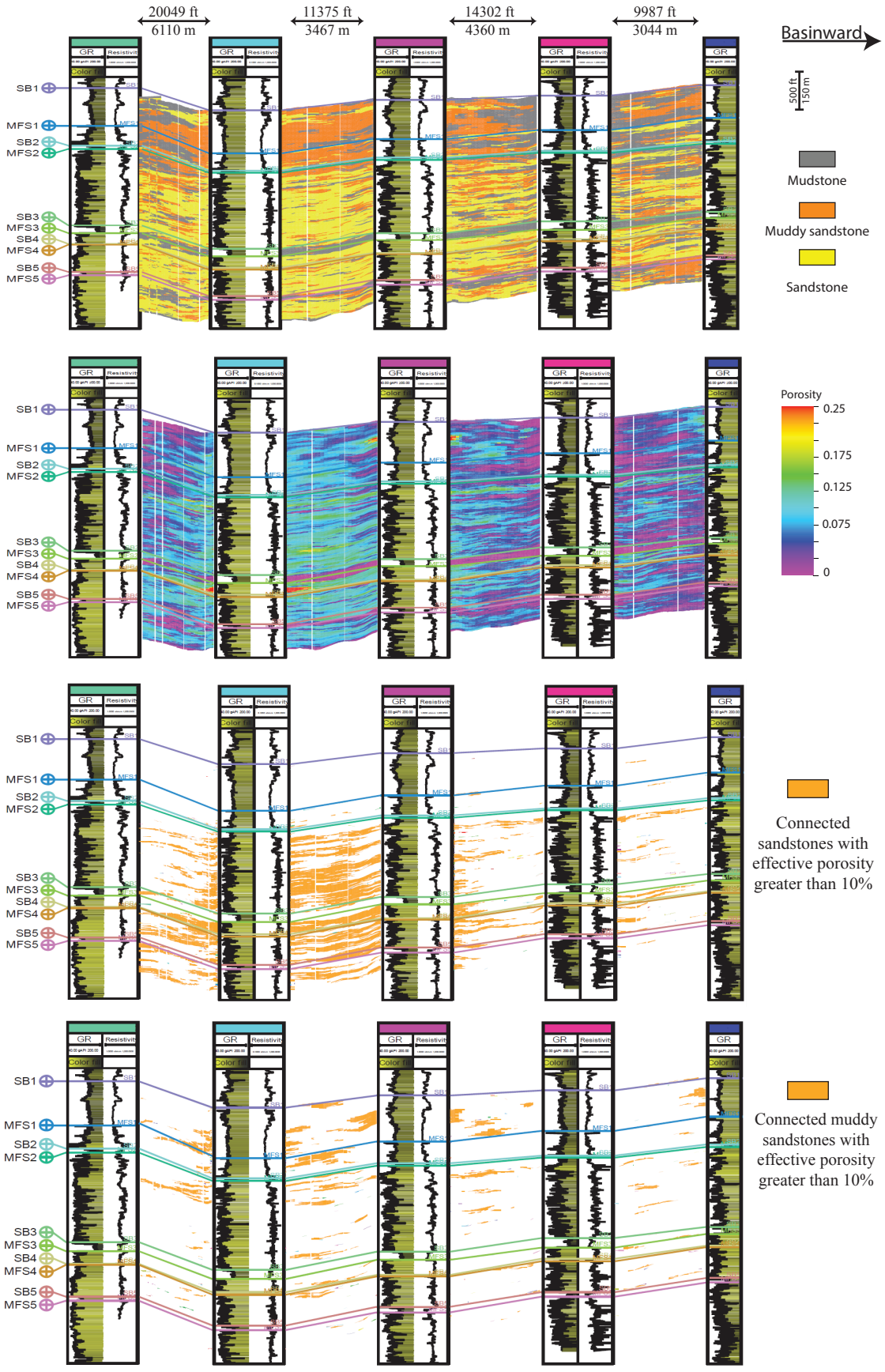
20049 ft
6110 m
11375 ft
3467 m
14302 ft
4360 m
9987 ft
3044 m
Basinward
500 ft
150 m
Mudstone
Muddy sandstone
Sandstone
Porosity
0.25
0.175
0.125
0.075
0
SB1
MFS1
SB2
MFS2
SB3
MFS3
SB4
MFS4
SB5
MFS5
Connected sandstones with effective porosity greater than 10%
Connected muddy sandstones with effective porosity greater than 10%

Figure 20. Structural cross section of the modeled properties (See Figure 3 for location). A) Lithologies, B) effective porosity, C) connected volume of sandstone with effective porosity greater than 10%, and D) connected volume of muddy sandstone with effective porosity greater than 10%. Sandstones have greater effective porosity than muddy sandstones in general. Moreover, sandstones have higher connectivity when compared to the muddy sandstones. Highest connectivity belongs to Sequence 4 for sandstones and Sequence 3 for muddy sandstones, 40% and 12% respectively.

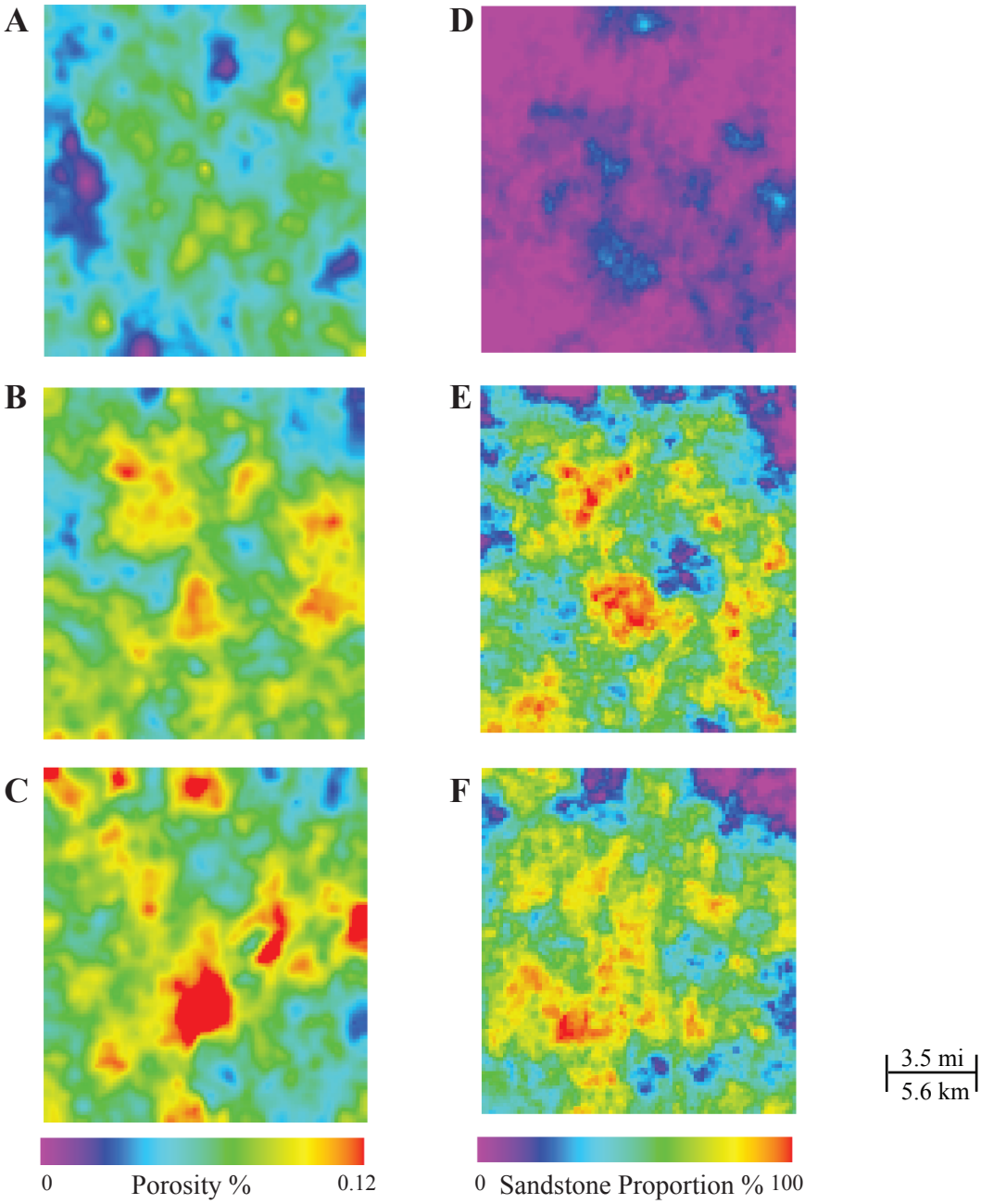

Figure 21. Average effective porosity maps of A) Marmaton, B) Granite Wash B, and C) Granite Wash E as examples from top to bottom. Sandstone proportion maps for D) Marmaton, E) Granite Wash B, and F) Granite Wash E as examples from top to bottom. These maps support the relationship between porosity and sandstone while also showing that porosity decreases upward as sandstone proportion decreases.

more chaotic which decreases effective porosity.

Static connectivity analysis of each system tract for connected porous sandstone and muddy sandstone lithologies were calculated using 10% porosity as a constraint. Results show that sandstones have higher connectivity compared to the muddy sandstones (Figure 22). The main reason for this can be the depositional characteristics of the two lithologies. Sandstones were mainly deposited at more distal settings as submarine fan lobes or channels. Whereas muddy sandstones were deposited at more proximal settings such as slopes and as debris flows and slumps. The chaotic bedding decreases porosity. Also, as muddy sandstones have much lower porosity due to their fine-grained content. Overall, connectivity shows a similar trend with porosity as expected and it decreases vertically. The Cherokee interval has the highest connectivity for both sandstone and muddy sandstone which is followed by Granite Wash E. Sandstones have the lowest connectivity in the Marmaton Wash interval whereas muddy sandstones have the lowest connectivity in the Granite Wash C interval (Figure 22A). Also, in terms of system tracts, LST+TST deposits always have higher connectivity when compared to the HST deposits except from the upper most system tracts. In general, LST+TST deposits are more connected due to the higher sandstone proportion, as sandstones tend to be more connected. But for the uppermost system tracts LST+TST 1 and HST 1, HST deposits have higher connectivity than LST+TST deposits although the overall connectivity of these deposits are relatively low when compared to the underlying system tracts. That is due to high muddy sandstone and very low sandstone content. The most connected LST+TST deposits is the LST+TST3 with 41% while the most connected HST deposits is the HST4 with 24% (Figure 22B).

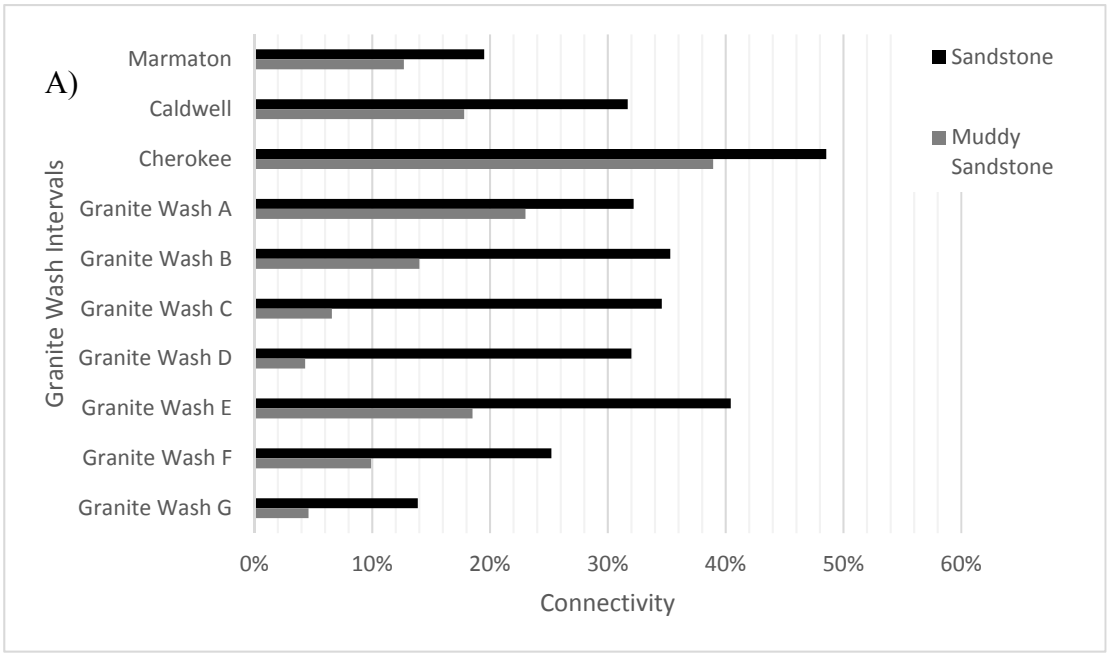
A)
Marmaton
Caldwell
Cherokee
Granite Wash A
Granite Wash B
Granite Wash C
Granite Wash D
Granite Wash E
Granite Wash F
Granite Wash G
Granite Wash Intervals
Sandstone
Muddy Sandstone
0%
10%
20%
30%
40%
50%
60%
Connectivity

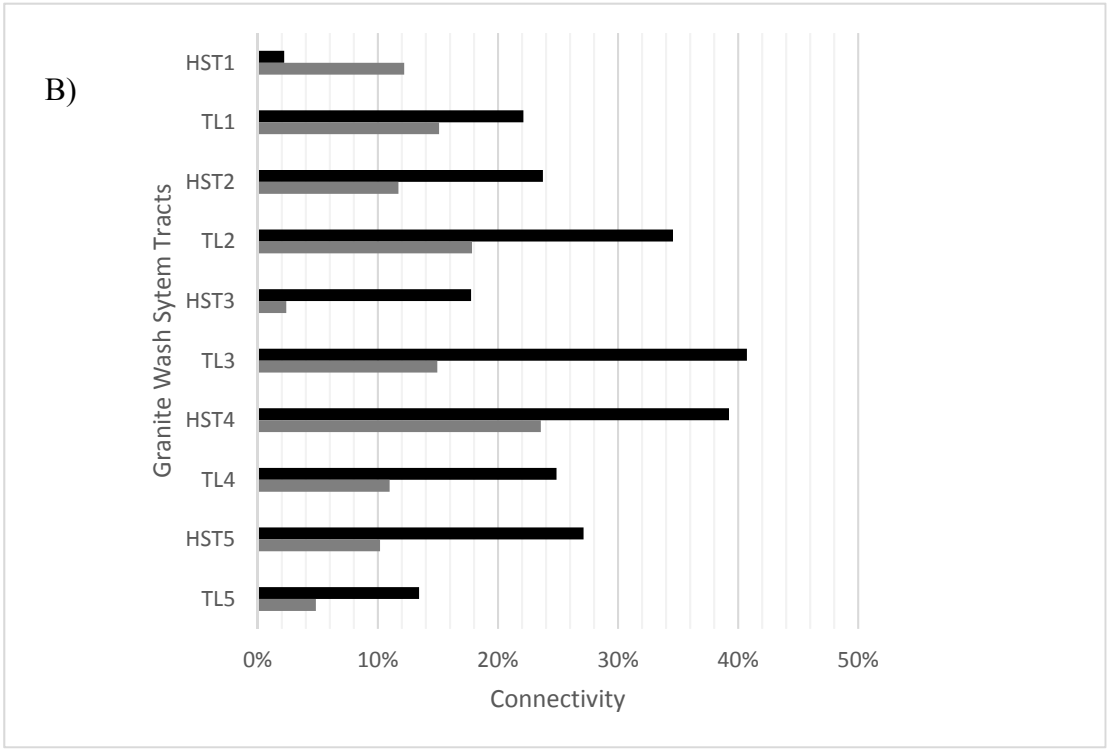
B)
HST1
TL1
HST2
TL2
HST3
TL3
HST4
TL4
HST5
TL5
Granite Wash Sytem Tracts
0%
10%
20%
30%
40%
50%
Connectivity

Figure 22. A) Connectivities (%) for sandstones and muddy sandstones for each zone. For connectivity, 10% porosity cut-off values were used as a constraint. The Cherokee interval has the highest connectivity for both sandstone (49%) and muddy sandstone (39%) which is followed by Granite Wash E. Sandstones have the lowest connectivity for the Granite Wash G interval (14%) whereas muddy sandstones have the lowest connectivity at Granite Wash C (4.3%) interval. B) Connectivities (%) for sandstones and muddy sandstones for each systems tract. For connectivity, 10% porosity cut-off values were used as a constraint. LST+TST 3 and HST4 deposits have the highest connectivity as 41% and 24%, respectively, while lowest connectivities LST+TST 1 and HST3 are 12% and 2% respectively. Also, note that except for first cycle, sandstones always have higher connectivities than muddy sandstones deposits.

CONCLUSION

Desmoinesian Series Granite Wash deposits of Buffalo Wallow field, Anadarko Basin, Texas consist of six lithofacies: mudstone, sandstone with mudstone clasts, interbedded mudstone and sandstone, dark gray muddy sandstone, fining upward sandstone, and laminated mudstone and sandstone. These deep-water deposits represent slumps, levee and channels, and submarine fan lobes.

A combined artificial neural network and well-log cutoff with gamma-ray, resistivity and Vshale logs were used to estimate lithology logs in non-cored wells with 84% accuracy.

The Desmoinesian Series consists of 10 stratigraphic intervals that are defined by laterally continuous and distinctive mudstone layers interpreted to be flooding surfaces. Furthermore, using well logs and a vertical proportion curve, a stratigraphic-framework was constructed and system tracts were evaluated. Reservoir models show that the amount of sandstone decreases going from southwest to northeast which is basinward. While sandstone proportion decreases stratigraphically upward, muddy sandstone increases suggesting an overall progradation within the study area. The effective porosity model shows that sandstones have higher porosity than muddy sandstone and muddy sandstones have higher porosity than mudstones. Static connectivity analysis shows that the Cherokee interval has the highest connectivity for both sandstone and muddy sandstone. The Marmaton interval has the lowest connectivity for sandstones which can be explained by low proportion of sandstone at this interval. In general sandstones tend to be more connected than muddy sandstones.

In terms of sequence stratigraphy, Desmoinesian Granite Wash was evaluated to consist of five third order cycles that are bounded by maximum flooding surfaces. In general, LST+TST deposits show greater connectivity when compared to HST deposits. This greater connectivity can be explained by the high sandstone content of LST+TST deposits. Also HST deposits become thicker vertically and together with the increase in the muddy sandstone occurrence which also suggests that there is an overall progradation within the study area as muddy sandstones represent more proximal deposits.

References

Allen, D. B., 2013, Geologically constrained electrofacies classification of fluvial deposits: an example from the Cretaceous Mesaverde Group, Uinta and Piceance Basins AAPG Bulletin, v. 100, no. 12, p. 1775-1801.

Al-Shaieb, Z., J. O. Puckette, A. A. Abdalla, and P. B. Ely, 1994, Megacompartment complex in the Anadarko Basin: a completely sealed overpressured phenomenon, AAPG Memoir 61, p. 55-68.

Anggraini, J., and M. Puspa, 2008, Supervised and unsupervised neural networks technique in facies classification and interpretation, *in* Indonesian Petroleum Association Thirty-Second Annual Convention & Exhibition: p. 1-8.

Ball, M. M., M. E. Henry, and S. E. Frezon, 1991, Petroleum geology of the Anadarko Basin Region, Province (115), Kansas, Oklahoma, and Texas: Open-File Report 88-450W.

Batista, A. M., 2010, Evaluation of 3D Seismic attributes and post stack inversion methods: Pennsylvanian Granite Wash reservoir characterization case study, Texas: master's thesis, University of Oklahoma, p. 1-8.

Blakey, R., 2013, Paleogeography and geologic evolution of North America, http://cpgeosystems.com/paleomaps.html, (accessed March, 2016).

Bouma, A.H., 2000, Fine-grained, mud-rich turbidite systems: model and comparison with coarse-grained, sand-rich systems, in A.H. Bouma and C.H. Stone, eds., Fine-grained turbidite systems: AAPG Memoir 72/SEPM Special Publication 68, p. 9-20.

Brouwer, F. C. G., D. Connolly, and K. Tingdahl, 2011, A Guide to the Practical Use of Neural Networks, in 31st Annual GCSSEPM Foundation Bob F. Perkins Research Conference 2011, p. 312-333.

Bruner, K. R., and R. Smosna, 2000, Stratigraphic-Tectonic Relations in Spain's Cantabrian Mountains: Fan Delta Meets Carbonate Shelf, Journal of Sedimentary Research, v. 87, no. 4, p. 1302-1314.

Campbell, J. A., C. J. Mankin, A. B. Schwarzkopf, and J. J. Raymer, 1988, Habitat of petroleum in Permian rocks of the midcontinent region; in, Permian Rocks of the Midcontinent, W. A. Morgan and J. A. Babcock, eds.: Midcontinent Society of Economic Paleontologists and Mineralogists, Special Publication No. 1, p. 13-35.

Duggins, W. T., 2013, Facies architecture and sequence stratigraphy of part of the Desmoinesian Granite Wash, Texas Panhandle and Western Oklahoma: master's thesis, University of Tulsa.

Dutton, S. P., 1985, Fan-delta Granite Wash of the Texas Panhandle: Oklahoma CityGeological Society Short Course, p. 1–144.

Dutton, S. P., and L. S. Land, 1985, Meteoric burial diagenesis of Pennsylvanian arkosic sandstones, southwestern Anadarko Basin, Texas: The American Association of Petroleum Geologists Bulletin, v. 69, no. 1, p. 22-38.

Evans, J., 1987, Major structural features of the Anadarko Basin: Tulsa Geological Society Special Publication no. 1, p. 97-114.

Foody, G. M., 2002, Status of land cover classification accuracy assessment, Remote Sensing of Environment, v. 80, p. 187.

Gavidia, G. E., 2012, Attribute supported seismic geomorphology and reservoir characterization of the Granite Wash, Anadarko Basin, Texas: master's thesis, Oklahoma State University, Oklahoma City, Oklahoma, p. 1-20.

Gilbert, M. C., 1983, Timing and chemistry of igneous events associated with the Southern Oklahoma aulacogen, *in* Morgan, P., and Baker, B.H., ed., Processes of continental rifting: Tectonophysics, v. 94, p. 439-455.

Gilman, J., 2012, Depositional patterns, source rock analysis identify Granite Wash fairways: The American Oil and Gas Reporter, August 2012 Cover Story.

Ham, W. E. and J. L. Wilson, 1967, Paleozoic epeirogeny and orogeny in the central United States: American Journal of Science, v. 265, no. 5, p. 332-407.

Haq, B. U., and S. R. Schutter, 2008, A chronology of Paleozoic sea-level changes: Science, v. 322, October, p. 64‐68.

Holmes, C. D., 2015, Stratigraphic architecture, facies characteristics, and distribution of deepwater deposits, Colony Granite Wash, Anadarko Basin, Oklahoma, master's thesis, University of Oklahoma, p. 1 – 166.

Iloghalu, E. M., and N. Azikiwe, 2003, Application of neural networks technique in lithofacies classifications used for 3-D reservoir geological modelling and exploration studies. - A novel computer-based methodology for depositional environment interpretation, in AAPG Annual Convention Salt Lake City, Utah: p. 1 – 7.

Janssen, L. F., and F. M. van der Wel, 1994, Accuracy assessment of satellite derived land cover data: a review. Photogrammetric Engineering and Remote Sensing, v. 60, 419 – 426.

Johnson, K. S., and K. V. Luza, 2008, Earth sciences and mineral resources of Oklahoma, Educational Publication 9, Oklahoma Geological Survey, 22 p.

Karis, A. M., 2015, Stratigraphy and reservoir characteristics of the Desmoinesian Granite Wash (Marmaton Group), Southern Anadarko Basin: University of Oklahoma, 1 – 87 p.

Kumar B., and M. Kishore, 2006, Electrofacies classification: a critical approach, *in* Proceedings of the 6th international conference and exposition on petroleum geophysics, Society of Petroleum Geophysicists (SPG): Kolkata, India, p. 822-825.

LoCricchio, E., 2012, Granite Wash play overview, Anadarko Basin: Stratigraphic framework and controls on Pennsylvanian Granite Wash production, Anadarko Basin, Texas and Oklahoma, AAPG Annual Convention and Exhibition: Long Beach, California, p. 1-17.

McConnell, D. A., M. J. Goydas, G. N. Smith, and J. P. Chitwood, 1989, Morphology of the frontal fault zone, southwest Oklahoma: Implications for deformation and deposition in the Wichita uplift and Anadarko basin: Geology, v. 18, no. 7, p. 34 – 637.

Mitchell, J., 2011, Horizontal drilling of deep Granite Wash reservoirs, Anadarko Basin, Oklahoma and Texas: Shale Shaker, v. 62, no. 2, p. 118–167.

Mitchell, J., 2015, Economic development of Pennsylvanian age Granite Wash reservoirs with horizontal wells in the Anadarko Basin, AAPG Education Directorate Forum, Granite Wash and Pennsylvanian Sand, Oklahoma City, Oklahoma, p. 1-59.

Moore, G. E., 1979, Pennsylvanian paleogeography of the southern Mid-Continent, *in* Hyne, N. J., ed., Pennsylvanian Sandstones of the Mid-Continent, Tulsa, OK, Tulsa Geological Society, vol. 91, p. 2-12.

Northcutt, R. A. and J. A. Campbell, 1995, Geologic provinces of Oklahoma: Oklahoma Geological Survey Open-File Report 5-95, 1 sheet, scale 1: 750,000,6-page explanation and bibliography.

Perry, W. J., 1989, Tectonic evolution of the Anadarko Basin region, Oklahoma, U.S. Geological Survey Bulletin 1866, p. A19.

Pyrcz, M. J., and C. V. Deutsch, 2014, Geostatistical Reservoir Modeling: New York, NY, Oxford University Press, 433 p.

Richards, B. C., 2013, Current status of the international carboniferous time scale: The Carboniferous-Permian transition, Bulletin 60, New Mexico Museum of Natural History and Science, p. 348 – 353.

Ross, C. A., and Ross, J. R. P., 1988, Late Paleozoic transgressive-regressive deposition: Society of Economic Paleontologists and Mineralogists Special Publication 42, p. 227 – 247.

Sahl, H. L., 1970, Mobeetie field, Wheeler County, Texas: Shale Shaker, V.20, p. 107-115.

Salantur, B., 2016, Continuity, connectivity and reservoir characteristics of Desmoinesian fan-delta conglomerates and sandstones, Elk city field, Anadarko Basin, Oklahoma, master's thesis, University of Oklahoma, p.1-53.

Weimer, P., and R.M. Slatt, 2006, Introduction to the petroleum geology of deep-water settings, AAPG Studies in Geology Series (CD book), 816p.

Vail, P. R., and W. W. Wornart, 1990, Well log-seismic sequence stratigraphy: an integrated tool for the 90's: Sequence Stratigraphy as an Exploration Tool: Gulf Coast Section–SEPM Foundation 11th Annual Research Conference Houston, p. 379-388.

Appendix A: Paleogeographic maps

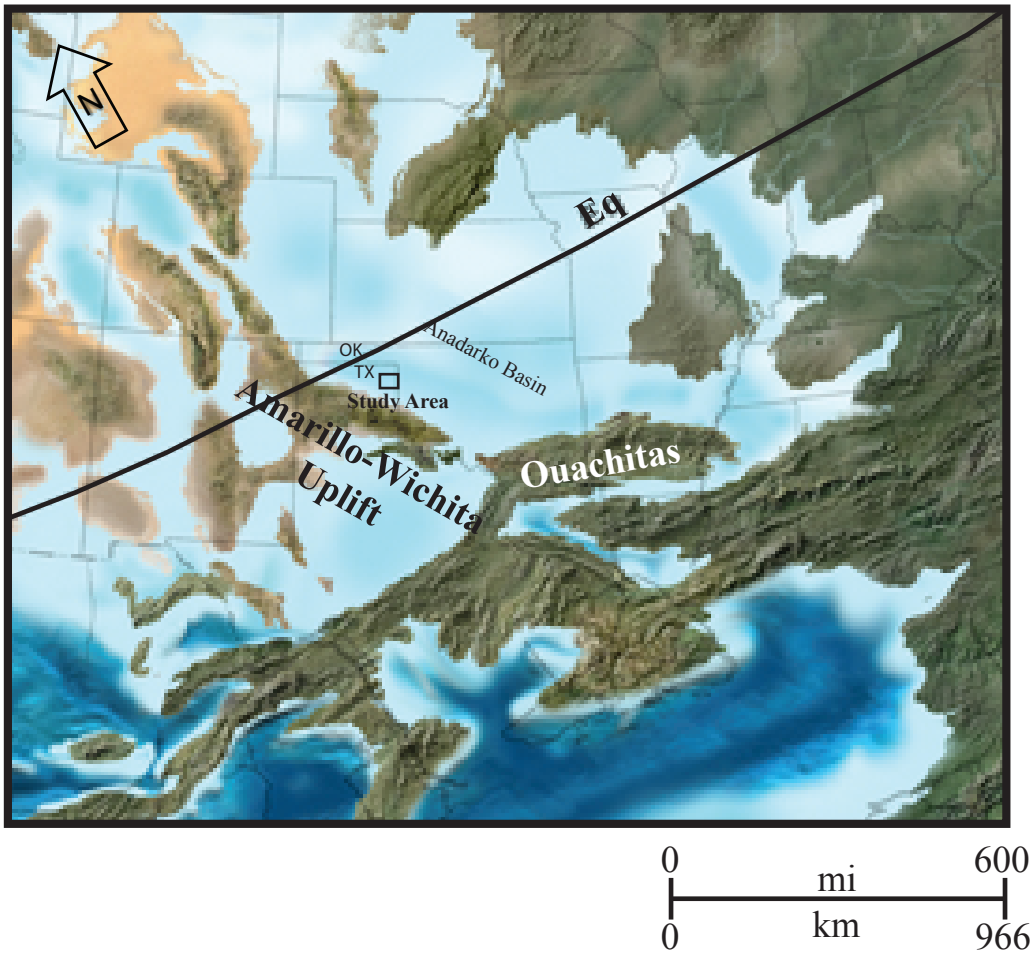

Figure A-1. Middle Pennsylvanian (308 Ma) paleogeographic map (modified from Blakey, 2013). Study area is shown by a black rectangle. The Amarillo-Wichita Uplift started to form in Early Pennsylvanian with the onset of the compressional regime while the Anadarko Basin started to subside. It is located in the southern Anadarko Basin, just in front of the Amarillo-Wichita Uplift. Sediments eroded from the Amarillo-Wichita Uplift were transported to the basin as alluvial fan, fan-delta, debris flow and turbidite deposits.

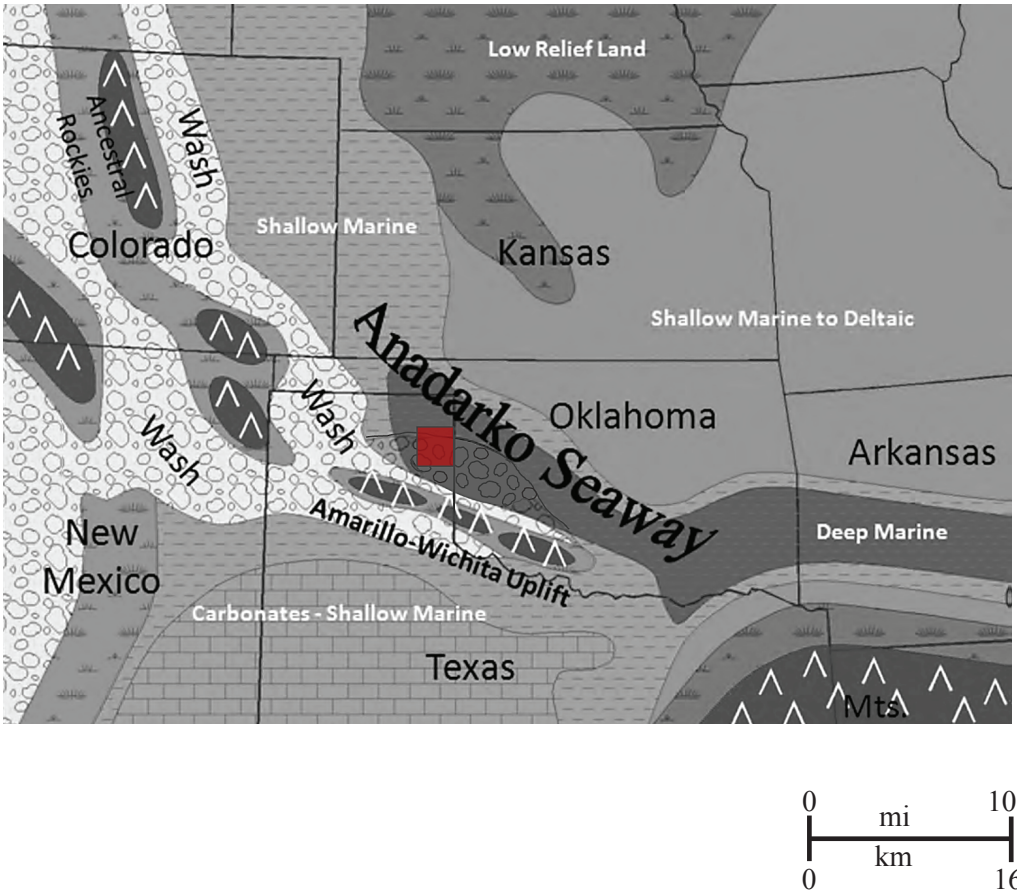

Figure A-2: Middle Pennsylvanian (Desmoinesian) paleogeography in Mid-Continent area (Modified from Moore, 1979 and Mitchell, 2011). Study area is shown in red rectangle and it corresponds to coarse grained deep marine depositional environment.

Appendix B: Core descriptions

Two cores, Shell 1-60 Hobart and Devon 1-3H Lott were described in terms of lithology, grain size, sorting, roundness, color, and sedimentary structures. The legend for the core description is as follows.

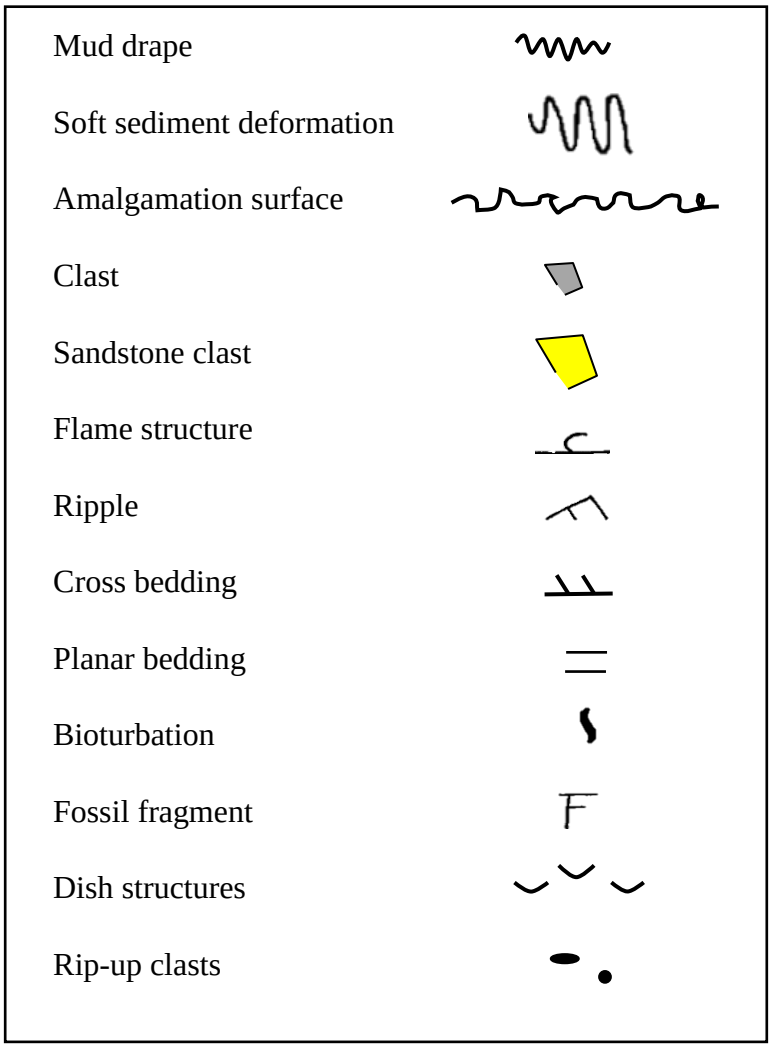

Shell 1-69 Hobart

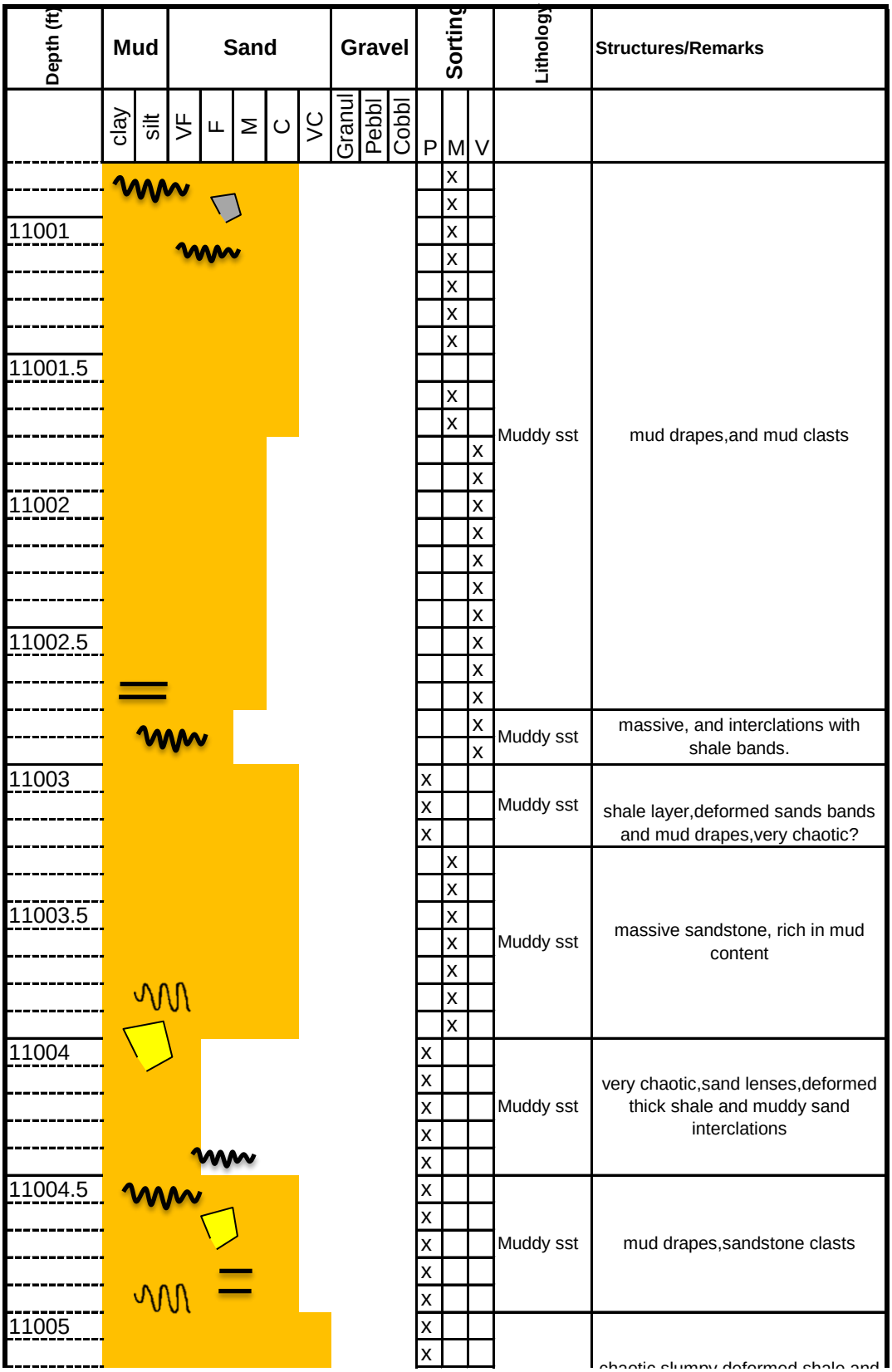

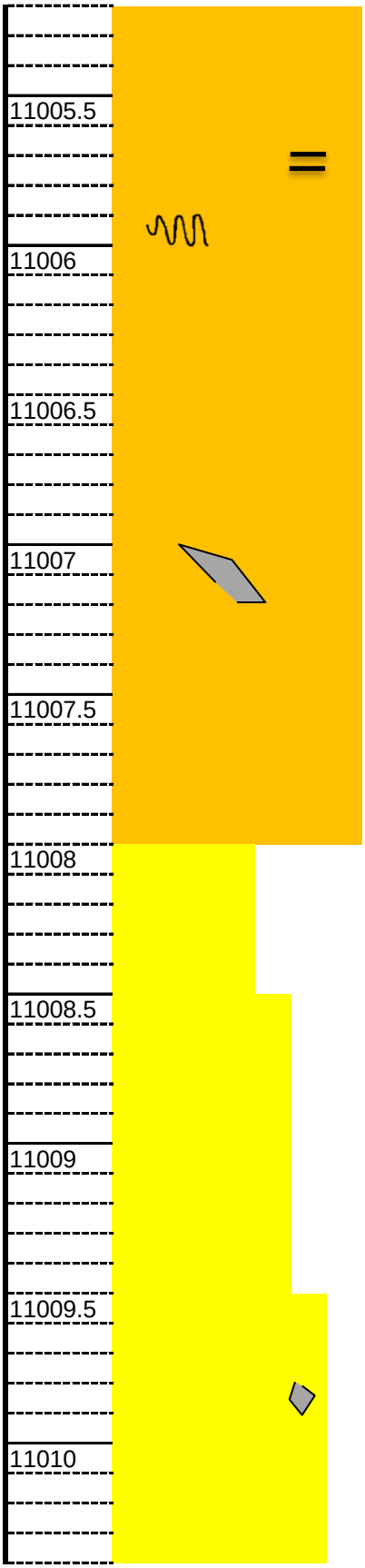

x				chaotic,slumpy,deformed shale and fine sandstone interclations
x				
x				
	x			massive sandstone,dark color because of high clay content
	x			
	x			
	x			
	x			
	x			chaotic,slumpy,deformed shale and fine sandstone interclations
	x			
	x			
	x			
	x		Muddy sst	
x				massive sandstone,dark color because of high clay content
x				
x				
x				
x				
x				very large elongated mud clast,sand clasts,upper part(below the boundary) is chaotic, slumpy?? Angular grains
x				
	x			
	x			
	x			
	x			massive sandstone,dark color because of high clay content
	x			
	x			
	x			
	x			
		x		massive sandstone
		x		
		x		
		x		
		x		
		x		
		x		
		x	Sandstone	
		x		
		x		
		x		
		x		
		x		
		x		
		x		
	x			massive, mud clasts
	x			
	x			
	x			
	x			
	x			
	x			
	x		Sandstone	
	x			

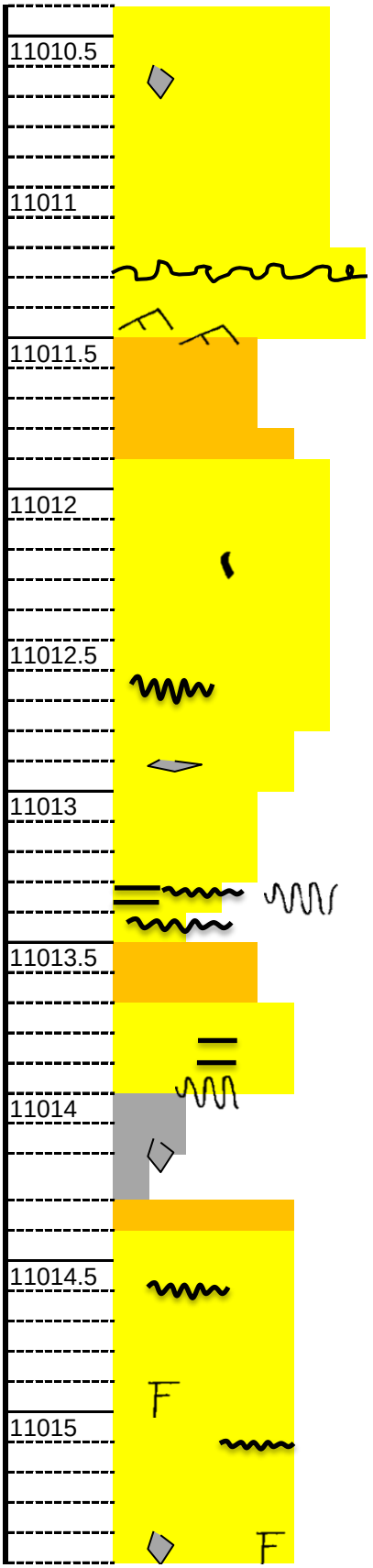

	x			
	x			
	x			
	x			
	x			
	x			
x			Sandstone	massive sandstone,slight fining upward, lower boundary is deliniated with subangular pebbly grains
x				
x				
x				
x				
x			Muddy sst	sand lenses
x				
x				
		x	Sandstone	a thick mud drape, elongated fine sandstone band
		x		
		x		
		x		
	x			
	x			
	x			
	x			
	x			
		x		
		x		
		x		
		x		
		x		
		x	Sandstone	highly stramatolitic,bioturbation
		x	siltstone	shale band,stramatolite at the top
x			Muddy sand	very chaotic, very poorly sorted,interclations of shale bands muddy sandstone and fine
x				
	x		Sandstone	massive
	x			
	x			
	x		siltstone	mud clasts, increasing clay content, sandstone grading into sandy mud and then muddy sand
	x			
x			sandy Mudstone	
	x		Muddy sand	
	x			
	x			
		x	Sandstone	fossils, mud clasts
		x		
		x		
		x		
		x		
		x		
		x		
		x		
		x		
		x	Sandstone	

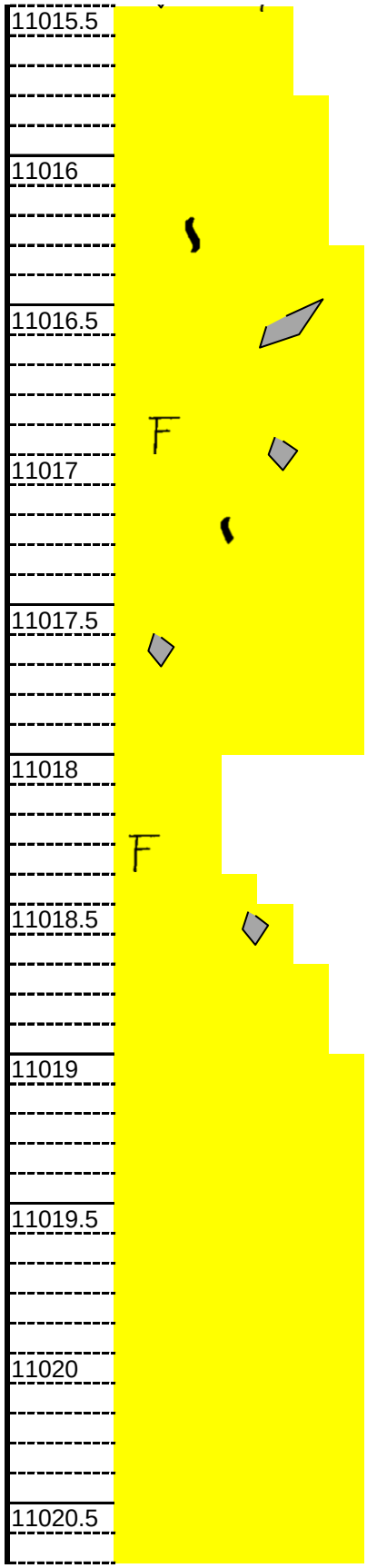

		x	Sandstone	
		x		
		x		
		x		
	x			
	x		Sandstone	massive,big elongated mud clasts embedded,bioturbation,fining upward
	x			
	x			
	x			
	x			
	x			
	x			
	x			
x			Sandstone	fossils,bioturbation, massive,abrupt change in grain size from very fine to very coarse
x				
x				
x				
x				
x				
x				
x				
x				
x				
x				
		x	Sandstone	fining upward,a few fossil traces
		x		
		x		
		x		
		x		
		x		
	x			
	x			
	x			
	x			
	x			
	x			
	x			
	x			
	x			
	x			
	x			
	x			
	x		Sandstone	Lower boundary is abrupt from very fine sand to very coarse sand. Boundary is deliniated with amalgamation surface
	x			
	x			
	x			
	x			
	x			
	x			
	x			
	x			
	x			
	x			
	x			
x				
x				
x				
x				
x				

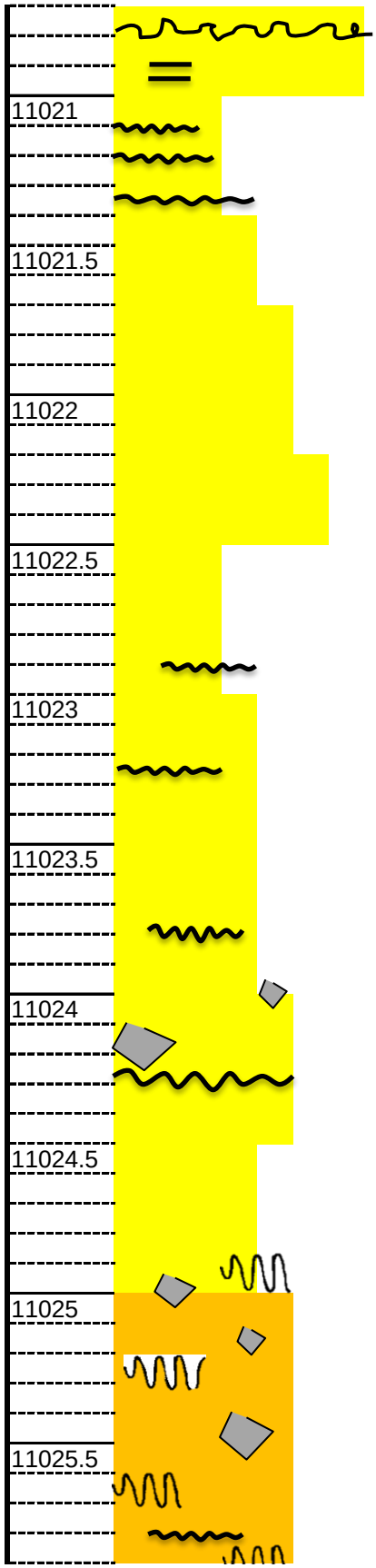

x				
x				
x				
		x	Sandstone	fining upward,
		x		
		x		
		x		
		x		
		x		
		x		
	x			
	x			
	x			
	x			
	x			
	x			
	x			
		x	Sandstone	very large black mud clast at the bottom of the section with deformed thin shale layer, mud clasts, a very big mud drape, fining upward
		x		
		x		
		x		
		x		
		x		
		x		
		x		
		x		
		x		
		x		
		x		
		x		
		x		
		x		
		x		
		x		
	x		Sandstone	massive sandstone
	x			
	x			
	x			
	x			
			Muddy sst	very chaotic slump? Elongated mud drapes, a huge mud clasts embeded
x				
x				
x				
x				
x				
		x		
		x		

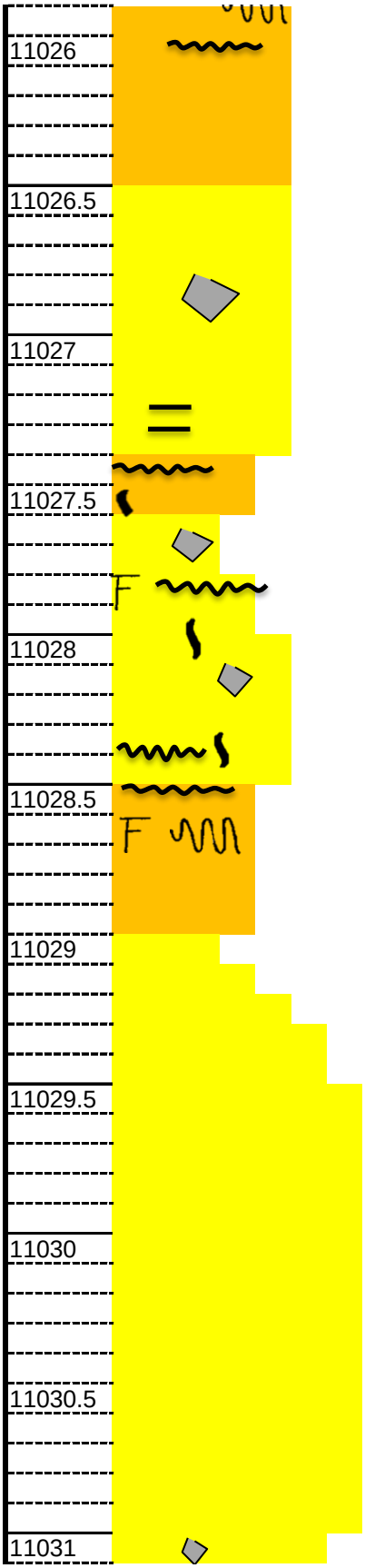

		X	Muddy sst	elongated mud drapes, big mud clasts
		X		
		X		
		X		
		X		
		X		
		X	Sandstone	a very large mud clast embedded inside of the core
		X		
		X		
		X		
		X		
		X		
X			Muddy sst	shle layers interclated with muddy sandstone
X				
		X	Sandstone	bioturbation,mud clasts, fining upward
		X		
		X		
		X		
		X	Sandstone	fossils,mud clasts,bioturbation thin shale layers at the upper boundary
		X		
		X		
		X		
		X		
		X	Muddy sst	muddy sandstone interclated with fine grained sandstone and thin shale layers. Fossils. Deformed sandstone, slump structures. Grains embedded in to mud drape, 1 cm thick shale layer, mud drapes
		X		
		X		
		X		
		X		
		X	Sandstone	massive sandstone with fining upward sequence, in the middle there is a thin siltstone bend
		X		
		X		
	X		Sandstone	massive sandstone
	X			
	X			
	X			
	X			
	X			
	X			
	X			
	X			
	X			
	X			
	X			
	X			
	X			
	X			
	X			

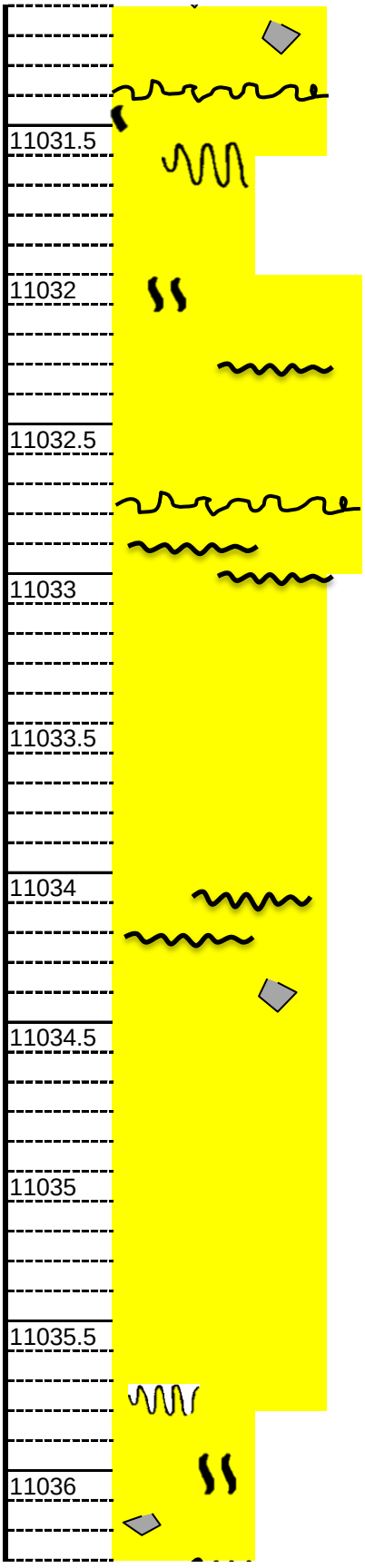

	x		Sandstone	massive, mud clasts
	x			
	x			
	x			
	x		Sandstone	interclated with muddy sandstone,bioturbation,upper boundary is deliniated with amalgamation surface
	x			
x				
x				
x				
	x		Sandstone	massive with bioturbation, mud drape
	x			
	x			
	x			
	x			
	x			
	x			
	x			
	x			
	x			
		x		mud drape. Amalgamation surface at the upper most boundary with very coarse sandstone
		x		
		x		
		x		
	x		Sandstone	mud clasts, mud drape, massive
	x			
	x			
	x			
	x			
	x			
	x			
	x			
	x			
	x			
	x			
	x			
	x			
	x			
	x			
	x			
	x			
	x			
	x			
	x			
	x			
	x			
	x			
	x		Sandstone	bioturbation, two bends of coarse sandstone,chaotic slump?, shale bend at the top boundary
	x			
	x			
	x			
	x			

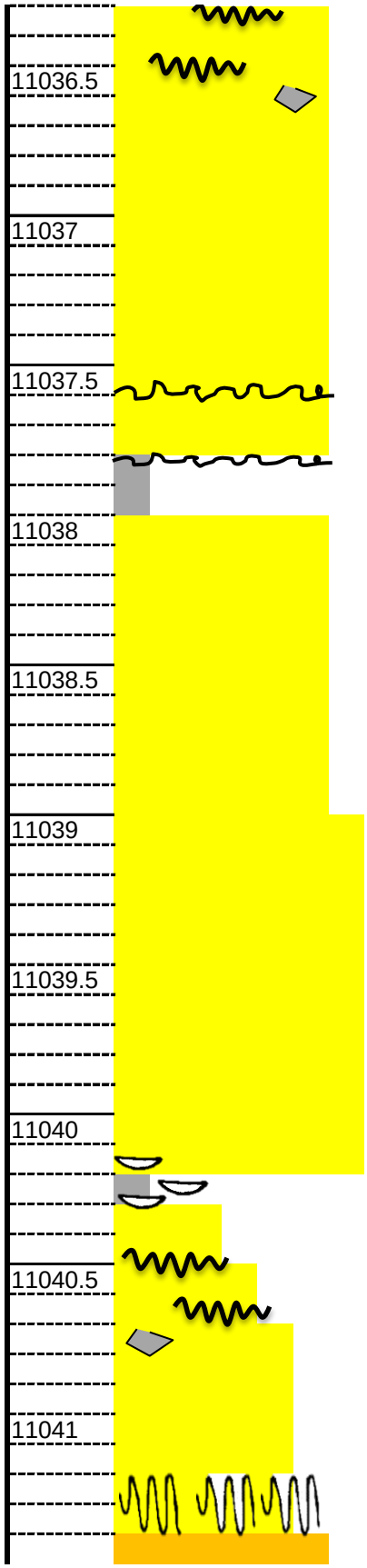

	x		Sandstone	mud drape, mud clasts.
	x			
	x			
	x			
	x			
	x			
	x			
	x			
	x			
	x			
	x			
	x			
	x			
		x	Mudstone	massive, highly thin laminated
		x		
	x		Sandstone	massive sandstone
	x			
	x			
	x			
	x			
	x			
	x			
	x			
x			Sandstone	abrupt change from shale to very coarse sand
x				
x				
x				
x				
x				
x				
x				
x				
x				
x				
			Mudstone	massive
			Sandstone	trough cross bedding, mud clast, mud drape, bioturbation?
		x	Sandstone	massive sandstone with mud drapes with an abrupt base
		x		
		x		
		x		
		x		
		x		
		x		
		x		
		x	Muddy sst	slump? Chaotic.

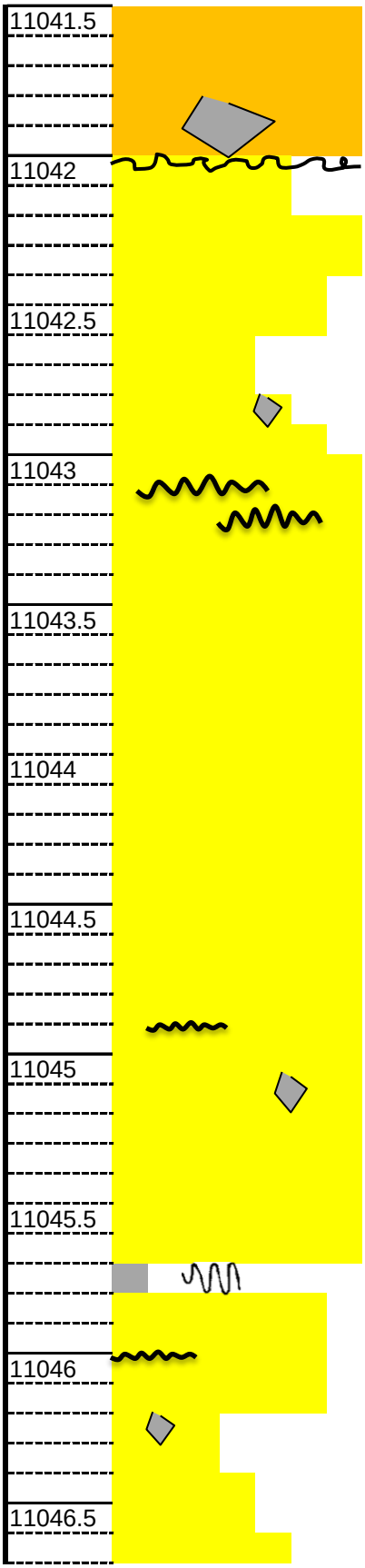

X			Muddy sst	massive sandstone
X				
X				
X				
X				
		X	Sandstone	a huge mud clast (8x3 cm)on top within fine sandstone, fining upward and then coarsenin upward sequence
		X		
		X		
		X		
		X		
		X		
		X		
		X		
		X		
X			Sandstone	massive sst
X				
X				
X				
X				
X				
X				
X				
X				
X				
X				
X				
X				
X				
X			Sandstone	massive sandstone, mud drape and mud clast
X				
X				
X				
X				
X				
X				
X				
X				
		X	Mudstone	massive shale band
			Sandstone	massive sandstone,grading into very fine sand, convolute bedding
		X		
		X		
		X	Sandstone	mud drape, mud clast,fining upward
		X		
		X		
		X		
		X		

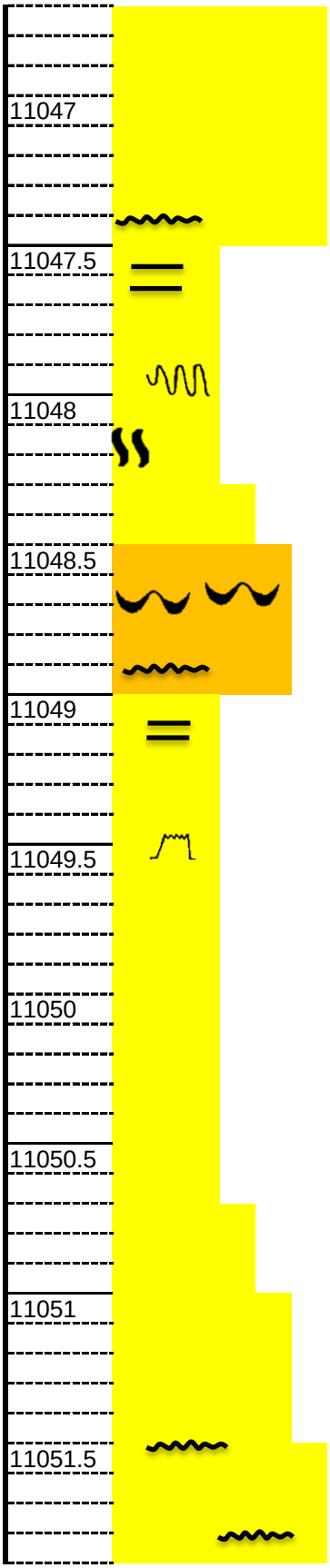

		x	Sandstone	massive sandstone
		x		
		x		
		x		
		x		
		x		
		x		
		x		
			Sandstone	thin shale layers and a thick shale bend at the top
				continued thick shale layers at the bottom, cleaning and fining upward sandstone, thin shale layers at the top part
	x		Muddy sst	flaser bedding within the lower third and thick shale layers abundant through section:fine sand interclations
	x			
	x			
	x			
	x			
		x	Sandstone	massive,styolite at the top and siltstone layers
		x		
		x		
		x		
		x		
		x		
		x		
		x		
		x	Sandstone	massive,fining upward
		x		
		x		
		x		
		x		
		x		
		x		
		x		
		x		
		x		
		x	Sandstone	
		x		
		x		
		x		
		x		
		x	Sandstone	massive, mud drapes
		x		
		x		
		x		
		x		

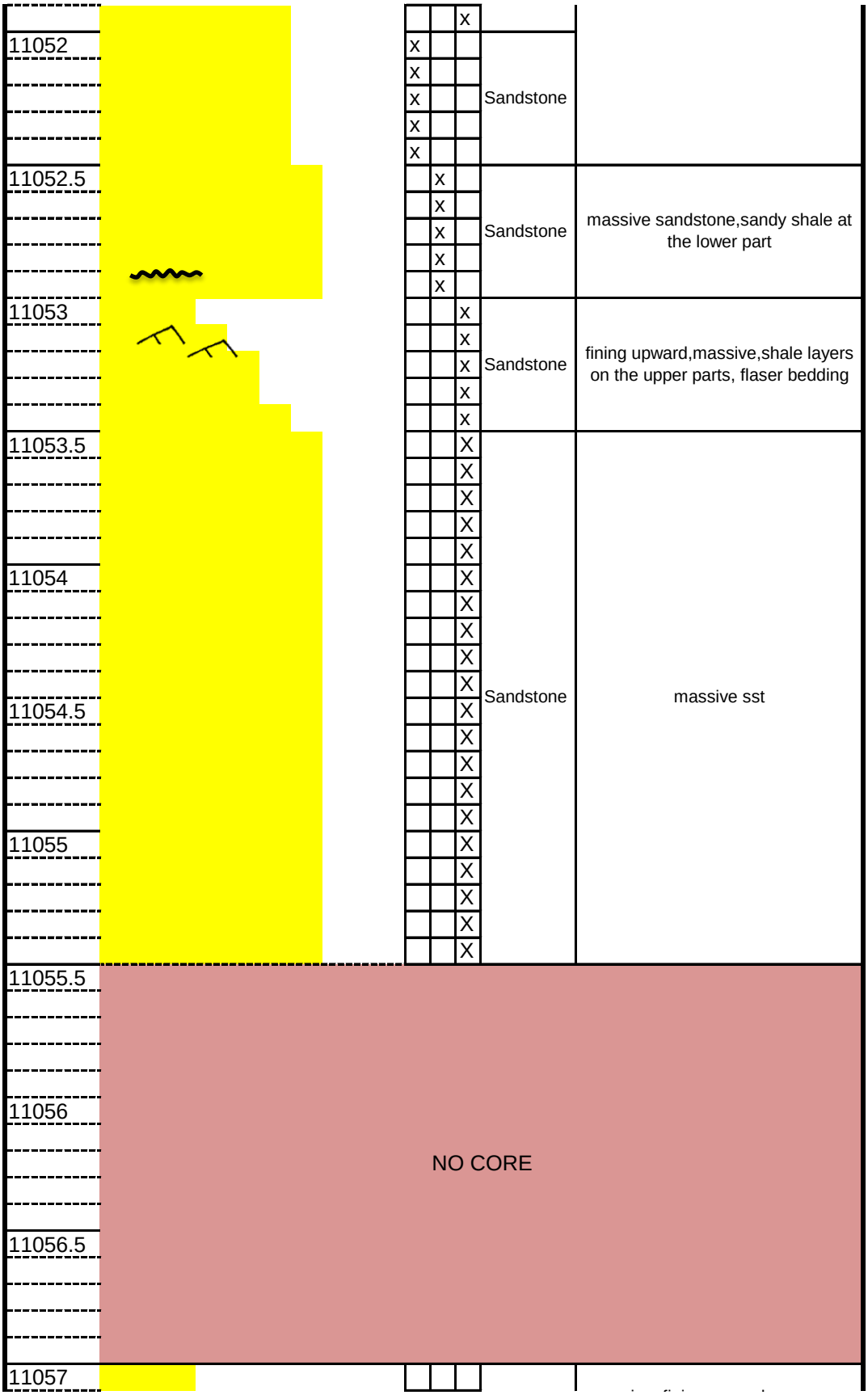
11052
11052.5
11053
11053.5
11054
11054.5
11055
11055.5
11056
11056.5
11057
Sandstone
Sandstone
massive sandstone,sandy shale at the lower part
Sandstone
fining upward,massive,shale layers on the upper parts, flaser bedding
Sandstone
massive sst
NO CORE

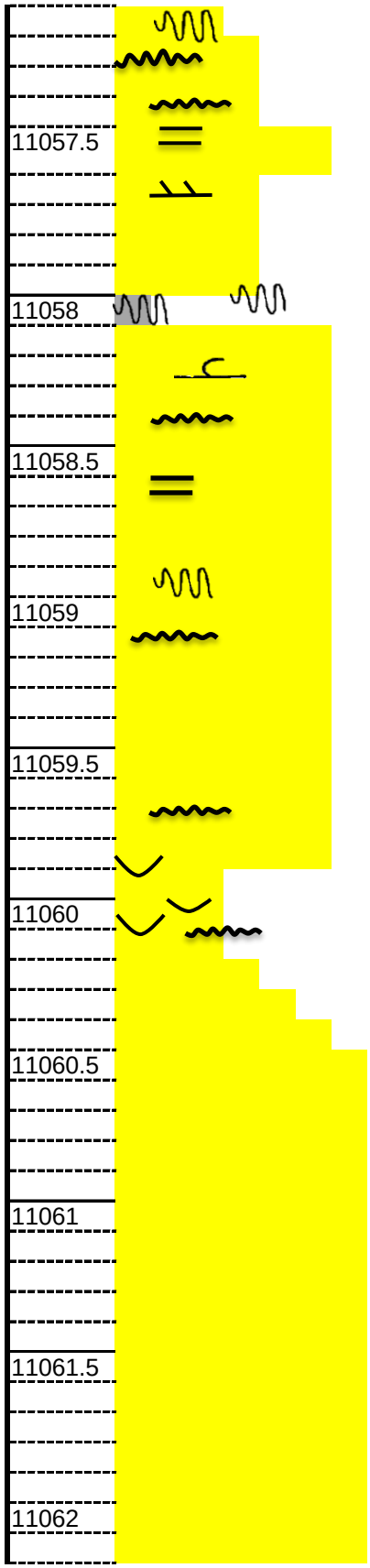

			Sandstone	massive, fining upward sequence, upper quarter is characterized by increasing abundance of thin shale layers, mud drapes
			Sandstone	massive,thin shale layers at the top in transition to upper shale layer
			Sandstone	massive sandstone, upper part is abundant with thin shale layers.
		x	Mudstone	massive shale layer
x			Sandstone	highly deformed bended shale layers,slump?, flame str, Topped with massive shale layer
	x		Sandstone	shale layers, deformed shale bands
		x	Sandstone	massive, dish structures and mud drapes
x			pebbly Sandstone	massive sst

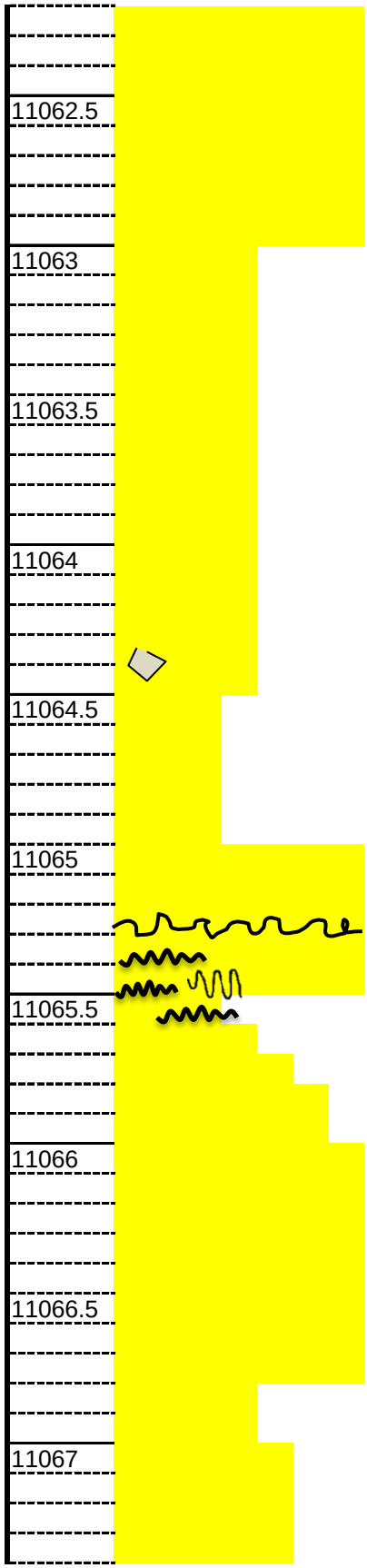

X				
X				
X				
X				
X				
X				
X				
		X	Sandstone	oblique shale layer cuts through and seperates fine grained sandstone from very fine grained sandstone. Possible reverse fault? Non-linear shale layer. Within the fine grained sst, an inclined shale layer parallel to fault.A large Interclast (2x2 cm) interclast at the the upper boundary and lateral grain size change.
		X		
		X		
		X		
		X		
		X		
		X		
		X		
		X		
		X		
		X	Sandstone	massive sandstone, lateral grain size change??
		X		
		X		
		X		
		X		
X			Sandstone	massive sandstone, big quartz grain embedded.lateral grain size change??
X				
X				
X				
X				
X			Sandstone	massive, amalgamation surface at the bottom
X				
X				
X				
X				
		X	Sandstone	fining upward,upper parts are dominant with mud drapes and deformed mud drapes
		X		
		X		
		X		
		X		
	X		Sandstone	massive sst
	X			
	X			
	X			
	X			
	X			
	X			
	X			
	X			
		X	Sandstone	massive sandstone with fining
		X		
		X		
		X		
		X		
		X		

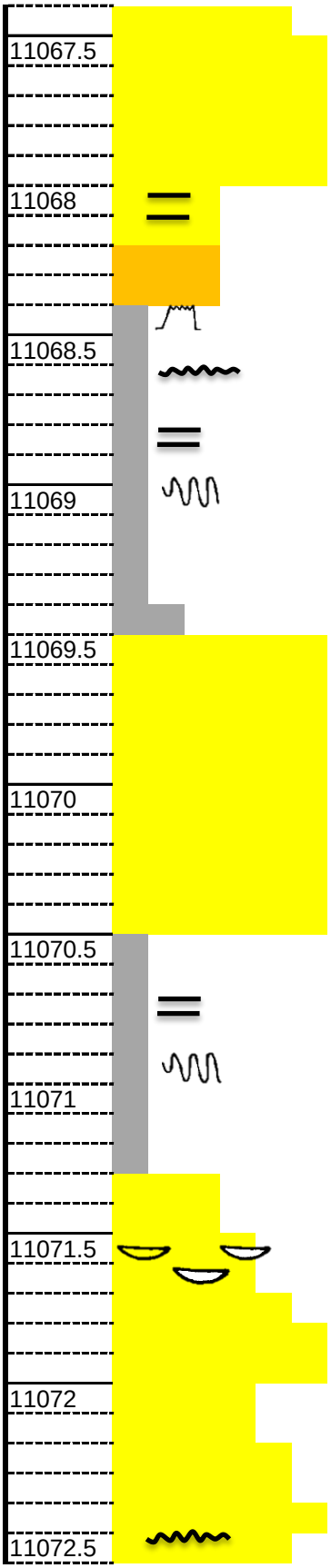

		X	Sandstone	upward sequence
		X		
		X		
		X		
		X		
		X		
		X	very fine Sandstone	interclations of muddy sand and sandy shale with stramatolites and mud drapes. Cleaning upwards to very fine sandstone
		X		
X			Muddy sst	
X				
		X	Mudstone	massive, within the sandy shale part shale/silt layers and stylolites and mud drapes
		X		
		X		
		X		
	X		sandy Mudstone	
	X			
	X			
	X			
	X			
		X	Mudstone	
		X	siltstone	
	X		Sandstone	abrupt change from shale to coarse sand in the upper and lower boundary
	X			
	X			
	X			
	X			
	X			
	X			
	X			
	X			
	X			
		X	Mudstone	bended shale interclated with sandy mud, mud drape
		X		
		X		
		X	sandy Mudstone	no structure
		X		
		X	sandy Mudstone	silt layers
		X		
		X		
		X	Sandstone	fining upward, massive. Upper part is very fine sand band which shows trough cross bedding and it passes abruptly to shale
		X		
		X		
		X		
	X			
	X			
		X		fining upward,massive
		X		
	X			
	X			
X				
	X			

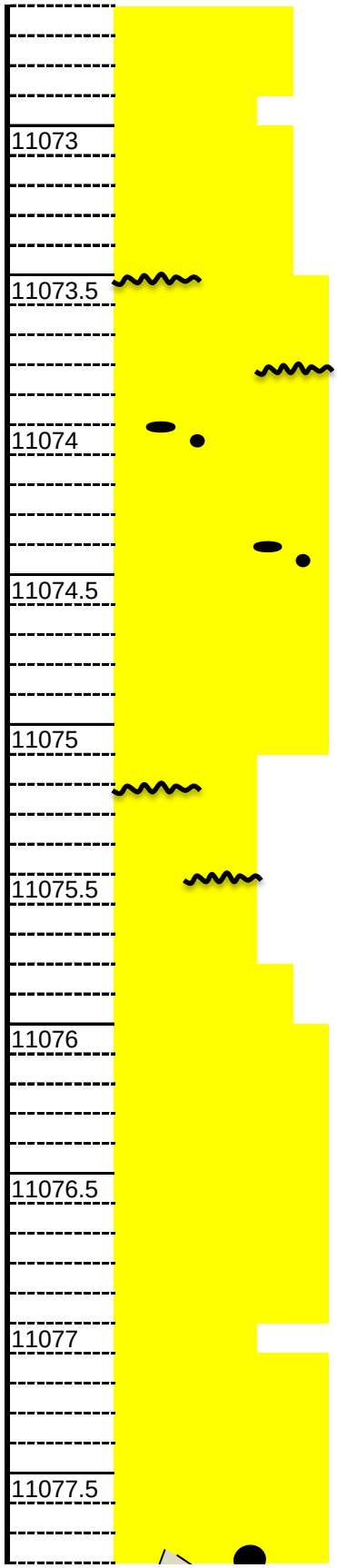

	x		Sandstone	massive sst with mud drapes
	x			
	x			
	x		Sandstone	massive, fining upward with large muddy clast? Mud drapes and possible fossil within the mud clast
		x		
		x		
		x		
		x		
		x		
	x		Sandstone	massive sst,mud clasts and drapes
	x			
	x			
	x			
	x			
	x			
	x			
	x			
	x			
	x			
	x			
	x			
	x			
		x	Sandstone	massive with mud drapes
		x		
		x		
		x		
		x		
		x		
		x		
		x		
		x		
		x		
		x		
		x		
		x		
	x		Sandstone	massive sandstone
	x			
	x			
	x			
	x			
			Sandstone	massive sandstone with fine sand band

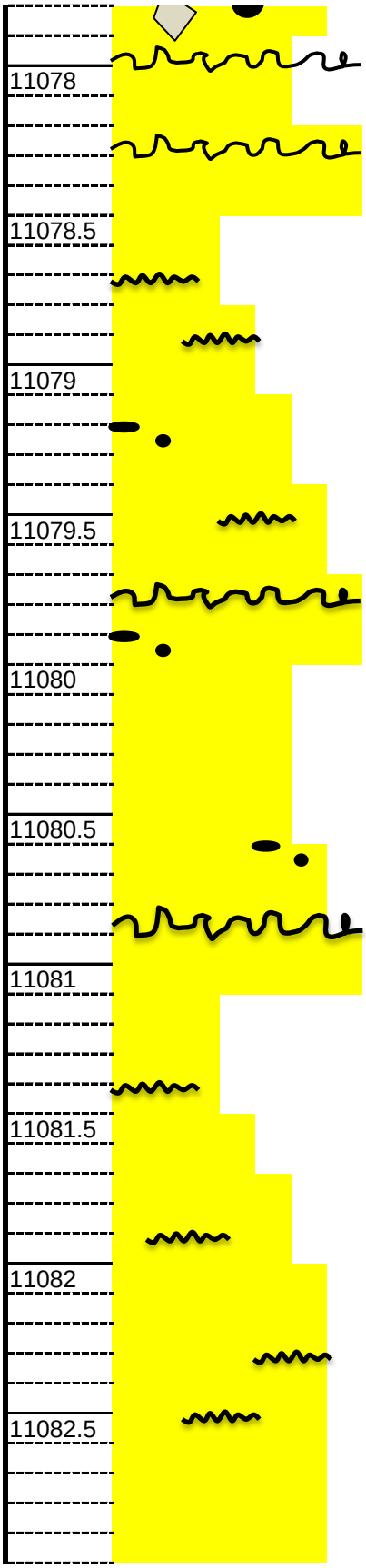

		x	Sandstone	big quartz clast, amalgamation surface with below coarse sand. Very large mud clasts embedded in the core
		x		
		x		
	x		Sandstone	abrupt change at the top and bottom. from very fine sand to coarse sand, clasts lying below the contact within the fine sand
	x			
	x			
		x	Sandstone	abrupt change, very coarse sand is fining upward to very fine sand
		x		
		x		
		x		
		x		
		x		
		x		
		x		
		x		
		x		
		x		
		x		
	x		Sandstone	very abrupt change at the base from very fine sand to pebbly sandstone.upper parts are massive sand with mud clasts.
	x			
	x			
	x			
	x			
	x			
	x			
	x			
	x			
	x			
	x			
x				
x				
			Sandstone	lots of mud drapes
		x	Sandstone	massive with mud drapes, finig upward,discoloration??
		x		
		x		
		x		
		x		
		x		
		x		
	x			deformed shale layer at the bottom topped with fine sand and a scoured base delinated by mud drapes;
	x			
	x			
	x			
	x			
	x			
	x			
	x			
	x			
	x			

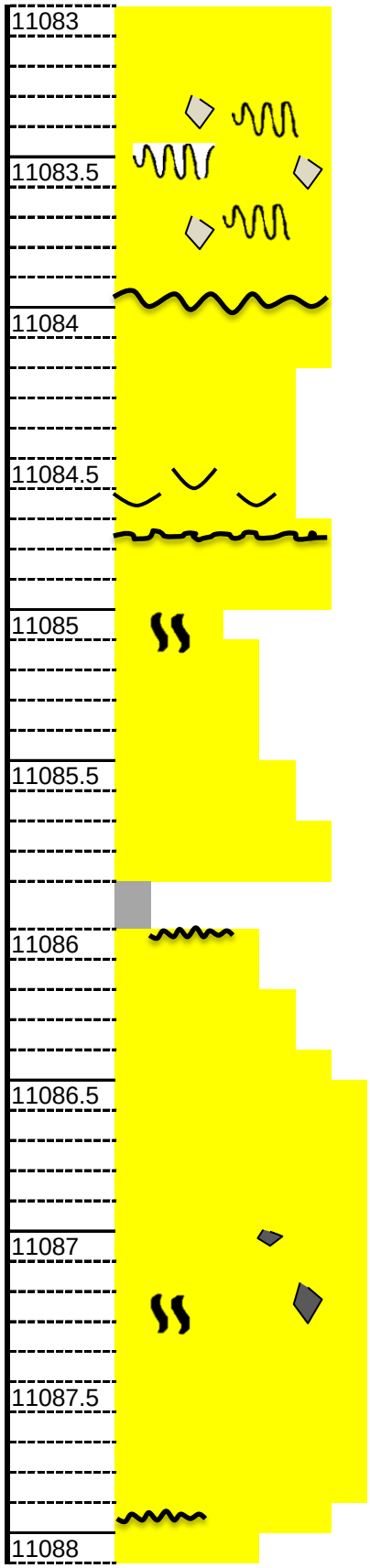

	x		Sandstone	representing an abrupt change with clasts.and a typical slump structure indicating chaotic deposition. Upper parts represented with massive sand with mud drapes
	x			
	x			
	x			
	x			
	x			
	x			
	x			
	x			
	x			
x				
x				
		x	Sandstone	amalgamation surface at the bottom,dish structures observed through upper parts
		x		
		x		
		x		
	x	x		
	x			
	x			
	x			
			Sandstone	increasing mud content through upward, fining upward, with two sand layer interclations,upper being coarse sand, lower being fine sand(pinching out shape)
		x	Mudstone	thin laminated shale band,abrupt change at the top and bottom
		x	Sandstone	massive with mud drapes
		x		
		x		
		x		
		x		
	x		Sandstone	massive with mud clasts
	x			
	x			
	x			
	x			
	x			
	x			
	x			
	x			
	x			
		x		
		x		

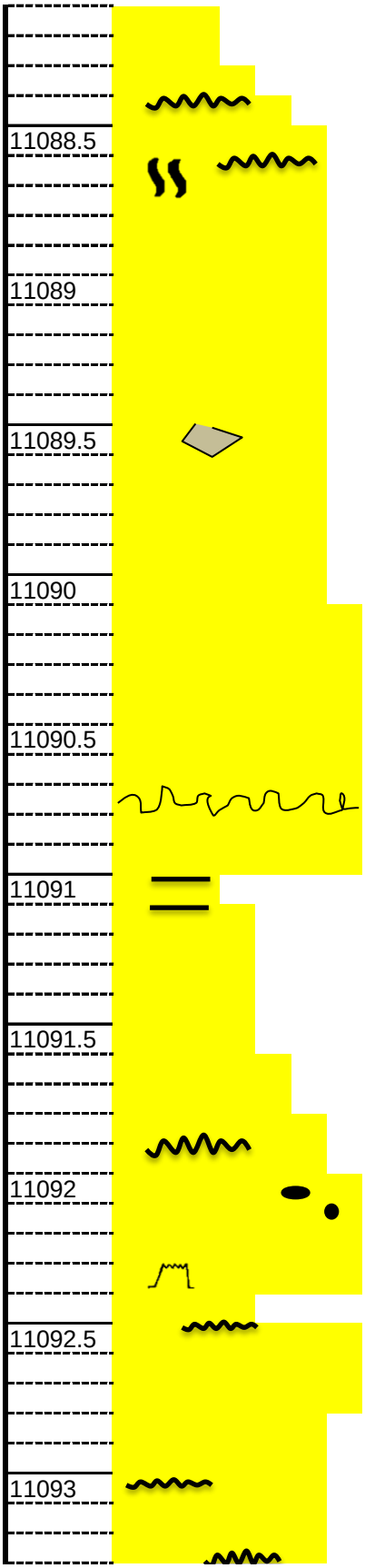

		x	Sandstone	massive with mud drapes
		x		
		x		
		x		
	x		Sandstone	massive sst with mud drapes and bioturbation
	x			
	x			
	x			
	x			
	x			
	x			
	x			
	x		Sandstone	fine sand layer with a quartz interclast
	x			
	x			
	x			
	x			
			Sandstone	massive
	x			
	x			
	x			
	x			
	x			
		x	Sandstone	shale layers with mud drapes,shale sand interclation
		x		
		x		
		x		
		x		
		x		
		x		
		x		
		x		
		x		
	x		Sandstone	massive with mud drapes, fine grain band with mud clast
	x			
	x			
	x			
		x		
		x	Sandstone	mud drapes, stylolites
		x		
		x		
		x		
		x		
	x		Sandstone	mud drapes, massive
	x			
	x			

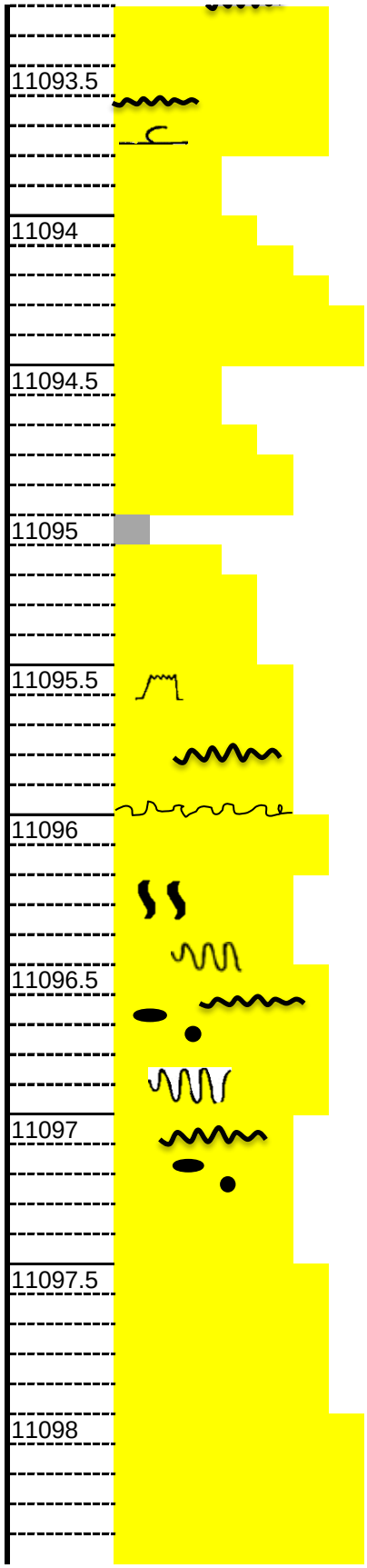

	x			
	x			
	x			
	x			
	x		Sandstone	flame str, mud drapes
	x			
	x			
	x			
	x			
	x		Sandstone	abrupt base at the bottom contact from very fine to granule,fining upward
	x			
	x			
	x			
		x		
		x		
		x	Sandstone	massive
		x		
		x		
		x	Mudstone	
		x		
		x	Sandstone	massive
		x		
		x		
		x		
		x		
		x		
		x	Sandstone	massive, some stylolites and mud drapes
		x		
		x		
		x		
		x		
x				
x				
x				
		x		
		x		
		x	Sandstone	mud clasts, slumping structures, mud drape at the top, muddy sandy mixture, soft sed deformation, bioturbation
		x		
		x		
	x			
	x			
	x		Sandstone	slumping,mud drapes, mud clasts, convolute bedding
	x			
	x			
		x		
		x		
		x	Sandstone	massive sst
		x		
		x		
x				
x				
x				
x				
x				

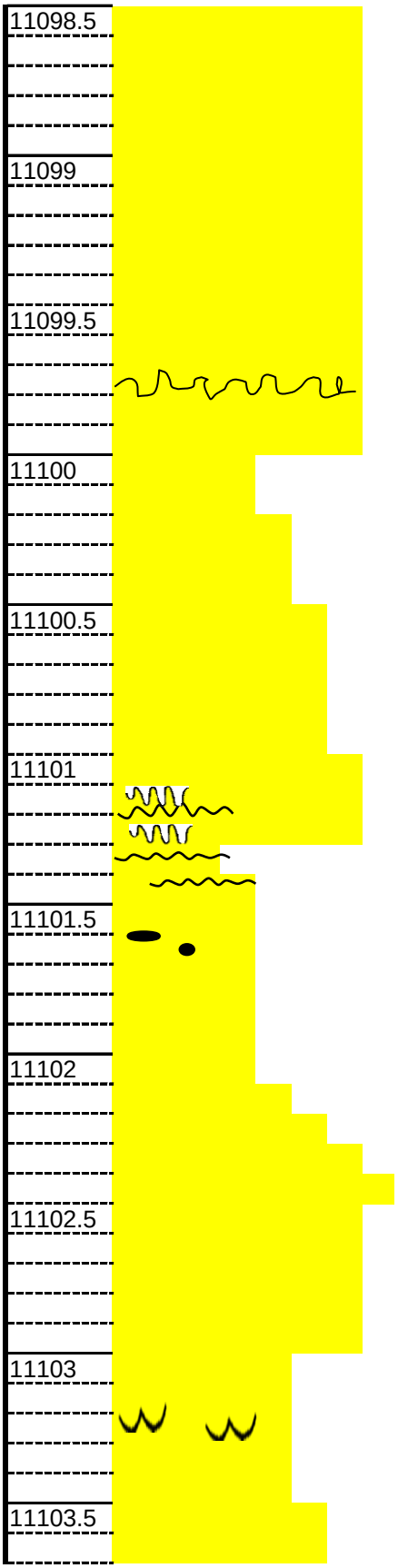

x			Sandstone	massive,
x				
x				
x				
x				
x				
x				
x				
x				
x			Sandstone	sharp contact, amalgamation surface at the bottom massive sandstone
x				
x				
x				
x				
x				
		x	Sandstone	massive with 4 cm clay rich band
		x		
		x		
		x		
		x		
		x		massive, fining upward
		x		
		x		
		x		
		x		
	x		s	an abrupt base at the bottom with mud drape, subangular grains
	x			
	x			
		x	Sandstone	mud drapes,increasing mud content as going upward,mud clasts, convolute bedding
		x		
		x		
		x		
		x		
		x		
		x	Sandstone	cont. finig upward
		x		
x			Sandstone	fining upward,shale bands
x				
x				
			Sandstone	scour base with large clasts at the bottom of the section bivalves(fossils),coarsening upward,subangular to subrounded grains within conglomerate
x			Sandstone	
x				
x				
x				
x				
		x		
		x		

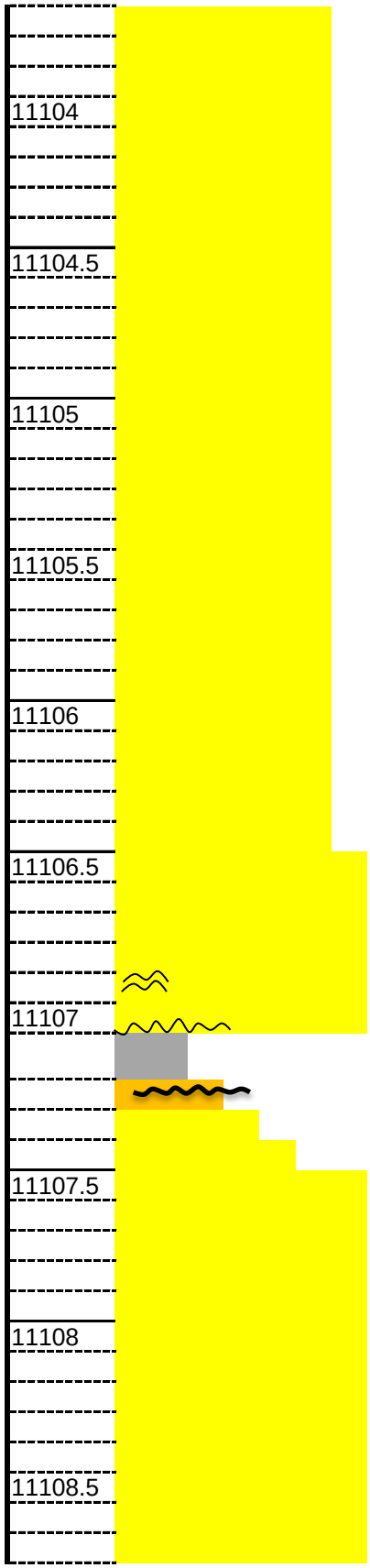

		x	Sandstone	massive sst,
		x		
		x		
		x		
		x		
		x		
		x		
		x		
		x		
		x		
		x		
		x		
		x		
		x		
		x		
		x		
		x		
		x		
		x		
		x		
		x		
		x		
		x		
		x		
		x		
x			Sandstone	massive sst
x				
x				
x				
x				
x				
		x	sandy Mudstone	sof sediment deformation (load cast)
		x	Muddy sst	fining upward,a muddrape,massive, abrupt boundary at the top with sst
		x	Sandstone	
		x		
	x		Sandstone	massive
	x			
	x			
	x			
	x			
	x			
	x			
	x			
	x			
	x			
	x			
	x			

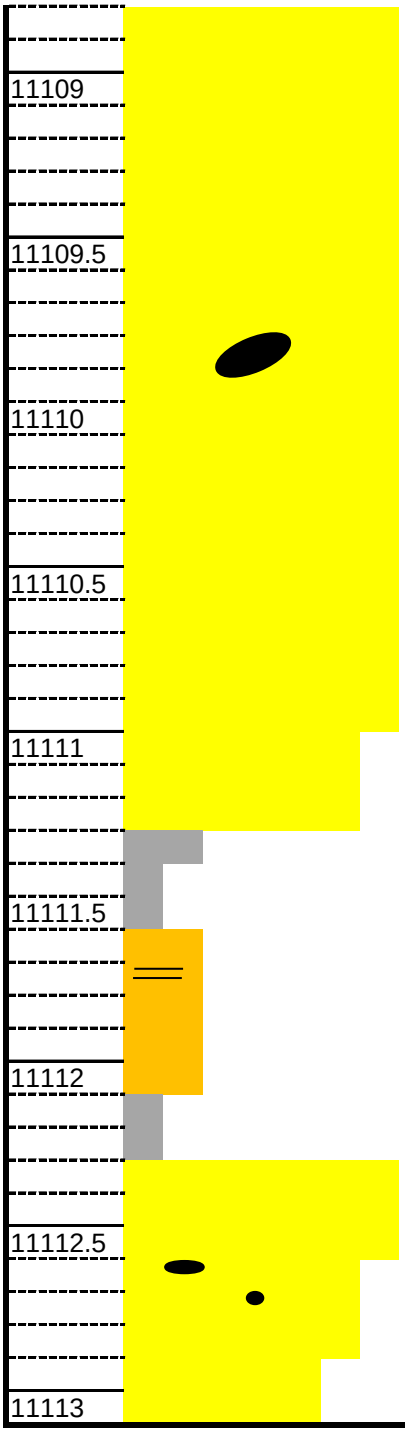

	x			
	x			
	x		Sandstone	massive sst
	x			
	x			
	x			
	x			
	x			
	x			
	x			
	x			
		x		a big elongated mud clast (5x1 cm) at 11.110 ft and fining upward, an abrupt change to massive very coarse sst
		x		
		x		
		x		
		x		
		x		
		x		
		x		
	x			
	x		Sandstone	massive sst,coarsening upward
	x			
		x		
		x		
		x		
	x			
	x		sandy Mudstone	coarsening upward
	x			
		x		
		x		
		x	silty Mudstone	laminated siltstone with black colored shale layering
		x		
		x		
			Mudstone	sharp contact at the bottom
		x		
		x		
		x		
		x		
		x	Sandstone	mud clasts,coarsening upward
		x		
		x		
		x		
		x		

Devon 1-3H Lott

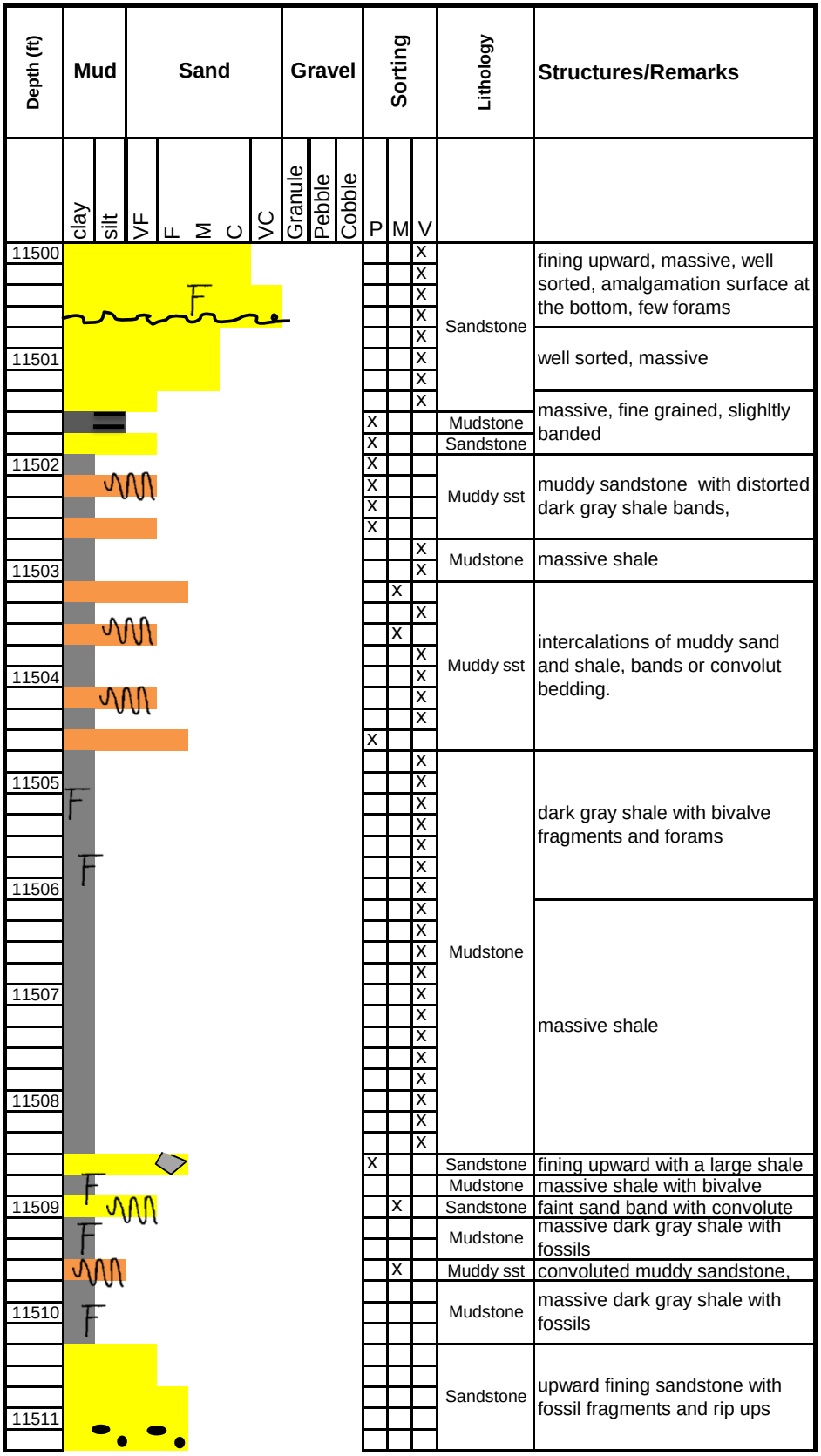

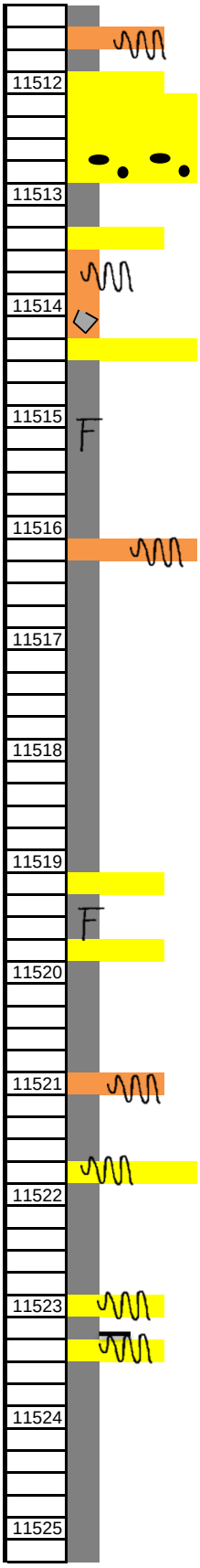

X			Mudstone	bands of shale, muddy sandstone , convolute bedding
X			Muddy sst	
X			Mudstone	
		X	Sandstone	fining upward sandstone with rip up clasts
		X		
		X		
	X			
	X			
		X	Mudstone	massive black shale
		X		
	X		Sandstone	massive sandstone
		X	Muddy sst	dark gray shale with convoluted muddy sandstone bands on the top part and a huge calcite clast
		X		
		X		
		X		
	X	X	Sandstone	massibe sandstone band
		X		dark gray shale with rare bivalve fragments
		X		
		X		
		X		
		X		
		X		
		X		shale and muddy sandstone, soft sediment deformed
X			Muddy sst	
		X	Mudstone	dark gray massive shale
		X		
		X		
		X		
		X		
		X		
		X		
		X		
		X		
		X		
		X		
		X		
		X		
		X	Sandstone	sandstone bed
		X		dark gray shale with bivalve fragments and forams
		X		
		X	Sandstone	sandstone bed
		X	Mudstone	dark gray massive shale
		X		
		X		
		X		
		X		
	X		Muddy sst	muddy sandstone intercalation
		X	Mudstone	dark gray massive shale
		X		
		X		soft sed deformed shale and muddy sandstone
		X	Sandstone	
		X	Mudstone	dark gray massive shale
		X		
		X		
		X		
		X		
	X		Sandstone	sof sed deformed sandstone layers within shale
	X		Mudstone	
X			Sandstone	
X				
	X			dark gray shale with an oblique
		X		
		X		
		X		
		X		
		X		
		X		
		X		

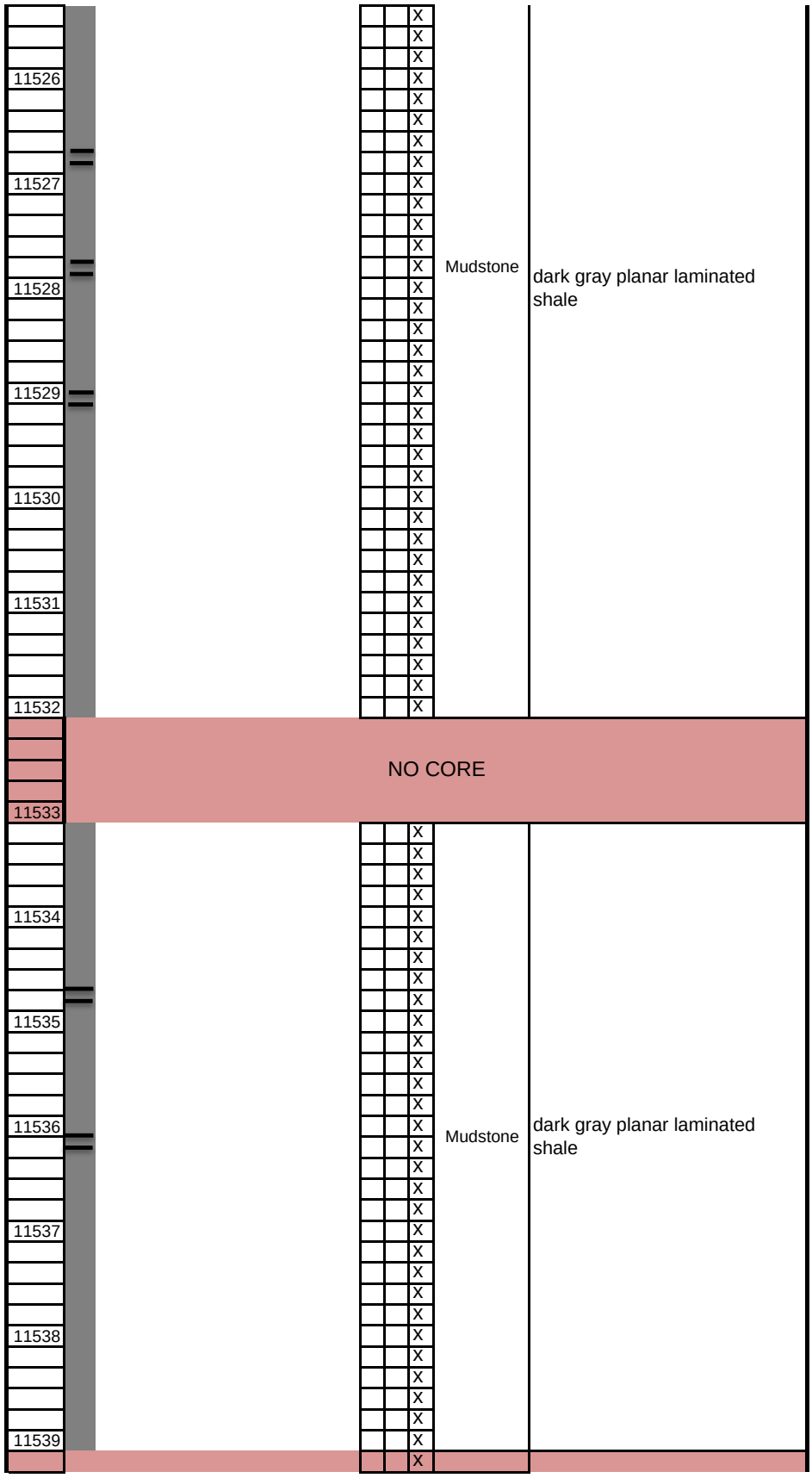
11526
11527
11528
11529
11530
11531
11532
11533
11534
11535
11536
11537
11538
11539
Mudstone
dark gray planar laminated shale
NO CORE
Mudstone
dark gray planar laminated shale

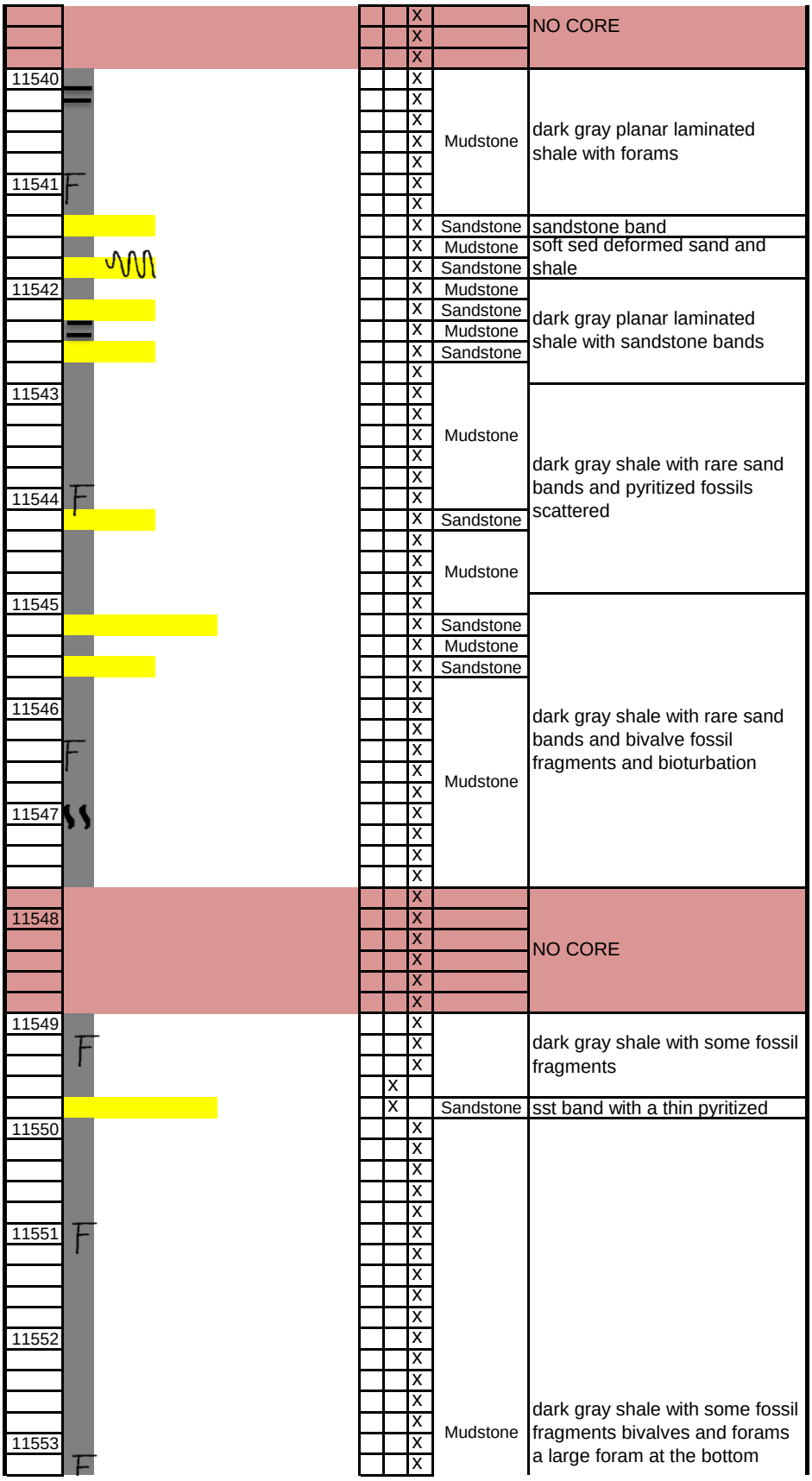
NO CORE
11540
11541
Mudstone
dark gray planar laminated shale with forams
Sandstone
sandstone band
Mudstone
soft sed deformed sand and shale
Sandstone
11542
Mudstone
Sandstone
Mudstone
Sandstone
dark gray planar laminated shale with sandstone bands
11543
11544
Mudstone
Sandstone
Mudstone
dark gray shale with rare sand bands and pyritized fossils scattered
11545
Sandstone
Mudstone
Sandstone
11546
11547
Mudstone
dark gray shale with rare sand bands and bivalve fossil fragments and bioturbation
NO CORE
11548
11549
dark gray shale with some fossil fragments
Sandstone
sst band with a thin pyritized
11550
11551
11552
11553
Mudstone
dark gray shale with some fossil fragments bivalves and forams a large foram at the bottom

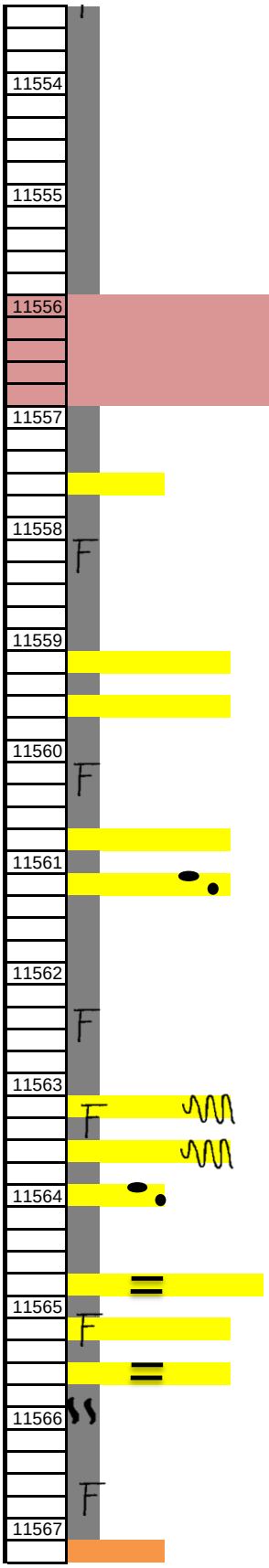

		X		
		X		
		X		
11554		X		
		X		
		X		
		X		
		X		
11555		X		
		X		
		X		
		X		
		X		
11556		X		NO CORE
		X		
		X		
		X		
		X		
11557		X		
		X	Mudstone	
		X		
		X	Sandstone	
		X		dark gray shale with some fossil fragments bivalves and forams
11558		X		
		X		
		X	Mudstone	
		X		
		X		
11559		X		laminated dark gray shale with thin layers of sandstone and some bivalves
	X		Sandstone	
		X	Mudstone	
	X		Sandstone	sandstone with some ripples
		X		
11560		X		
		X	Mudstone	dark gray shale with some fossil fragments bivalves and forams
		X		
		X		
	X		Sandstone	sandstone layers with some biturbation and rip up clasts
11561		X	Mudstone	
	X		Sandstone	
		X		
		X		
		X		
11562		X		
		X	Mudstone	dark gray shale with some fossil fragments bivalves and forams
		X		
		X		
		X		
11563		X		
X			Sandstone	sandstone with a deformed
		X	Mudstone	dark gray shale wih bivalve
X			Sandstone	sst with rip up clasts and soft
		X	Mudstone	
	X		Sandstone	
11564		X		dark gray shale with some fossil fragments bivalves and forams and planar thin sand/shale layers
		X	Mudstone	
		X		
	X		Sandstone	
11565		X	Mudstone	
X			Sandstone	
X			Mudstone	soft sed deformed sand and shale
X			Sandstone	
X				dark gray shale woth some bioturbation
11566		X		
		X		
		X	Mudstone	dark gray shale with few bivalve fossils
		X		
		X		
11567		X		
	X		Muddy sst	muddy sand band

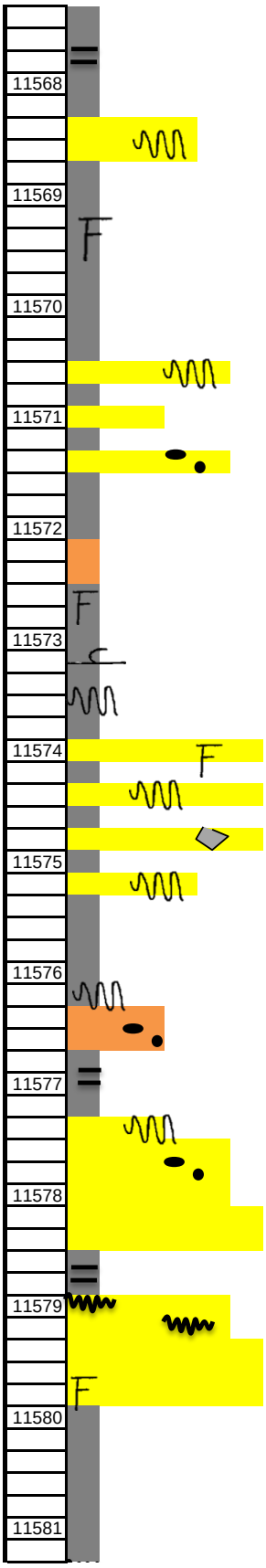

	X		Mudstone	dark gray shale with some sand layers within laminated or distorted slighltly
	X			
	X			
	X			
	X			
	X		Sandstone	sandstone with some thick convoluted shale layers
	X			
	X			
		X	Mudstone	dark gray massive shale with bivalves
		X		
		X		
		X		
		X		
		X		
		X		
		X		
	X		Sandstone	convolute bedding sand and shale
X			Mudstone	
X			Sandstone	
X			Mudstone	large shaly rip ups witihin sandstone
X			Sandstone	
		X	Mudstone	irregular sand bands within
		X		dark gray layered shale with bivalve fragments
		X		
		X	Muddy sst	layered shale and coarse grained muddy sandstone
		X		
		X	Mudstone	dark gray shale with a calcite nodule and bivalves
		X		
		X		dark gray shale with convoluted sand layers, flame structure is also present with bivalve fragments
		X		
		X		
		X		
		X		
		X	Sandstone	dark gray shale with irregular sand layers, bivalves and bioturbation
		X	Mudstone	
		X	Sandstone	
		X	Mudstone	
		X	Sandstone	dark shale with calcite nodule
		X	Mudstone	sand and shale soft sediment deformation
		X	Sandstone	
		X		
	X		Mudstone	muddy sandstone with some irregular and distorted shale layers and rip up clasts.
	X			
	X			
	X			
	X		Muddy sst	
	X			
	X		Mudstone	dark gray shale laminated
	X			
	X			
		X	Sandstone	laminated sandstone
X				sst with rip up clasts and soft
	X			massive sst capped with a shale layer
	X			
	X			massive sst capped with a shale layer
	X			
		X	Mudstone	dark gray laminated shale
		X		
		X	Sandstone	fining upward sandstone
		X		
		X		
		X		
		X		massive sanstone with bivalves
		X	Mudstone	dark gray shale
		X		
		X		
		X		
		X		
		X		
		X		

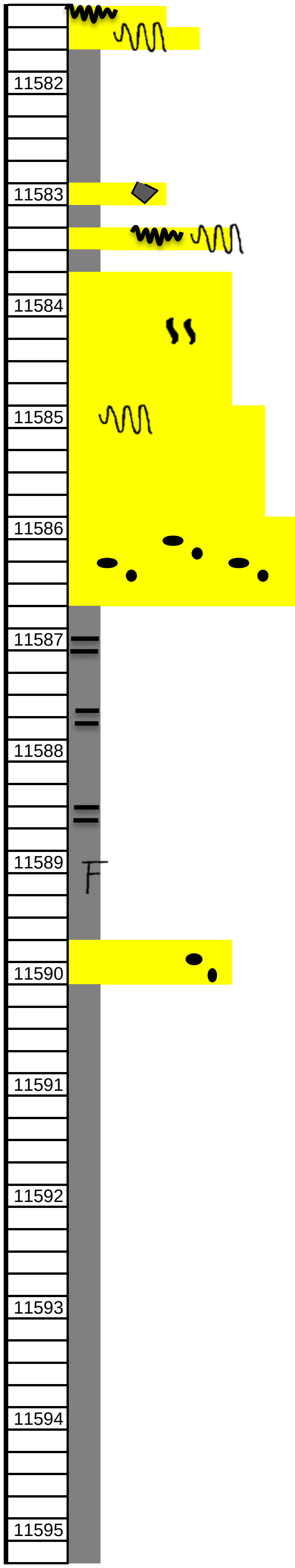

		X	Sandstone	sandstone with convuluted shale layers and a mud clast
		X		
		X	Mudstone	dark gray laminated shale
		X		
		X		
		X		
		X		
		X		
		X	Sandstone	sandstone with mud clast
		X	Mudstone	dark gray laminated shale
		X	Sandstone	sandstone and concoluted shale
		X	Mudstone	dark gray laminated shale
		X	Sandstone	fining upward sandstone bioturbated, convoluted at some places and couple of rip up clasts
		X		
		X		
		X		
		X		
		X		
		X		
		X		
		X		
X				
X				
		X		
		X		
		X		
		X		
		X	Mudstone	dark gray laminated shale with some forams
		X		
		X		
		X		
		X		
		X		
		X		
		X		
		X		
		X		
		X		
		X		
		X		
		X		
		X		
		X	Sandstone	fining up sandstone with rip up clasts
		X		
		X	Mudstone	
		X		
		X		
		X		
		X		
		X		
		X		
		X		
		X		
		X		
		X		
		X		
		X		
		X		
		X		
		X		
		X		
		X		
		X		
		X		
		X		
		X		
		X		
		X		
		X		
		X		

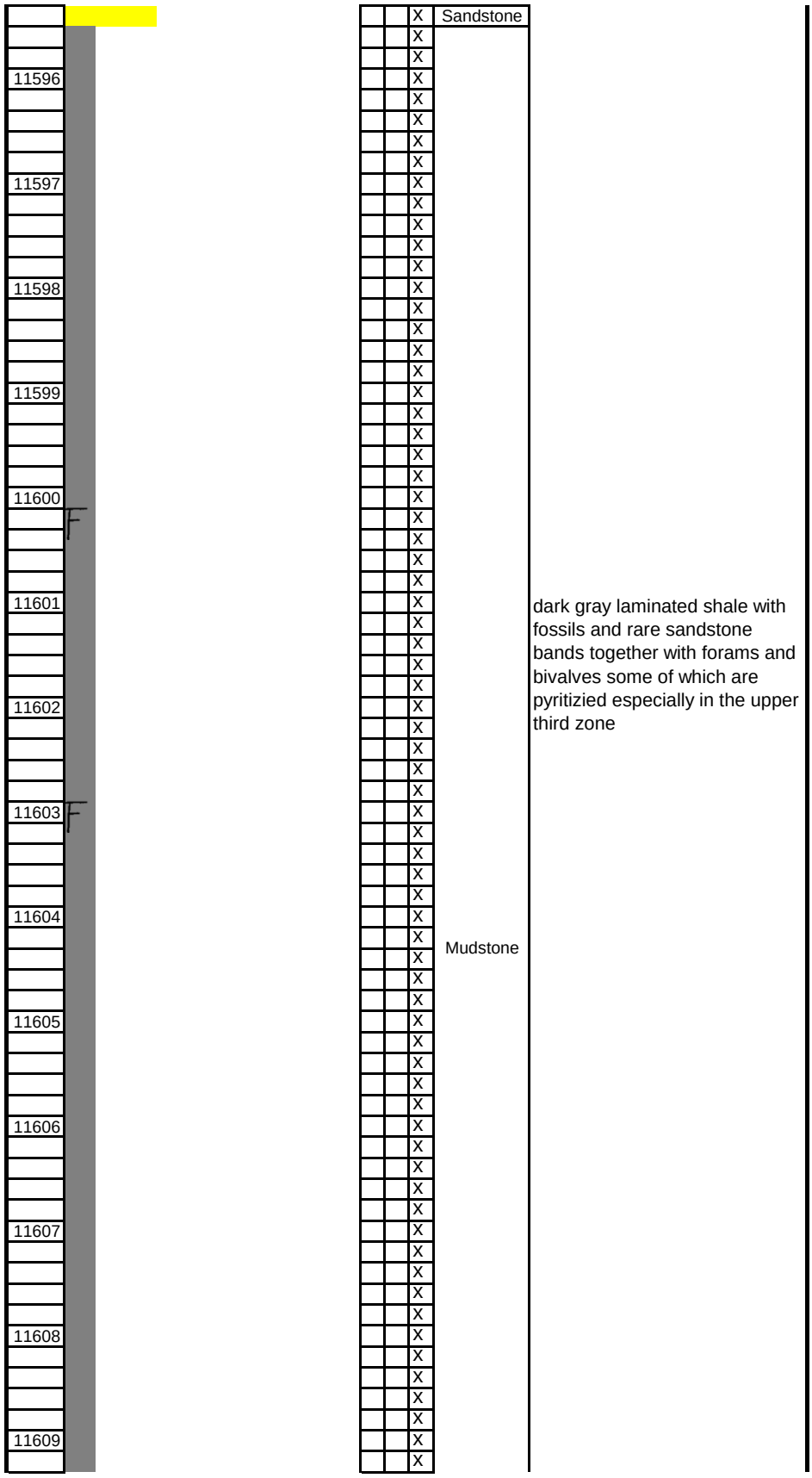
11596
11597
11598
11599
11600
F
11601
11602
11603
F
11604
11605
11606
11607
11608
11609
Sandstone
Mudstone
dark gray laminated shale with fossils and rare sandstone bands together with forams and bivalves some of which are pyritizied especially in the upper third zone

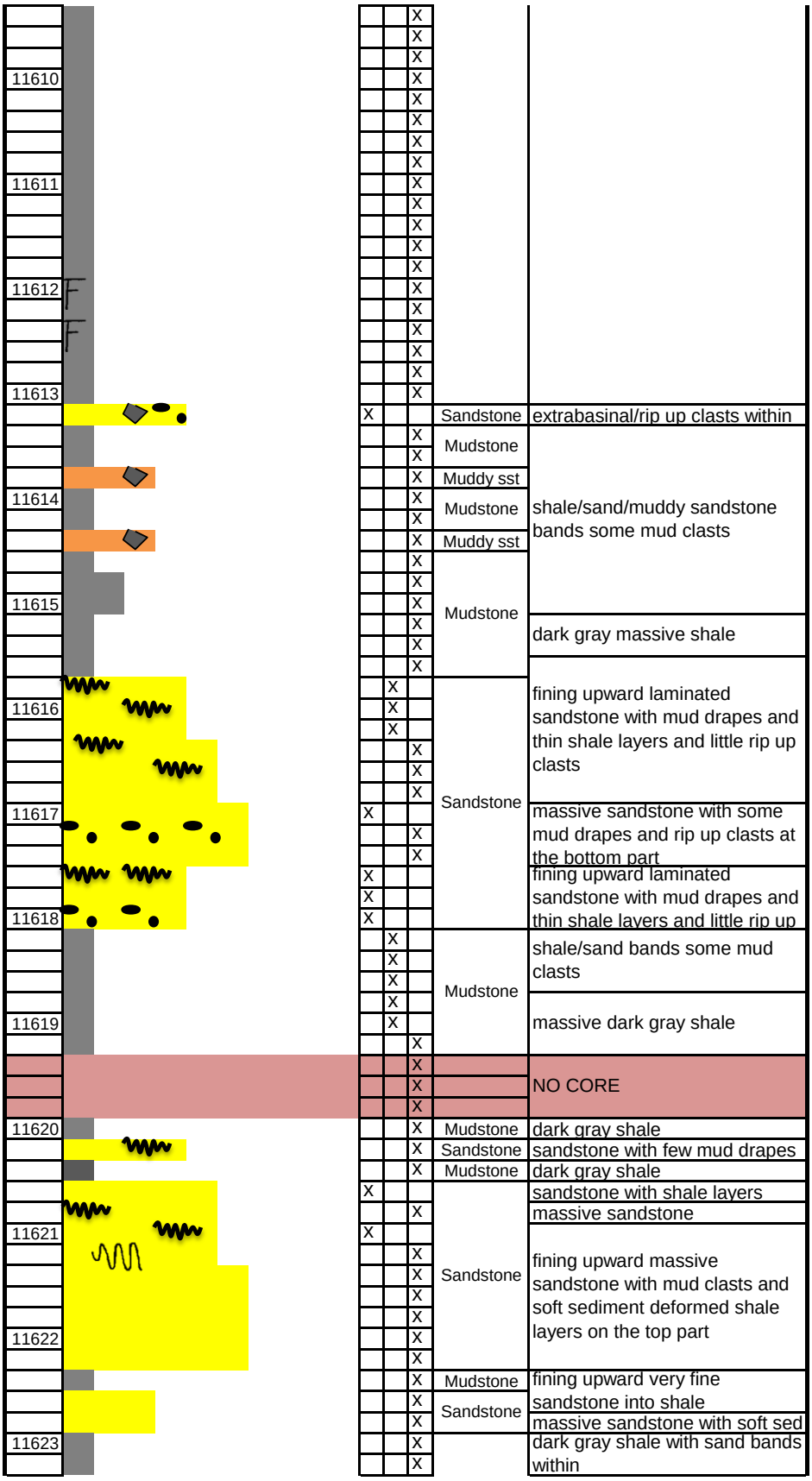
11610
11611
11612
F
F
11613
11614
11615
11616
11617
11618
11619
11620
11621
11622
11623
Sandstone
extrabasinal/rip up clasts within
Mudstone
Muddy sst
Mudstone
shale/sand/muddy sandstone bands some mud clasts
Muddy sst
Mudstone
dark gray massive shale
Sandstone
fining upward laminated sandstone with mud drapes and thin shale layers and little rip up clasts
massive sandstone with some mud drapes and rip up clasts at the bottom part
fining upward laminated sandstone with mud drapes and thin shale layers and little rip up
Mudstone
shale/sand bands some mud clasts
massive dark gray shale
NO CORE
Mudstone
dark gray shale
Sandstone
sandstone with few mud drapes
Mudstone
dark gray shale
sandstone with shale layers
massive sandstone
Sandstone
fining upward massive sandstone with mud clasts and soft sediment deformed shale layers on the top part
Mudstone
fining upward very fine sandstone into shale
Sandstone
massive sandstone with soft sed
dark gray shale with sand bands within

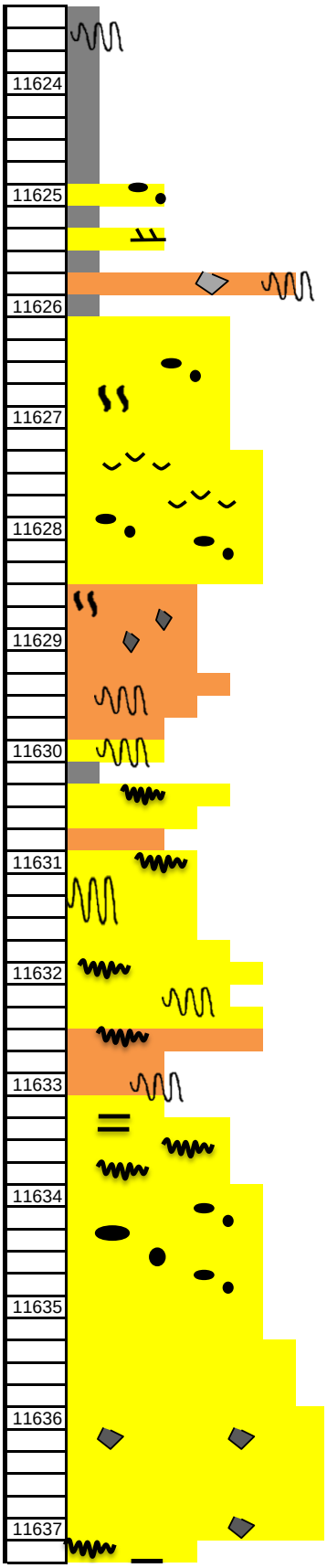

		X	Mudstone	shale/sand soft sed def
		X		banded shale/sand
		X		
		X		
		X		
		X		
		X		laminated shale
		X		massive calc shale
X			Sandstone	sandstone with rip up clasts at
X			Mudstone	fining upward from vf sst to
X			Sandstone	shale and sst is cross bedded
X			Mudstone	muddy sandstone with some
X			Muddy sst	irregular and distorted shale
			Mudstone	layers and a large clast.
		X	Sandstone	massive sandstone with some
		X		rip up clasts, bioturbation,
		X		
	X			
	X			
	X			
		X		massive sandstone with some
		X		rip up clasts and dish structures
		X		at the lower half.
		X		
		X		
		X		
	X		Muddy sst	muddy sandstone with
	X			bioturbation and some mud
	X			clasts
X				soft sed deformed sand and
X				muddy sand
X				
X				
X			Sandstone	soft sediment deformation with
X			Mudstone	convolute bedding and flame
X			Sandstone	sandstone with a mud drape
X				sandstone banded with shale
X			Muddy sst	massive muddy sandstone with
X			Sandstone	sandstone with lots of rip up
X				clasts and a few mud clasts, soft
X				
		X		fining upward massive
		X		sandstone
		X		
		X		massive sandstone with
X				muddrape and concolute
X			Muddy sst	muddy sandstone with mud
X				clasts, drapes and convolute
X				bedding.
X			Sandstone	fining upward laminated
	X			sandstone/cong with mud
	X			drapes and increasing
	X			abundanca of large rip up clasts
	X			and extrabasinal clasts
	X			especially on the lower third
	X			
	X			
	X			
	X			
	X			
	X			
	X			
X				
X				
X				
X				
X				
X				
X				
		X		slightly laminated sandstone

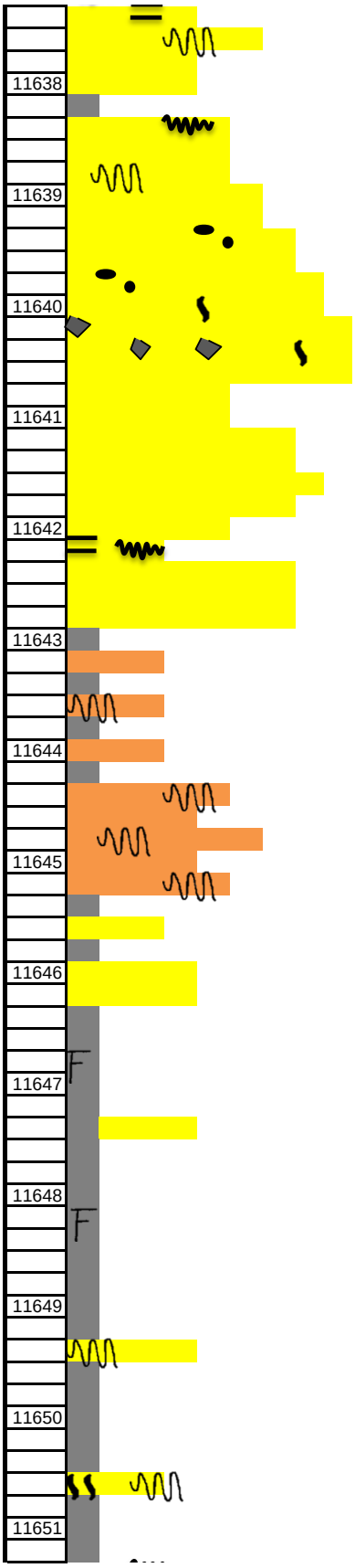

		X		with some mud drapes, rip up clasts and extra basinal clasts, convolute bedding also observed, deformed shale
X				
X				
X				
		X	Mudstone	
		X	Sandstone	fining upward sandstone. Shale band at the top. Convolute bedding and deformed shale bands at the upper part within sandstone. Rip up clasts and large extrabasinal clasts are also present. Within the lower half some bioturbation is observed and size of the extrabasinal clast increased,
		X		
	X			
X				
X				
X				
X				
X				
X				
X				
X				
X				fining upward sequence from medium sst to cong. Very large extrabasinal clasts up to 5cm.
X				
X				
X				
X				
X				coarsening upward massive sandstone
X				
	X			banded shale/sand
	X			massive sandstone with mud clasts and a thin shale layer
	X			
		X		
		X	Muddy sst	massive shale with some sandstone and muddy sandstone layers, deformed mud drapes
		X		
		X		
		X		
		X		
		X		
		X		muddy sandstone and shale soft sed deformation
		X		
		X		
		X		
		X		
		X	Mudstone	layers of sand and shale
		X	Sandstone	
		X	Mudstone	
		X	Sandstone	
		X		
		X		
		X	Mudstone	massive dark gray shale with few bivalve
		X		
		X		
		X	Sandstone	massive sst
		X		
		X		
		X		
		X		
		X	Mudstone	massive dark gray shale with few bivalve
		X		
		X		
		X		
		X		
		X	Sandstone	sandstone with soft sed def at
		X		
		X		
		X	Mudstone	massive dark gray shale
		X		
		X		
		X	Sandstone	bioturbated and soft sed def sst
		X		
		X	Mudstone	massive dark gray shale
		X		

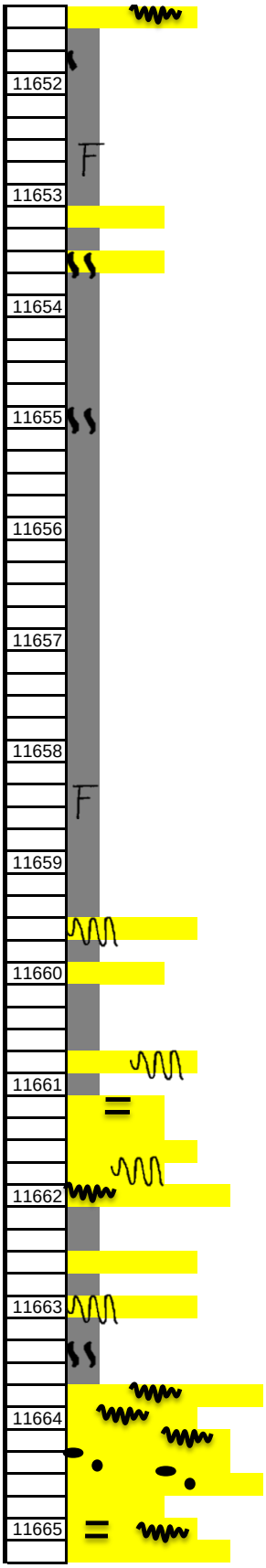

		X	Sandstone	sst with mud drape
		X	Mudstone	dark gray massive shale with bioturbation and few bivalves
		X		
		X		
		X		
		X		
		X		
		X		
		X		
		X	Sandstone	bioturbated dark gray shale with some sst bands
		X	Mudstone	
		X	Sandstone	
		X	Mudstone	bioturbated dark gray shale with some sst bands and bivalves
		X		
		X		
		X		
		X		
		X		
		X		
		X		
		X		
		X		
		X		
		X		
		X		
		X		
		X		
		X		
		X		
		X		
		X		
		X		
		X		
		X		
		X	Sandstone	sandstone with deformed shale
		X	Mudstone	dark gray massive shale layered with sandstone
		X	Sandstone	
		X	Mudstone	
		X		
		X		
		X	Sandstone	massive sandstone with
		X	Mudstone	shale with thin sst layers
		X	Sandstone	faintly laminated sst
		X		
		X		
		X		
		X		sandstone with shale laminations and deformed mud
	X		Mudstone	
		X		dark gray sandstone with thin sst laminations
		X	Sandstone	
		X	Mudstone	
	X		Sandstone	bioturbated and soft sed def sst
		X	Mudstone	dark gray shale with sst bands and bioturbation
		X		
		X		
	X		Sandstone	massive sst
		X		fining upward sst with mud drapes at the top, some deformed, rip ups.
		X		
		X		
		X		
		X		fining upward massive sandstone very fine shaly
		X		
		X		

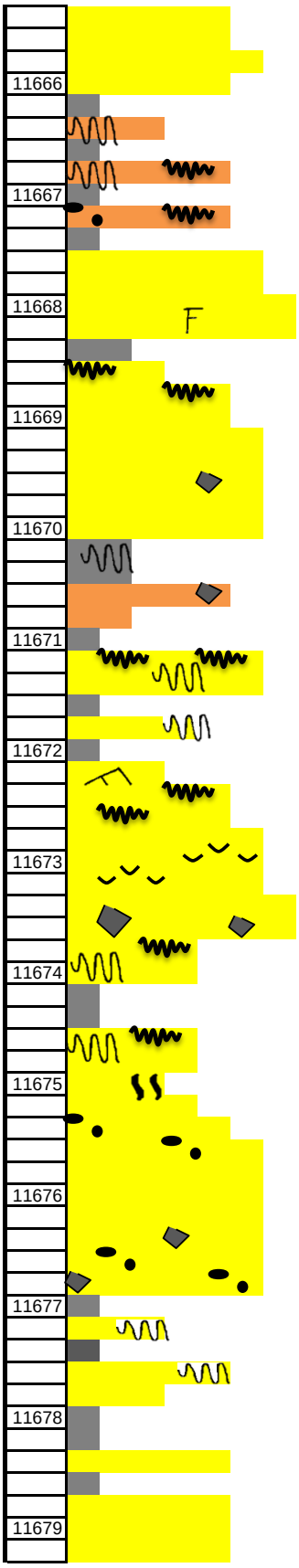

		X		laminations at top
		X		fining upward massive sandstone
	X			
	X			coarsening upward massive
X			Muddy sst	shale/muddy sandstone/sandstone deformed bands, convoluted bedding, mud drapes, mud clasts, rip up clasts
X				
X				
X				
		X		
	X			
		X		
		X	Sandstone	massive sandstone, slightly fining upward few bivalves
		X		
		X		
		X		
		X	Mudstone	fininf upward massive sandstone. At the top thin shale bands, slightly inclined, a mud drape, calcite nodule
		X	Sandstone	
		X		
		X		
		X		
		X		
		X		
		X		
		X	Mudstone	shale with some sand layers deformed, convoluted
		X		
	X		Muddy sst	muddy sandstone with laminated shale and muddy sst
	X			
	X			faintly laminated shale
	X		Sandstone	massive sst with a deformed mud drape on top
	X			
	X		Mudstone	layers of sand and shale, slight soft sed deformed.
	X		Sandstone	
	X		Mudstone	
X			Sandstone	fining upward sandstone: Laminations and faint ripples on the top part with few mud drapes. Rest is massive with abundant dish structures. Two mud clasts at the bottom one of them is very large. Grains are subangular and moderately
		X		
		X		
		X		
		X		
	X			
	X			
X				
X				sandstone with deformed mud
X				
		X	Mudstone	soft sediment deformed sand and shale intercalations with some bioturbation
		X		
	X			
	X			
	X			fining upward massive sandstone. Upper part is dominated with soft sed deformed mud drapes and shale bands, some fine rip up clasts
	X			
	X			
		X		
		X		
		X		part of upper f.u. sequence but different in character. Very large rip ups and a huge mud clast.
		X		
		X		
		X		
		X	Mudstone	2 sandstone packages with thin shale layers at the top them.
		X	Sandstone	
		X	Mudstone	soft sed deformed shale and massive sandstone
		X	Sandstone	
		X		fine grained massive sst with
		X	Mudstone	massive dark gray shale
		X		
		X	Sandstone	thick sand band interruption
		X	Mudstone	
		X		
		X		
		X		

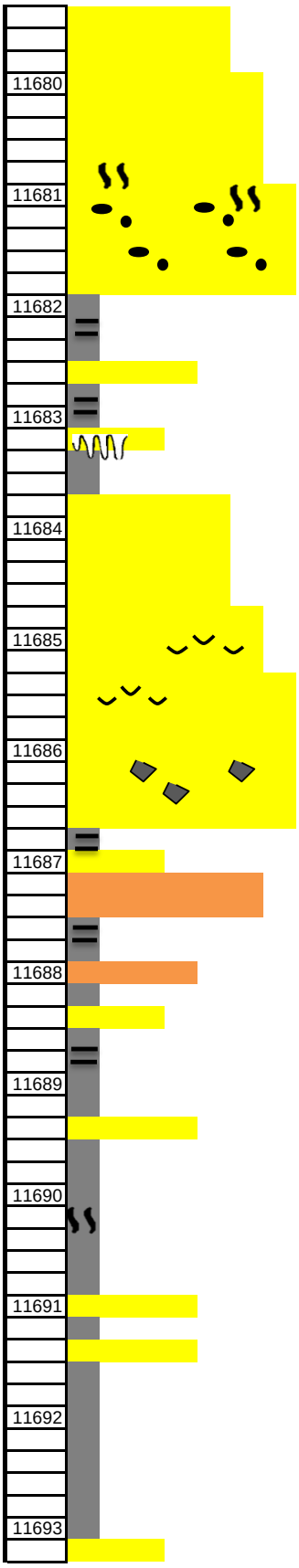

		X	Sandstone	fining upward massive sandstone with few rip up mud clasts and some bioturbation in the lower 1 feet
		X		
		X		
		X		
		X		
		X		
		X		
		X		
		X		
		X		
		X		
		X		
		X	Mudstone	laminated dark gray shale
		X		
		X		
		X	Sandstone	fine sand layer between shales
		X	Mudstone	laminated dark gray shale
		X		
		X	Sandstone	faintly laminated sandstone on
		X	Mudstone	soft sed deformed shale and minor sand on top than
		X		
		X	Sandstone	massive fining upward sandstone, some dish structures at the lower half. Subangular grains
		X		
		X		
		X		
		X		
		X		
		X		
		X		
		X		
		X		
	X			
	X			
	X			
	X			
	X		Mudstone	laminated dark gray shale
	X		Sandstone	sandstone with thin shale layers
	X		Muddy sst	massive muddy sandstone
	X			
	X		Mudstone	faintly layerted shale with some minor thin sand bands
	X			
	X		Muddy sst	sandy muddy shaly laminations
	X		Mudstone	faintly layered shale
	X		Sandstone	massive sst
		X	Mudstone	faintly layered shale
		X		
		X		
		X		
		X	Sandstone	sandstone with thin shale layers
		X		dark gray shale with occasional thin sand bands and bioturbations
		X		
		X		
		X		
		X		
		X		
		X		
	X		Sandstone	bioturbated and convoluted sandstone with mud drapes. Shalier at top
	X		Mudstone	
	X		Sandstone	
		X	Mudstone	dark gray massive shale with rare thin sand bands
		X		
		X		
		X		
		X		
		X		
		X		
		X	Sandstone	sandstone with deformed thin

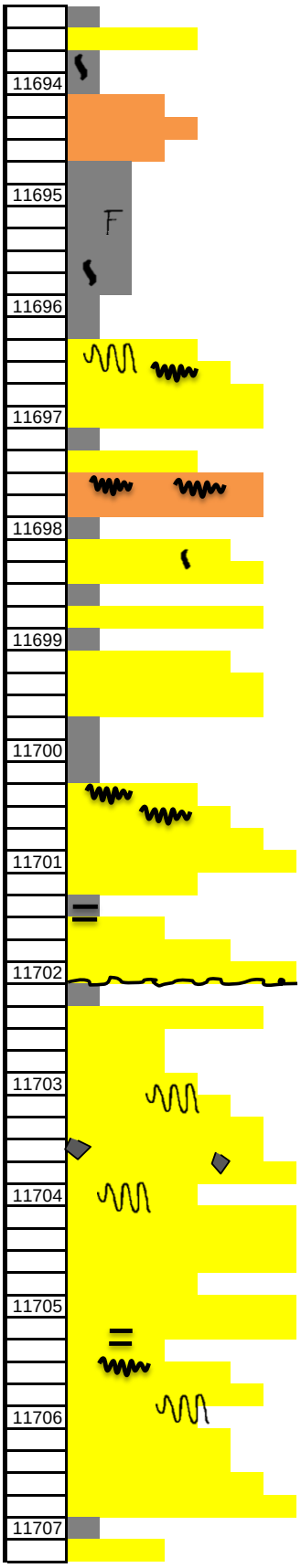

		X	Mudstone	shale with some thin sand layers on top. Bioturbated. Also some pyritization is observed.
X			Sandstone	
X			Mudstone	
		X		
		X	Muddy sst	soft sed deformed muddy sandstone and sandstone. Mud drapes and rip ups are present.
X				
X				
		X	Mudstone	massive dark gray shale with fossils
		X		
		X		
		X		
		X		
		X		
		X		
	X			shale with some sand bands. Bioturbated.
	X			
	X		Sandstone	fining upward sandstone. Upper parts more shaly and soft sed deformed.
	X			
	X			
X				
X			Mudstone	massive bioturbated dark gray
X			Sandstone	massive sandstone
X			Muddy sst	layers of shale and muddy sandstone. Bioturbated. Mud
X				
		X	Mudstone	massive shale
		X	Sandstone	fining upward massive sandstone with thin biot. shale
		X		
		X	Mudstone	deformed shale by the upper sst
		X	Sandstone	fu sst to biot shale bands
		X	Mudstone	massive shale
		X	Sandstone	f.u. massive sandstone
		X		
		X	Mudstone	massive dark gray shale with sand bands, few mud drapes and bioturbation
		X		
		X		
		X	Sandstone	fining upward massive sandstone with few mud drapes
		X		
		X		
		X		massive sandstone
		X	Mudstone	fining upward sst with shale layering at the top. Mud drapes are present and an amalgamation surface
		X	Sandstone	
		X		
		X	Mudstone	fininf upward sandstone from coarse sst to shale
		X	Sandstone	fining upward sandstone. Upper part shale layered and soft sed deformed. Mud clast at the bottom
		X		
		X		
		X		
		X		
		X		
		X		
		X		
	X			fine sandstone with soft sed def
	X			massive sandstone
	X			
	X			
	X			massive sandstone
	X			
		X		massive sandstone
		X		
		X		fining upward into shale laminations, mud drapes slightly sof sed def.
		X		
		X		
		X		massive fining upward sandstone
		X		
		X		
		X		
		X		
		X	Mudstone	massive dark gray shale
	X			shale layers and mud drapes

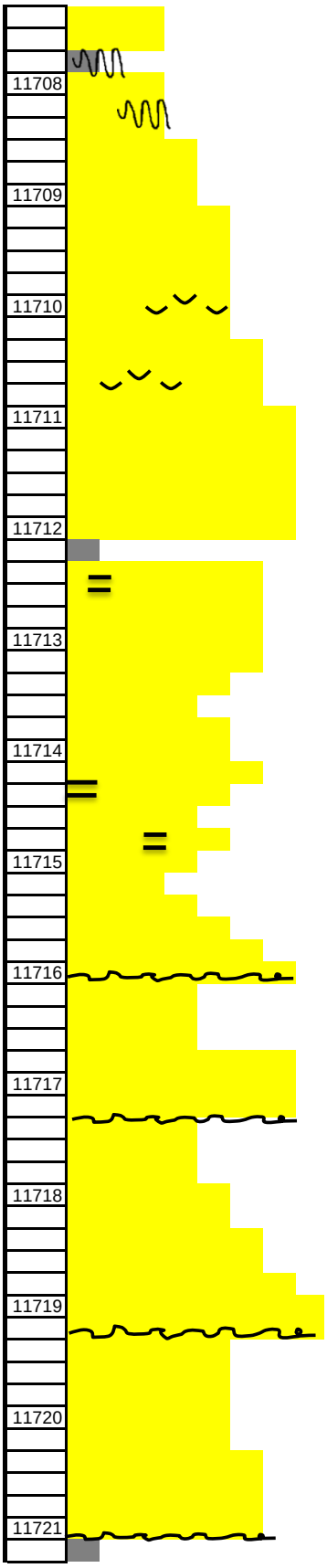

	X		Sandstone	laminated on top and convoluted at bottom part
	X			
		X	Mudstone	convoluted shale layer
		X	Sandstone	fining upward sandstone. Upper parts are slightly soft sed deformed. Middle part has some dish structures.
		X		
		X		
		X		
		X		
		X		
		X		
		X		
		X		
		X		
		X		
	X			
	X			
	X			
	X			
	X			
	X			
		X	Mudstone	massive shale
		X	Sandstone	massive sandstone. Some laminations of fine grained sst on top
		X		
		X		
	X			
	X			
		X		soft sed deformed sst
		X		fining upward massive sandstone
		X		
		X		
		X		bands of laminated fine and medium grain sized sst
		X		
		X		
		X		fining upward massie sst
		X		
		X		
		X		
		X		
		X		
		X		
		X		upward fining massive sandstone
		X		
X				
	X			
	X			
	X			
		X		fining upward sandstone, massive, subangular grains. Around 11718 ft lotf of large rip up clasts.
X				
		X		
		X		
		X		
		X		
		X		
X				
X				
		X		massive fining upward sandstone. Few dish str and bioturbation
		X		
		X		
		X		
		X		
		X		
		X		
X			Mudstone	massive shale with few sand

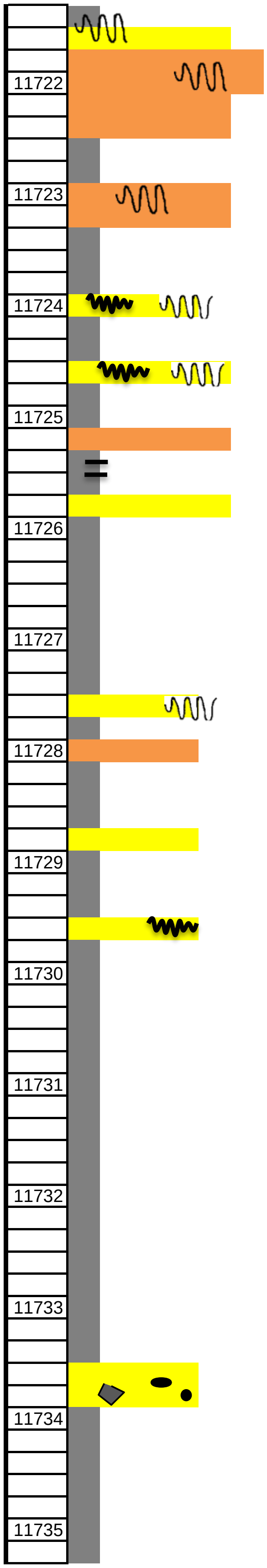

X			Mudstone	bands which are convoluted
X			Sandstone	sst with soft sed def shale layer
X			Muddy sst	muddy sandstone is deformed with some shale and sand, muddy sandstone with a huge rip up clast in it and some
X				
X				
X				
		X	Mudstone	massive dark gray shale
		X		
X			Muddy sst	muddy sandstone with deformed shale layer at the top part,
	X		Mudstone	shale with some thick sandstone layers and deformed mud drapes in them. Little
	X			
	X			
	X		Sandstone	sandstone with soft sed
	X		Mudstone	massive shale with some sand layers
	X			
	X		Sandstone	sandstone with soft sed
X			Mudstone	massive shale
X				
		X	Muddy sst	massive muddy sandstone
		X	Mudstone	laminated dark gray shale
		X		laminated shale with some sand
		X	Sandstone	massive muddy sandstone
		X	Mudstone	massive shale with couple of slightly inclined sandstone layers
		X		
		X		
		X		
		X		
		X		
		X		
		X		
		X	Sandstone	soft sediment deformation.
		X	Mudstone	shale with some sandstone
	X		Muddy sst	massive muddy sandstone
	X		Mudstone	massive shale with downward increasing abundance of sandstone layers
		X		
		X		
		X	Sandstone	
		X	Mudstone	massive shale
		X		
		X		
		X	Sandstone	sandstone with a mud drape
		X	Mudstone	massive shale
		X		
		X		
		X		
		X		
		X		
		X		
		X		
		X		
		X		
		X		
		X		
		X		
		X		
		X		
		X		
		X		
		X		
		X		
		X	Sandstone	massive sandstone with little mud clasts/ rip ups
		X		
		X		
		X		
		X		
		X		
		X		
		X		
		X		

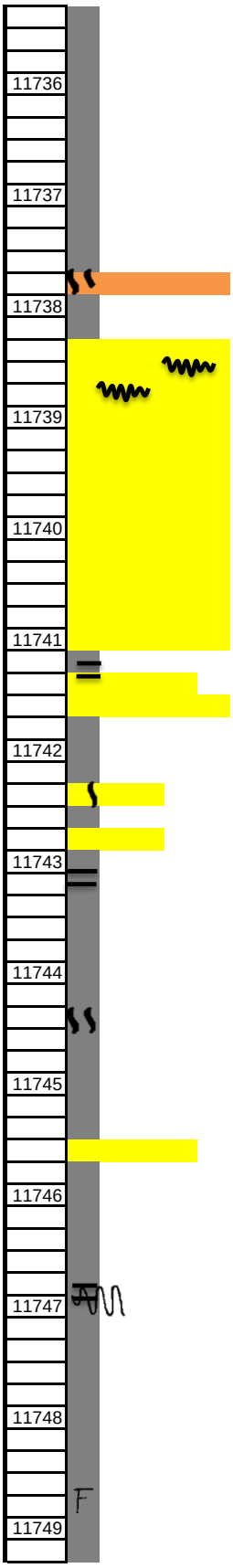

Mudstone	
Muddy sst	massive muddy sandstone
Mudstone	massive dark gray shale
Sandstone	massive sandstone with a mud drape on top part
Mudstone	layered dark gray shale
Sandstone	fining upward sst with shale laminations on top portion and
Mudstone	layered dark gray shale
Sandstone	bioturbated sst
Mudstone	layered dark gray shale
Sandstone	massive sst
Mudstone	layered dark gray shale with few thin sst layers and bioturbation
Sandstone	massive sst
Mudstone	layered dark gray shale
Mudstone	slightly layered dark gray shale with some fossils, some pyritization

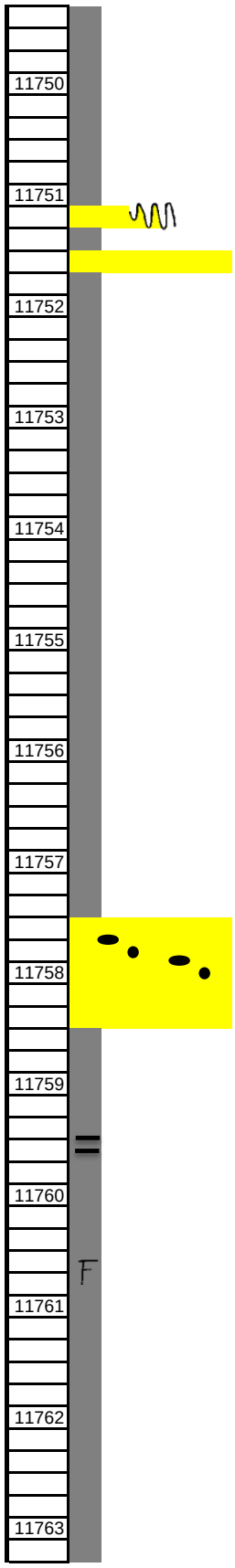

Sandstone	shale with a deformed sand
Mudstone	layered shale
Sandstone	massive sand btw syn-sed faults
	shale with a thin deformed sand layers in it
Mudstone	layered dark gray shale rare pyritizied fossils
Sandstone	massive sandstone with rip ups at the top part
Mudstone	massive to slightly layered shale with pyritized forams and pyritization at some places

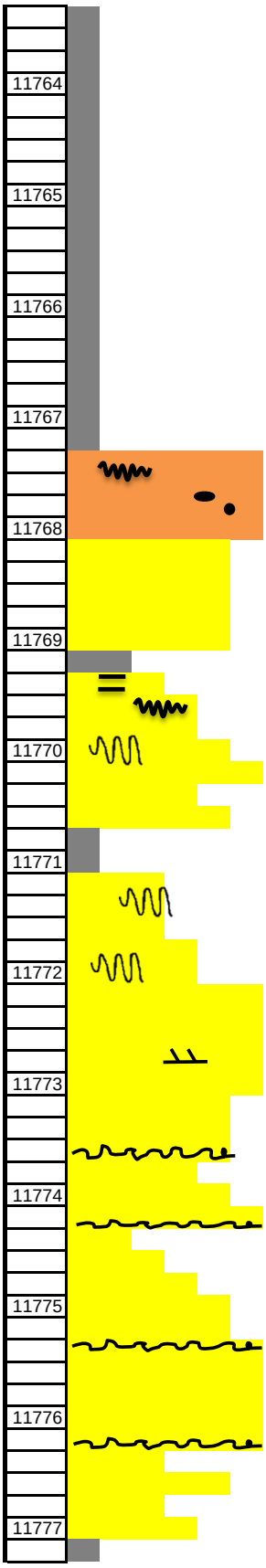

Muddy sst	massive muddy sandstone with few rip ups and mud drapes at the top and bottom	
Sandstone	massive sandstone	
Mudstone		
Sandstone	fining upward sandstone, laminated on the top. Mud drapes soft sed def. at the bottom.	
	massive sandstone with rip ups	
	massive sst slightly deformed	
	shale/sand layers soft sed	
Sandstone	shale and sand highly convoluted, soft sed deformation.	
	coarser part is massive with some bioturbation and one large mud clast. Lower finer part is showing faint cross bedding in the middle	
	fining upward sandstone, laminated on the top. Thin coarse sand band in the middle	
	fining upward sandstone with finw shale band at the top. And a mud clast at the bottom	
	massive sandstone	
	fining upward sand with mud drapes on top	
	fining upward sand with mud drapes on top	
	bands of sand and shale	

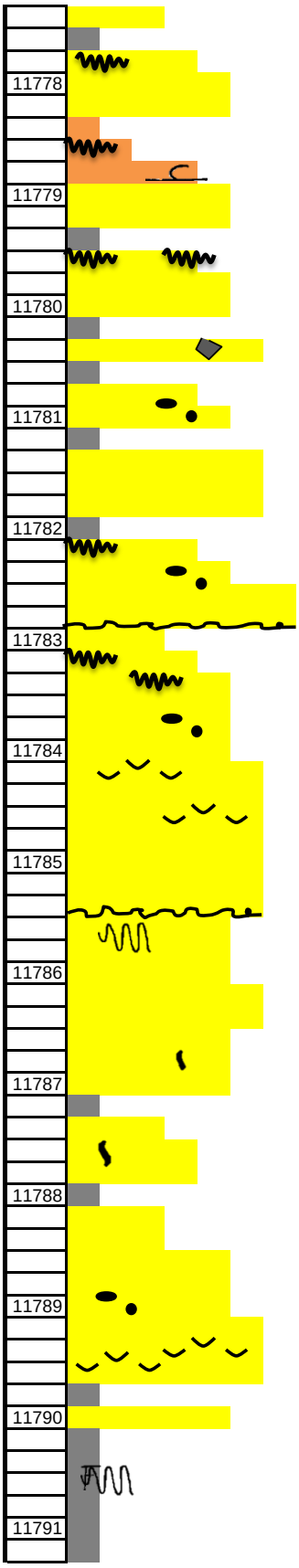

		X	Sandstone	convoluted
		X	Mudstone	fining upward sandstone with mud drapes on top
	X		Sandstone	
		X		
		X		
	X		Muddy sst	fining upward dark muddy sandstone with mud drapes on top and a flame str at the bottom
	X			
X				
		X	Sandstone	massive sandstone
		X		
	X		Mudstone	fining upward sandstone with mud drapes on top
		X	Sandstone	
		X		
		X		
		X	Mudstone	massive shale
		X	Sandstone	sandstone with some mud clasts
		X	Mudstone	massive shale
	X		Sandstone	fining upward sandstone getting shaly at the top part with a little
		X		
		X	Mudstone	massive shale with a sandsy
		X	Sandstone	massive sandstone
		X		
		X		
	X		Mudstone	fining upward massive sandstone with mud drapes and rip ups on top.
		X	Sandstone	
		X		
		X		massive sandstone, subrounded grains, amalgamation suface at
		X		
	X			fining upward sandstone. Couple of mud drapes on top. Followed by very large rip ups. Then dish structures to the end. Amalgamation surface at the bottom.
	X			
		X		
		X		
		X		
		X		
		X		
		X		
		X		
		X		
		X		
		X		
		X		
		X		
		X		massive sandstone. Concoluted middle part. Laminated bottom part.
		X		
		X		
		X		massive sst
		X		
		X		massive sandstone with some bioturbation
		X		
		X	Mudstone	fining upward sandstone with a shale band at the top with few bioturbation.
	X		Sandstone	
		X		
		X		
		X	Mudstone	
	X		Sandstone	fining upward sandstone into shale. Some rip ups where grain size changes into medium sand. And then dish str.
		X		
		X		
		X		
		X		
		X		
		X		
		X		
		X	Mudstone	layered shale
		X	Sandstone	massive sandstone
		X	Mudstone	layered shale with few fossils
		X		
		X		
		X		
		X		
		X		

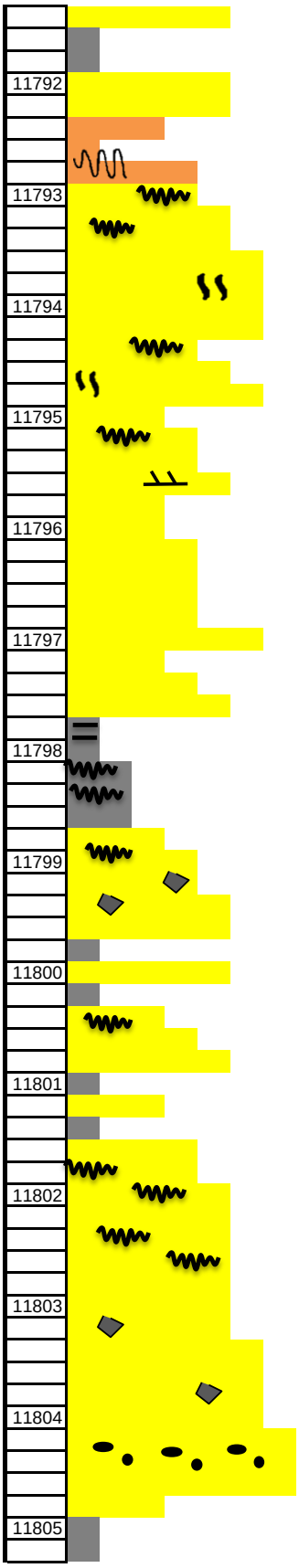

		X	Sandstone	massive sandstone
		X	Mudstone	layered shale
		X		
		X	Sandstone	massive sandstone
		X		
X			Muddy sst	muddy sandstone with some shale, concoluted, soft sed deformed and bioturbated.
X				
X				
		X	Sandstone	fining upward sandstone with some mud drapes towards bottom. Bioturbated
		X		
		X		
		X		
		X		
		X		
		X		
		X		fining upward sandstone with a shale band at the top with some bioturbation.
		X		
		X		
		X		fining upward sandstone with some cross bedded mud drapes at the top.
		X		
		X		
		X		
		X		fining upward sandstone with mud drape on top part
		X		
		X		
		X		
		X		
		X		
		X		fining upward sandstone with laminated mud drapes on top
		X		
		X		
		X		layered shale
		X		
		X		siltstone with lots of mud drapes and large/small rip ups and mud clasts
		X		
		X		
		X		
		X	Sandstone	fining upward sandstone with mud drape laminations on top and some mud clasts scattered. Mud drape at the top as
		X		
	X			
	X			
	X			massive sandstone
		X	Mudstone	layered shale
		X	Sandstone	massive sandstone
		X	Mudstone	
		X	Sandstone	fining upward sandstone with layered mud drapes on top and a shale band at the very top.
		X		
		X		
		X	Mudstone	shale
		X	Sandstone	massive sandstone
		X	Mudstone	shale
		X	Sandstone	fining upward sandstone wth laminated mud drapes on top. Some bioturbation common. Mud-clasts scattered, at the very bottom a huge rip up clast.
		X		
		X		
		X		
		X		
		X		
		X		
		X		
		X		
		X		
		X		
		X		
		X		
		X		
		X		
		X		
		X		
	X			
	X			massive sandstone
		X	Mudstone	shale with some thin sand bands
		X		

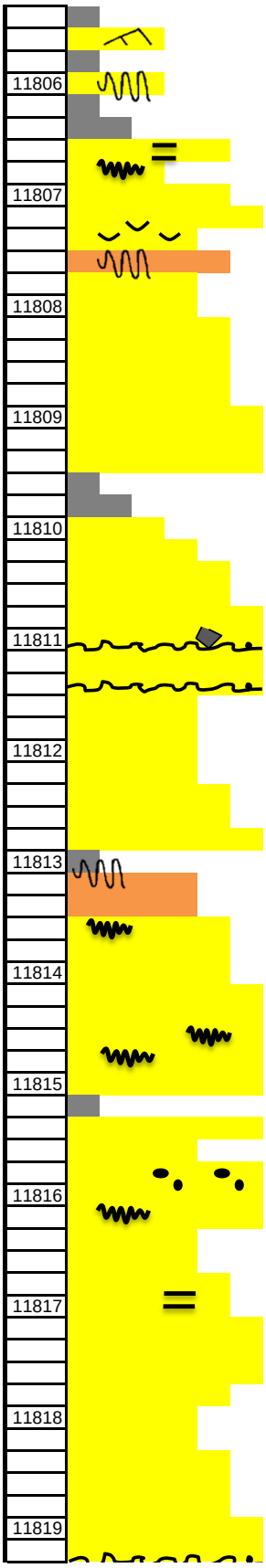

		X		bands
		X	Sandstone	sandstonw with ripples
		X	Mudstone	layered shale
X			Sandstone	sand and shale soft sed deformed
		X	Mudstone	
		X		siltstone and shale laminated
		X	Sandstone	massive sandstone
		X		fining upward sandstone. Mud drape laminations on top then some pillar str.
		X		
		X		
		X		
		X		massive sandstone
X			Muddy sst	muddy sandstone with slight
		X	Sandstone	fining upward sandstone
		X		
		X		
		X		
		X		
		X		
		X		
		X		
		X	Mudstone	
		X		
		X	Sandstone	fining upward sandstone into silt and shale. Upper parts are more shaly and darker in color. Mud clast.
		X		
		X		
		X		
		X		
		X		
		X		
		X		coarsening upward massive sandstone with mud drapes in the finer part. Slightly cross bedded
		X		
		X		
		X		
		X		
		X		fining upward sandstone. Deformed mud drapes in the top part. And some bioturbation.
		X		
		X		
		X		
		X	Mudstone	convoluted silt/shale
	X		Sandstone	fining upward sandstone. Muddy at top part. A mud drape at the lower part. Subrounded grains.
	X			
		X		
		X		
		X		
		X		
		X		
		X		
		X		
		X	Mudstone	shale with some thin sand
		X		massive sandstone
		X		massive sand with some rip ups
		X		massive sandstone
X				sandstone with lots of extrabasinal clasts and some
X				
X				fining upward sandstone slightly laminated
X				
X				
X				
X				
	X			
	X			
		X		fu massive sandstone with amalgamation surface at the bottom
		X		
		X		
		X		
		X		
		X		
		X		
		X	Sandstone	

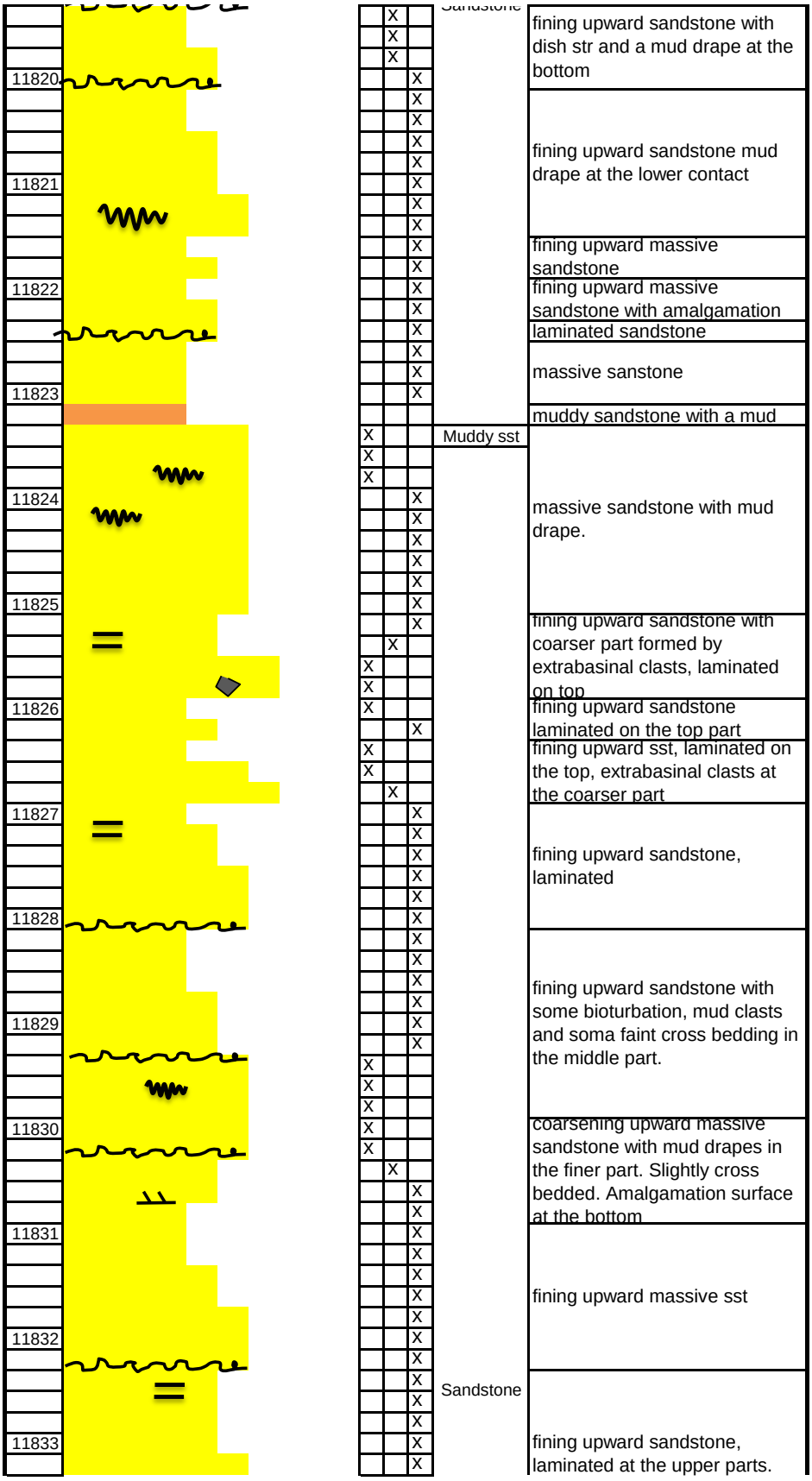
11820
11821
11822
11823
11824
11825
11826
11827
11828
11829
11830
11831
11832
11833
Muddy sst
Sandstone
fining upward sandstone with dish str and a mud drape at the bottom
fining upward sandstone mud drape at the lower contact
fining upward massive sandstone
fining upward massive sandstone with amalgamation
laminated sandstone
massive sanstone
muddy sandstone with a mud
massive sandstone with mud drape.
fining upward sandstone with coarser part formed by extrabasinal clasts, laminated on top
fining upward sandstone laminated on the top part
fining upward sst, laminated on the top, extrabasinal clasts at the coarser part
fining upward sandstone, laminated
fining upward sandstone with some bioturbation, mud clasts and soma faint cross bedding in the middle part.
coarsening upward massive sandstone with mud drapes in the finer part. Slightly cross bedded. Amalgamation surface at the bottom
fining upward massive sst
fining upward sandstone, laminated at the upper parts.

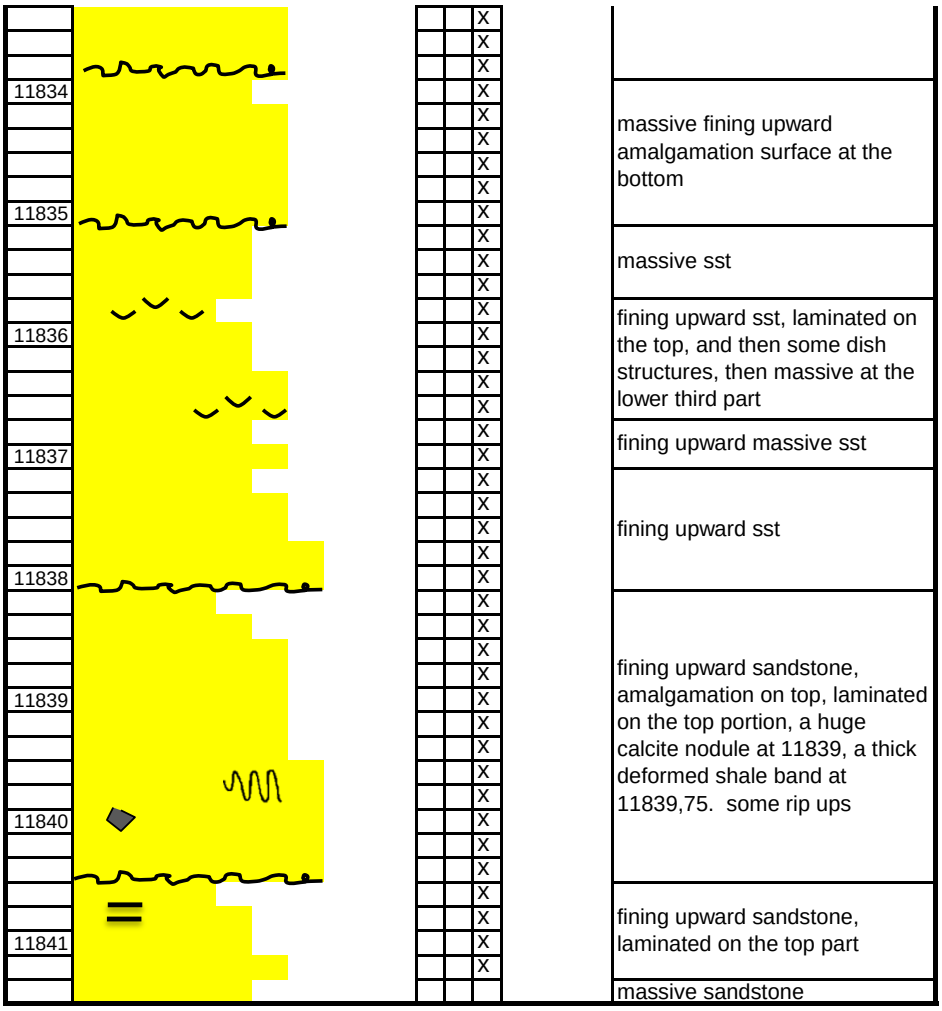
11834
11835
11836
11837
11838
11839
11840
11841
massive fining upward amalgamation surface at the bottom
massive sst
fining upward sst, laminated on the top, and then some dish structures, then massive at the lower third part
fining upward massive sst
fining upward sst
fining upward sandstone, amalgamation on top, laminated on the top portion, a huge calcite nodule at 11839, a thick deformed shale band at 11839,75. some rip ups
fining upward sandstone, laminated on the top part
massive sandstone

Appendix C: Seismic to well tie

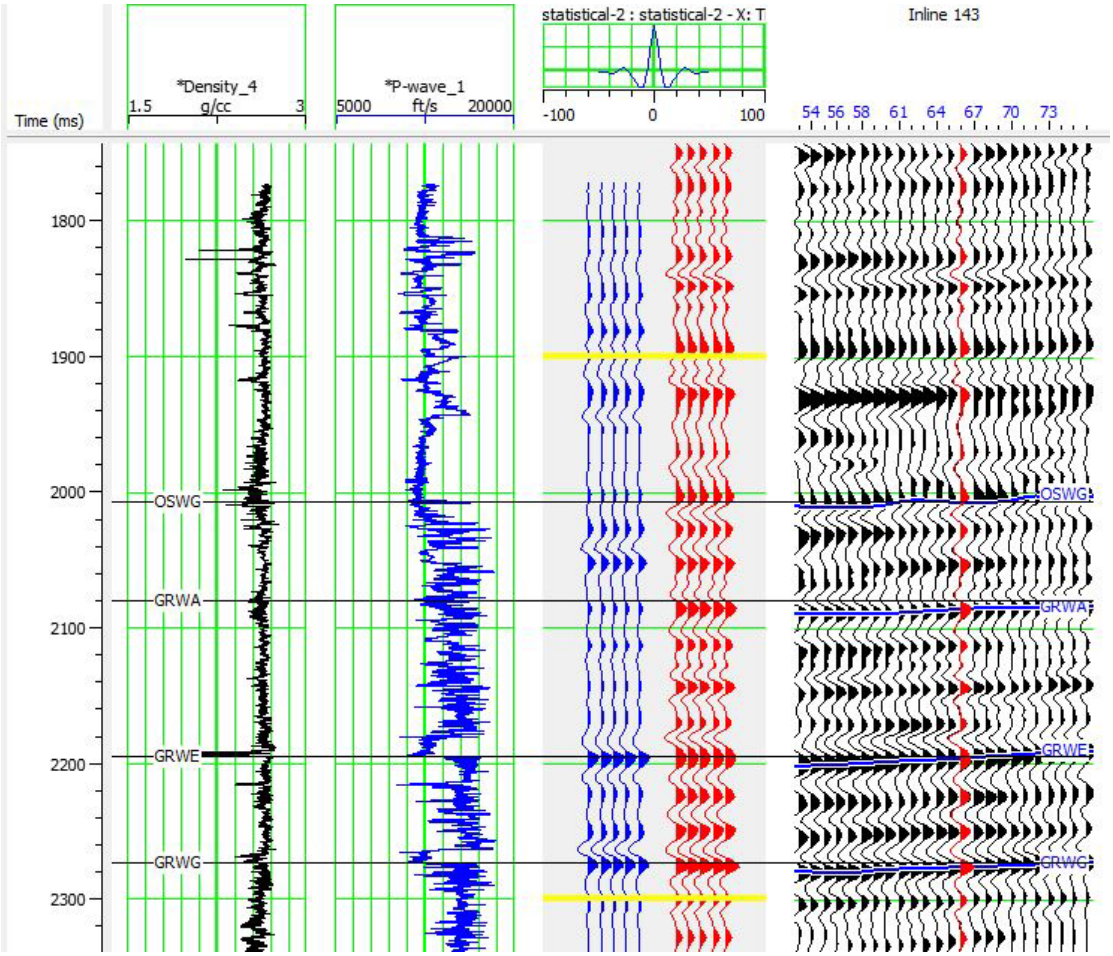

Figure C. Density and P-wave logs, synthetic seismogram, and extracted seismic trace. There is a good correlation between the synthetic and extracted seismic traces (correlation = 0.79).

Appendix D: AI cutoff values and probability maps

Zones	min AI	max AI
Marmaton Wash	32000	35000
Caldwell	32000	35000
Cherokee	37000	40000
Granite Wash A	37000	40000
Granite Wash B	37000	40000
Granite Wash C	39000	42000
Granite Wash D	39000	42000
Granite Wash E	39000	42000
Granite Wash F	39000	42000
Granite Wash G	39000	42000

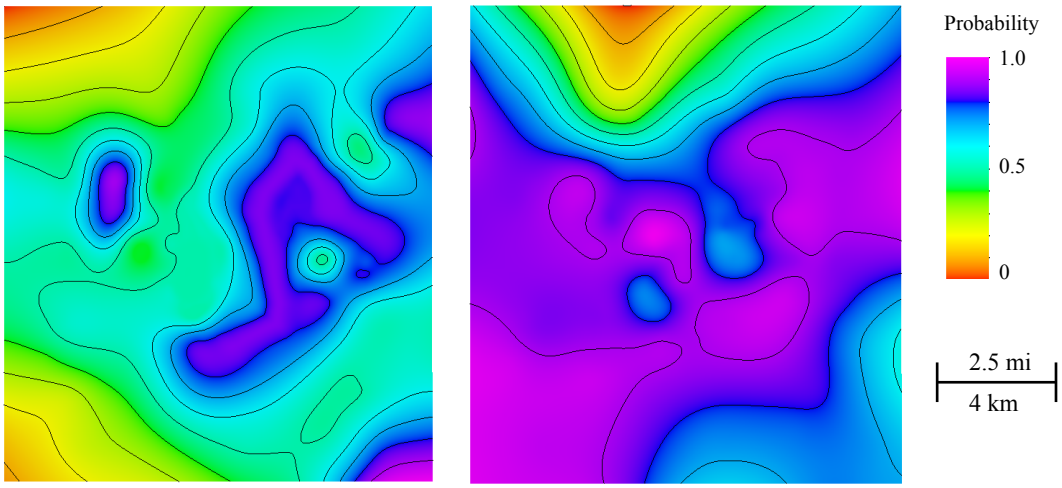

Figure D. 1) As AI is increasing with depth, different cut-off values are determined for each zone in order to be used for creating sandstone probability maps and an average AI surface attribute map is generated for each zone. 2) Examples of resultant sandstone probability maps. The map on the right belongs to Marmaton Wash while the map on the left represent Granite Wash E interval. It is seen that the probability of the sandstone occurence is greater for Granite Wash E interval compared to Marmaton Wash.

Appendix E: Variograms

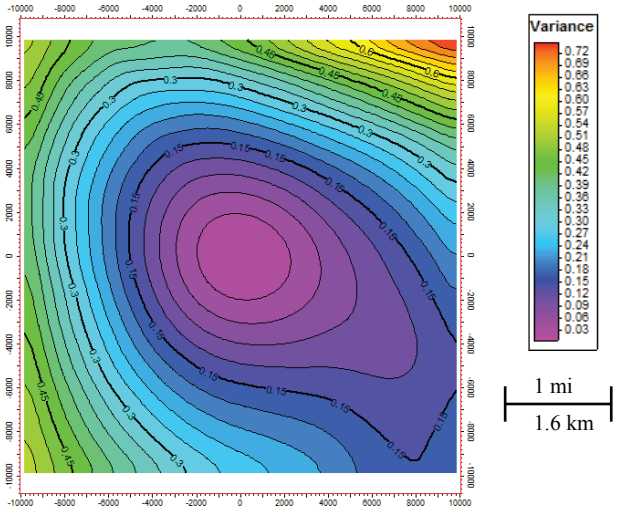

Granite Wash E - Sandstone	
Major range (ft)	16071.816
Minor range (ft)	12105.104
Vertical range (ft)	126.193
Azimuth (degree)	130

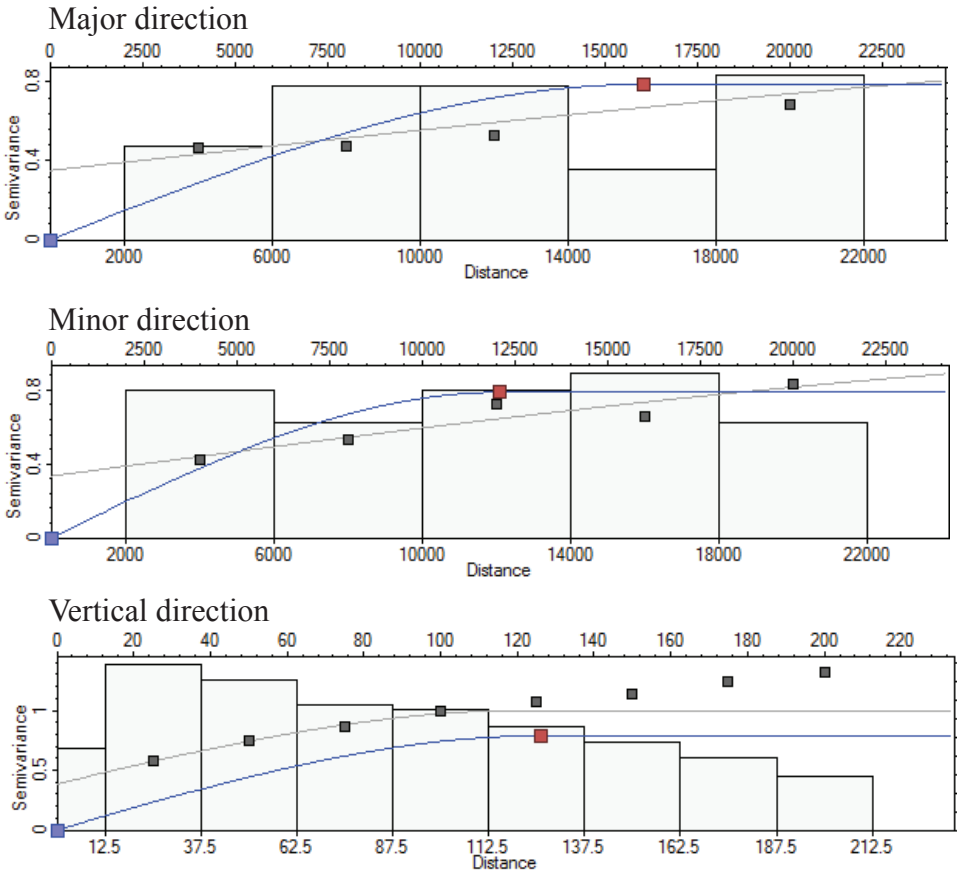

Figure E-1. Variogram models and horizontal variogram map for sandstone in GraniteWash E interval.

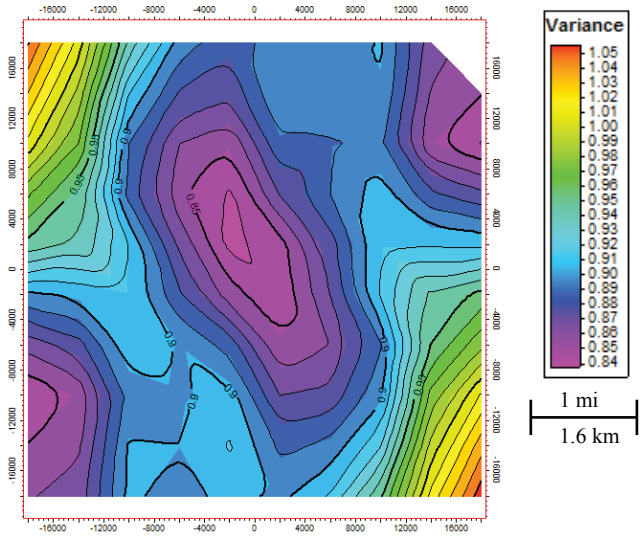

Granite Wash E - Muddy Sandstone	
Major range (ft)	20057.216
Minor range (ft)	11984.854
Vertical range (ft)	109.032
Azimuth (degree)	175

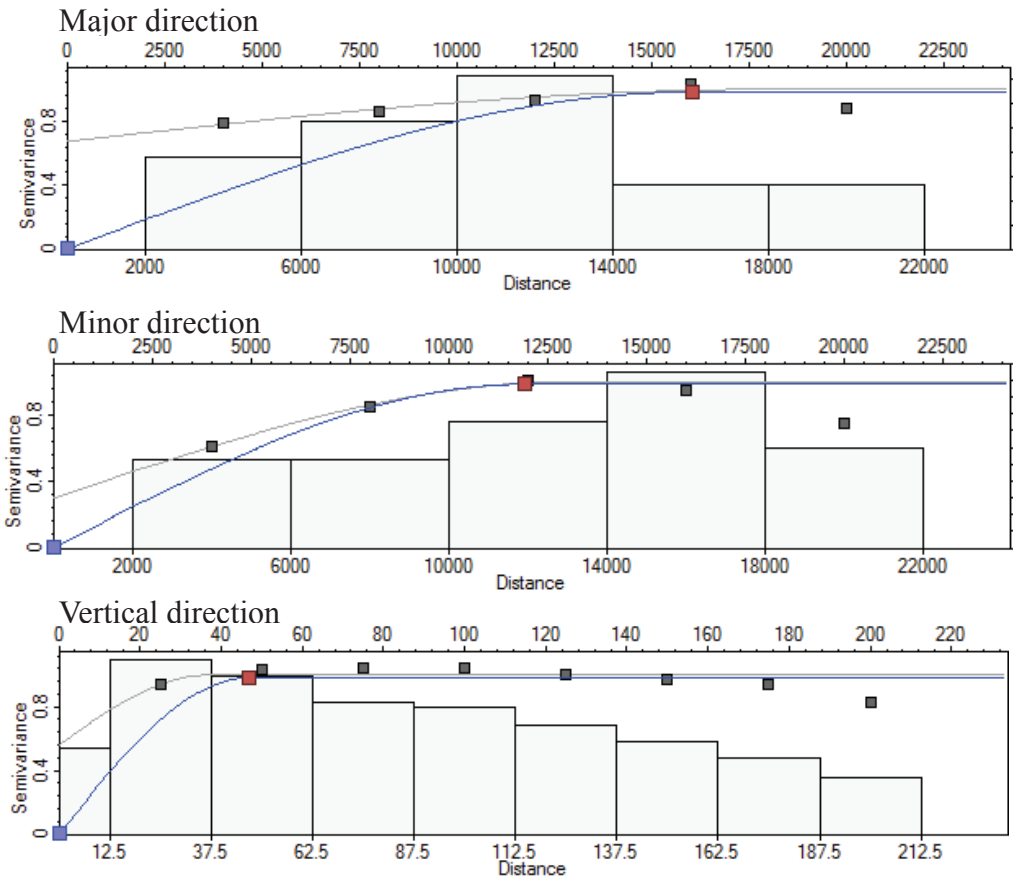

Figure E-2. Variogram models and horizontal variogram map for muddy sandstone in GraniteWash E interval.

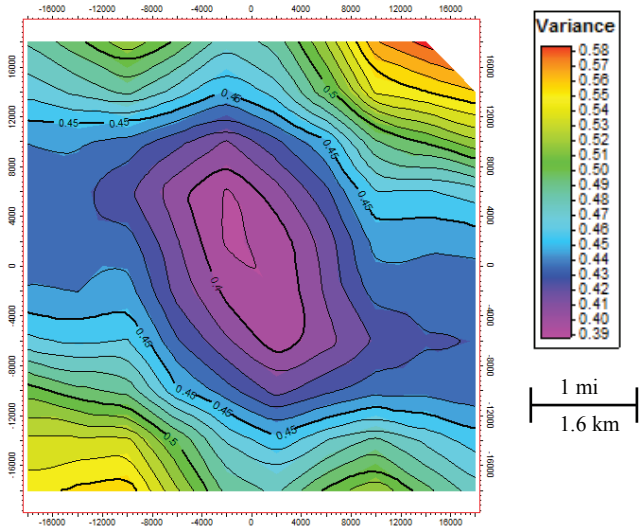

Granite Wash E - Mudstone	
Major range (ft)	16071.817
Minor range (ft)	11949.368
Vertical range (ft)	46.821
Azimuth (degree)	170

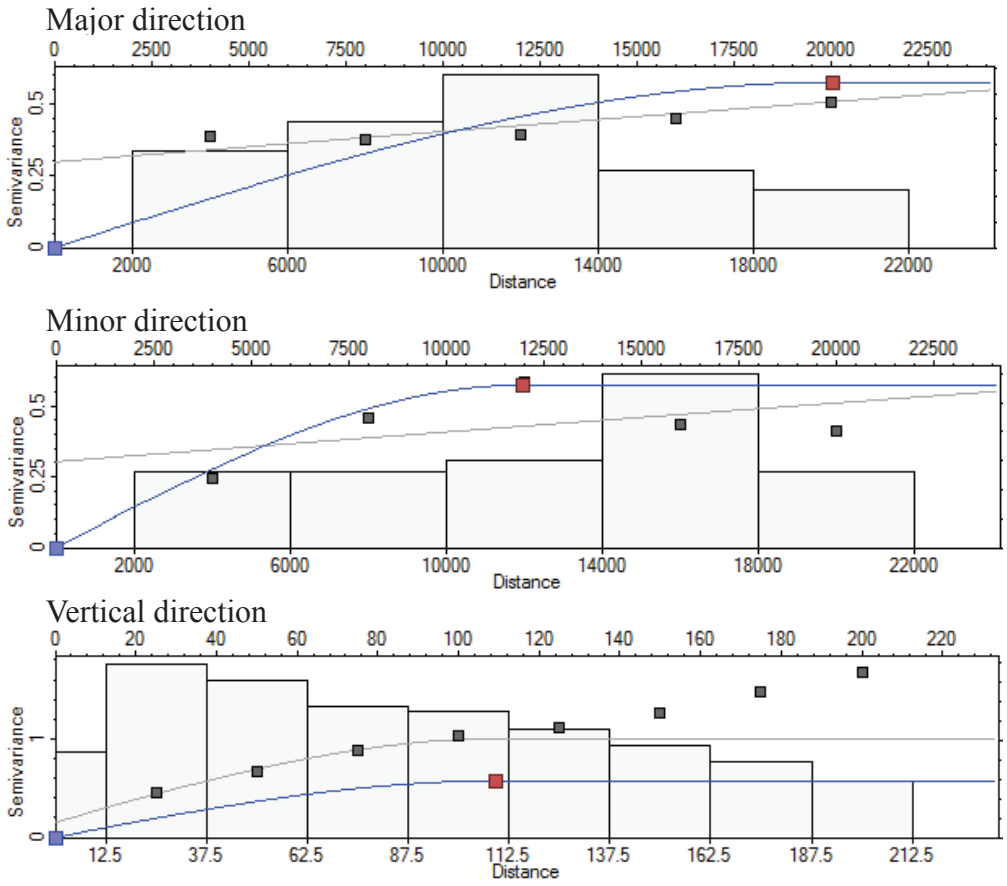

Figure E-3. Variogram models and horizontal variogram map for mudstone in GraniteWash E interval.

		Sandstone	Mudstone	Muddy Sandstone
Marmaton	Major range	20057.216	11021.442	9105.186
	Minor range	15989.643	8020.259	7419.417
	Vertical range	74.601	199.215	101.984
	Azimuth	15	155	150
Caldwell	Major range	10002.618	20031.05	19946.048
	Minor range	7525.806	12283.153	15947.426
	Vertical range	49.996	98.763	73.41
	Azimuth	80	145	130
Cherokee	Major range	16112.903	16161.274	11829.432
	Minor range	11880.985	12162.651	5623.236
	Vertical range	49.996	52.526	50.514
	Azimuth	70	115	45
Granite Wash A	Major range	20057.216	12098.51	19976.174
	Minor range	8183.191	8019.411	12146.103
	Vertical range	99.207	125.796	150.401
	Azimuth	45	95	145
Granite Wash B	Major range	10278.608	12099.478	19847.822
	Minor range	7936.672	8111.092	15852.594
	Vertical range	74.998	128.247	74.204
	Azimuth	80	145	145
Granite Wash C	Major range	20016.129	12186.057	8882.492
	Minor range	14181.834	8188.566	7511.239
	Vertical range	77.375	75.792	73.41
	Azimuth	90	140	125
Granite Wash D	Major range	16071.816	20057.216	16071.817
	Minor range	12105.104	11984.854	11949.368
	Vertical range	126.193	109.032	46.821
	Azimuth	130	175	170
Granite Wash E	Major range	20016.129	20016.129	12074.183
	Minor range	20016.129	12024.166	8205.307
	Vertical range	92.909	84.126	74.998
	Azimuth	0	50	175
Granite Wash F	Major range	19892.869	15938.038	12315.187
	Minor range	12209.677	7959.724	10513.386
	Vertical range	100.969	103.175	51.187
	Azimuth	100	150	40
Granite Wash G	Major range	19975.042	16146.988	12129.981
	Minor range	16482.683	12068.456	8171.877
	Vertical range	150.004	123.018	125.399
	Azimuth	100	125	10

Figure E-4. Variogram ranges of lithologies per zone.

Appendix F: Variogram ranges of porosity at each lithology per zone.

		Sandstone	Mudstone	Muddy Sandstone
Marmaton	Major range	10028.608	5510.721	4552.593
	Minor range	7994.8215	4010.1295	3709.7085
	Vertical range	37.3005	99.6075	50.992
Caldwell	Major range	5001.309	10015.525	9973.024
	Minor range	3762.903	6141.5765	7973.713
	Vertical range	24.998	49.3815	36.705
Cherokee	Major range	8056.4515	8080.637	5914.716
	Minor range	5940.4925	6081.3255	2811.618
	Vertical range	24.998	26.263	25.257
Granite Wash A	Major range	10028.608	6049.255	9988.087
	Minor range	4091.5955	4009.7055	6073.0515
	Vertical range	49.6035	62.898	75.2005
Granite Wash B	Major range	5139.304	6049.739	9923.911
	Minor range	3968.336	4055.546	7926.297
	Vertical range	37.499	64.1235	37.102
Granite Wash C	Major range	10008.0645	6093.0285	4441.246
	Minor range	7090.917	4094.283	3755.6195
	Vertical range	38.6875	37.896	36.705
Granite Wash D	Major range	8035.908	10028.608	8035.9085
	Minor range	6052.552	5992.427	5974.684
	Vertical range	63.0965	54.516	23.4105
Granite Wash E	Major range	10008.0645	10008.0645	6037.0915
	Minor range	10008.0645	6012.083	4102.6535
	Vertical range	46.4545	42.063	37.499
Granite Wash F	Major range	9946.4345	7969.019	6157.5935
	Minor range	6104.8385	3979.862	5256.693
	Vertical range	50.4845	51.5875	25.5935
Granite Wash G	Major range	9987.521	8073.494	6064.9905
	Minor range	8241.3415	6034.228	4085.9385
	Vertical range	75.002	61.509	62.6995

Figure F. Variogram ranges of porosity for each lithology per zone.

Appendix G. Upscaled lithology logs

A

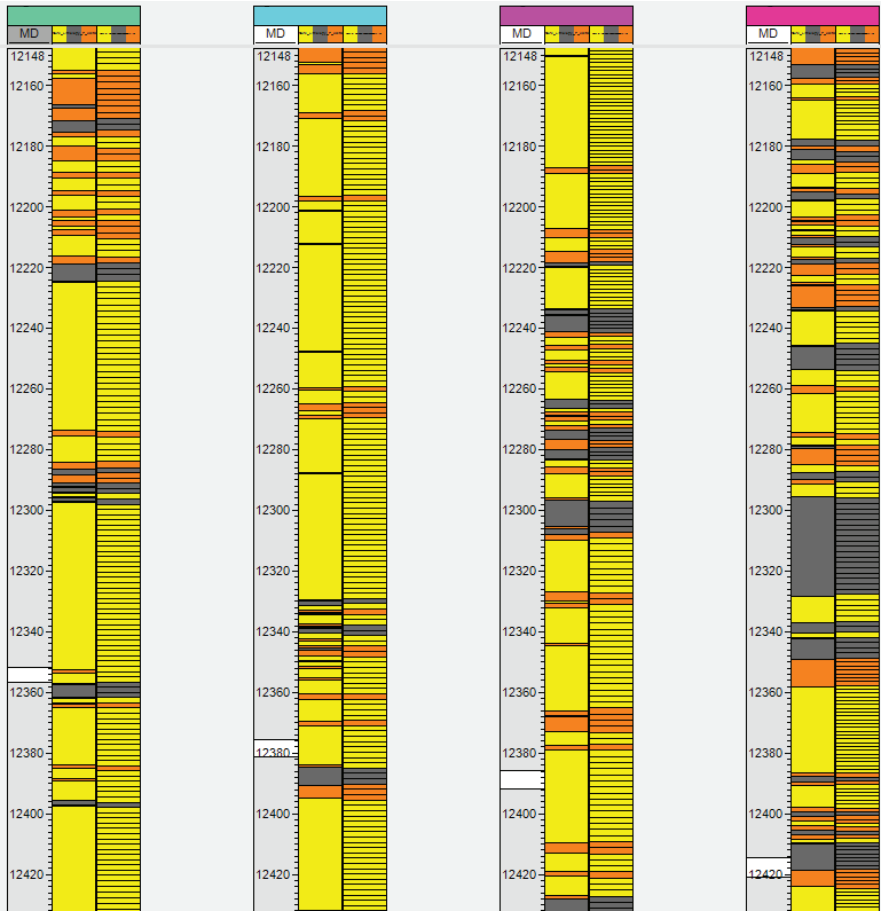

B

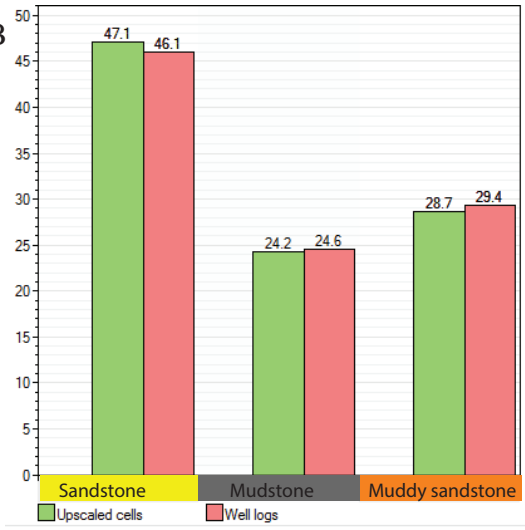

Figure G. Figure H. A) Structural cross section of wells shows the estimated lithology logs (left) and the upscaled lithology logs (right). Layers are 4 ft (1.2 m) thick on average vertically B) Histogram shows the percentage of the lithologies in the estimated lithology logs and the upscaled lithology logs. The values are satisfactory as there is little difference between them. No significant amount of data disappear through the upscaling process and the upscaled lithology log is suitable for modeling.

Appendix H: Subdivisions and sea level curves of Carboniferous-Permian

A

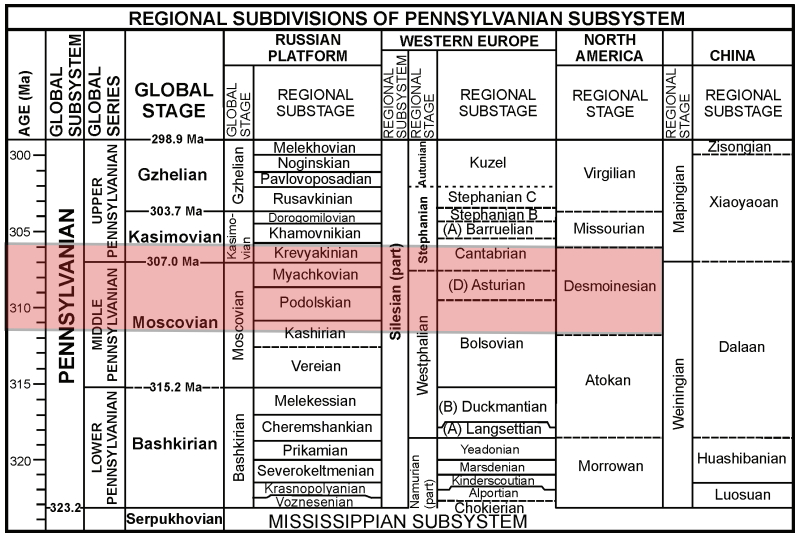

B

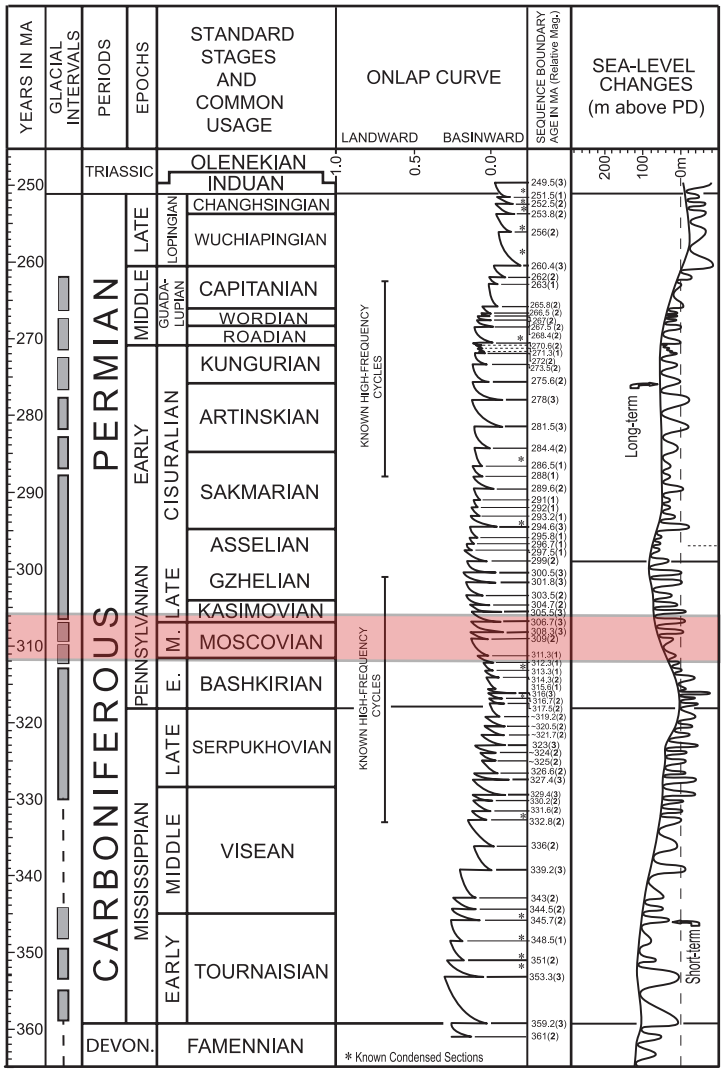

Figure H. A) Regional subdivisions of Pennysylvanian time. North American Desmoinesian time shown with a red box. (modified from Richards, 2013). B) Global sea-level cycles, Pennsylvanian time consists of 16 and Desmoinesian time consist of 5 depositional cycles that are 1 million years each in duration approximately (Modified from Haq and Schutter; 2008). The Desmoinesian Series corresponds to the upper Moscovian and lower Kasimovian stages between 306-312 mya in the international time scale. This interval consists of 5 sea-level cycles in the global sea-level curve, which also corresponds to the 5 depositional sequences that are estimated on the vertical proportion curve.

Appendix I: Average effective porosity maps for lithologies

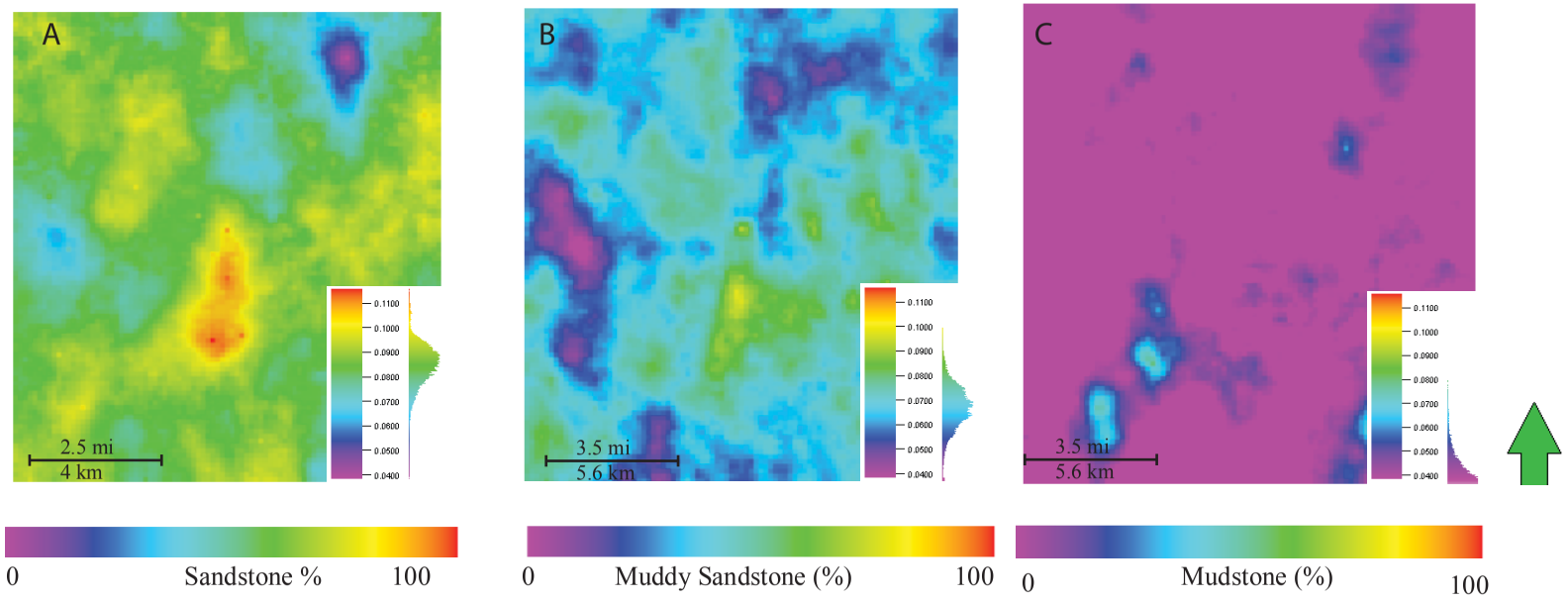

Figure I: A) Average effective porosity map for sandstone lithology. B) Average effective porosity map for muddy sandstone lithology. C) Average effective porosity map for mudstone lithology. Porosity decreases from sandstone to muddy sandstone and to mudstone. This is primarily due to the increase in the fine grained material in muddy sandstone and mudstone lithologies.